DYNAMICS AND PERFORMANCE OF FLYING DISCS

A thesis submitted to the University of Manchester for the degree of

Doctor of Philosophy

in the Faculty of Engineering and Physical Sciences

2011

Noorfazreena Mohammad Kamaruddin

School of Mechanical, Aerospace and Civil Engineering

Table of Contents

Final Word Count: 31, 036.

List of Figures

List of Tables

Nomenclature

$AdvR$	advance ratio
d	disc diameter (m)
c	chord (m)
C_D	drag coefficient
C_L	lift coefficient
C_M	pitching moment coefficient
C_X	axial coefficient
C_Z	normal coefficient
C_Y	side coefficient
$C_{M_{CG}}$	pitching moment coefficient about centre of gravity
C_{M_0}	zero lift pitching moment coefficient
C_N	yawing moment coefficient
C_R	rolling moment coefficient
F_X	axial force (N)
F_Z	normal force (N)
F_Y	side force (N)
F_R	rolling moment (N)
L	lift force (N)
D	drag force (N)
g	gravitational acceleration (m s^{-2})
k_n	static margin

L, M, N	rolling, pitching and yawing moments (N m)
m	mass (kg)
p, q, r	body axis roll, pitch and yaw rates (rad s^{-1})
q_∞	dynamic pressure (N m^{-2})
S	planform area (m^2)
t	time (s)
u, v, w	body axis velocity components (m s^{-1})
V_∞	freestream wind speed (m s^{-1})
xyz	generic coordinate system
$\mathbf{x}$	position vector (m)
α	angle of attack
ϕ, θ, ψ	roll, pitch and yaw Euler angles
ρ_∞	air density (kg m^{-3})
W	weight (kg)

Subscripts

L	launch

Embellishments

*	dimensionless variable

Abbreviations

AoA	angle of attack
cg	centre of gravity
cp	centre of pressure
ac	aerodynamic centre
R	dimensional range (m)
R^*	dimensionless range
θ_L	launch pitch angle (degree)
ϕ_L	launch roll angle (degree)
V^*	dimensionless speed
t	time (s)
t^*	dimensionless time
T_{total}	total time (s)
V_L	launch speed (m s^{-1})
V_o	initial speed (m s^{-1})
t/d	thickness-to-diameter ratio
c/t	cavity height-to-thickness ratio
t	time (s)
L/D	lift-to-drag ratio

Abstract

ABSTRACT OF THESIS submitted by **Nurfazreena Mohammad Kamaruddin** for the Degree of Doctor of Philosophy and entitled '**Dynamics and Performance of Flying Discs**'.

Submitted October 2011

The study of dynamics and performance of flying discs is motivated by how variations in their design features influence the aerodynamic characteristics and flight performance, particularly range. Reviews in the literature focus on the development of fundamental research in flying discs and on the performance of sports projectiles. Theoretical background on disc dynamics, range and sensitivity are given. This work investigates disc aerodynamics by performing wind tunnel experiments to measure aerodynamic loads on a set of generic parametric discs and a set of commercial golf discs. The parametric discs isolate various geometrical features such as thicknesses, cavities, leading edge curvatures and cambers to study the influence of these parameters on aerodynamic characteristics. The commercial golf discs consist of three different categories known as putter, mid-range and driver: these discs are used for short, medium and long flight range, respectively. To study the performance, aerodynamic data of the golf discs are used as inputs in numerical simulations to predict their flight trajectories and range. Effects of launch attitude on range are assessed to study the optimal initial launch conditions to achieve maximum range. Further, the simulation provides a direct approach to analyse range sensitivity on launch parameters.

Results from the experiments show a number of significant findings on disc geometry. First, a cavity is fundamentally important for a disc to have satisfactory flying qualities: the presence of the cavity produces a significant aft shift in the aerodynamic position to minimize the pitching moment about the centre of the disc. Hence, the disc will have a minimal tendency to roll about the flight axis. Second, the thickness of a disc has a significant effect on its profile drag: increasing the thickness increases the profile drag. Third, a disc with a positive camber produces a relatively higher lift-to-drag ratio (C_L/C_D) compared to one with no camber. Fourth, the effect of tapering a flat leading or trailing edge of a disc leads to a reduction in its lift (within the angles of attack tested in the study) with a significant reduction in its drag. Fifth, it is shown that peak lift-to-drag ratio of a free flying disc is not necessarily a good indicator of performance because the angle of attack (and hence, lift-to-drag ratio) varies widely through a typical flight. Furthermore, a disc with a significant pitching moment will roll significantly about the flight path direction, further reducing the achievable range for a given lift or drag characteristic. Finally, a novel method to quantify disc sensitivity with respect to changes in launch conditions has been developed. The simulations show that the range sensitivity of each disc with respect to launch pitch angle varies significantly, with discs design for long range being much more sensitive (and therefore harder to throw accurately) than discs designed for short range.

Declaration

No portion of the work referred to in the thesis has been submitted in support of an application for another degree or qualification of this or any other university or other institute of learning.

Noorhazreena Mohammad Kamaruddin, October 2011.

Copyright Statement

Further information on the conditions under which disclosure, publication and commercialisation of this thesis, the Copyright and Intellectual Property and/or Reproductions described in it may take place is available in the University IP Policy (see http://documents.manchester.ac.uk/medialibrary/policies/intellectual-property.pdf), in any relevant Thesis restriction declarations deposited in the University Library, The University Library's regulations (see http://www.library.manchester.ac.uk/about/regulations/) and in The University's policy on Presentation of Theses.

Acknowledgement

In the Name of God, the Most Gracious, the Most Merciful. All Praises to the Almighty God Who has given me so much strength throughout my PhD journey and with His Will, I manage to complete this thesis.

My life has been like a roller-coaster for the past 4 years, but without help from the people around me, it would be impossible to endure the ride. To my supervisor, Dr. William Crowther, who taught me to be strong to face criticism, I will forever be indebted for his help and guidance. To Dr. Jonathan Potts, my mentor, whom I went to for advice and guidance throughout my research, I hope one day we will find the 'Magic number' if it ever exists. To my friend Kailash who helped me to find a job, when I didn't even have a pound to ride the bus, I will never forget your kindness. To Chip, Chris, Paul, Ben, John, Matt, Phil, Steve and David, thank you for the friendship, I now know how to brew a proper English tea. To Andrew and Ian who helped me out when the wind tunnel decides to take a 'break', I am very grateful for the assistance. To the skilful lab technicians, Mike and Ken who let me drilled my disc models even without safety clearance, I truly appreciate it. To Dave, thank you for driving me out to Barton every day. I also would like to acknowledge the financial support from my sponsors, the Universiti Sains Malaysia and the Ministry of Higher Education Malaysia.

To my parents, Kamaruddin and Fadzillah, who have shaped me to be who I am today, who support me all the time, I am eternally grateful for everything and for all the prayers. Without their blessing, I don't think I will be able to go this far. To my brother, Ariffuddin, and his wife, Ekin, who are always there when I need them the most, I really missed you guys.

I am deeply grateful that God has blessed me with a beautiful princess, Hanya Syifaa, who stays late at night and constantly asking me what time I will finish my work, who made me smile every day and means everything to me. Most of all, I am truly grateful to my beloved husband, Zulfaa, who supports me throughout everything, who sacrifices his career so I can pursue my dream, who never gives up on me and always believe in me. There are no words enough to describe how grateful I am to have someone like him in my life. I pray to the Almighty, that we will always be together.

Chapter 1

Introduction

This chapter introduces the study presented in this thesis on flying discs and describes the motivation behind it. A background on golf discs, which are studied extensively in this work as models for the flying discs, is presented first with a particular focus on their characteristics and flight dynamics. Two major phases of this study are then described to highlight the significance of each phase. The aim of this thesis is defined following the introduction. Finally, the objectives of each chapter are described to establish the foundation of this thesis.

1.1 Introductory remarks

The game of disc golf was invented by Ed Headrick in the late 1960's as an adapted version of the standard game of golf. The game is similar to that of golf but uses discs commonly known as golf discs instead of golf balls. The goal of a player is to throw his or her disc with the least number of throws possible into a target hole, which is a metallic basket placed above the ground on a pole looped with chains to help capture the disc (a scene at a game of disc golf is shown in Figure 1.1). The game is relatively new in the United Kingdom but has been increasingly popular in the United States and managed by the Professional Disc Golf Association (PDGA).

Figure 1.1: A disc-golf player player throwing a golf disc towards a target basket on a pole above the ground (Taken from PDGA).

Golf discs are generally categorized into three distinct types designed to have different flight characteristics. The generic names of these types are 'driver', 'mid-range' and 'putter' discs. Each disc type is named to associate it with the flight range (i.e. the horizontal distance) it covers. (The word 'range' will be extensively used throughout this thesis to refer to the horizontal distance covered during a flight). A driver disc is typically used for a target range of more than 75 m, a putter disc for a range of less than 50 m, and a mid-range disc for the intermediate range between 50 m and 75 m. The variations in the flight range and characteristics of the discs are generally governed by the differences in their geometry. These discs differ mainly in their thickness-to-diameter ratios, depths of the cavities at the lower surfaces, cambers, and curvatures of the edge rims.

The cross sectional profiles of the three types of discs are shown in Figure 1.2. The typical diameters of the discs are approximately between 20 cm to 25 cm and their weights vary between 150 g to 180 g (further geometrical descriptions of the discs are detailed in Chapter 4: Method). In addition to the discs described above, another type of a flying disc is the Frisbee disc which is commonly used in recreational activities but not played in the game of disc golf. The geometrical and flight characteristics of a frisbee disc are similar to that of a putter, i.e. shorter flight range and thicker disc profile.

The geometrical properties of a disc have a primary influence on its aerodynamic characteristics (i.e. the aerodynamic forces and moments acting on the disc) that in turn determine its unique flight characteristics. In addition, these geometrical properties have a secondary influence on the moment of inertia of the disc given that its mass is fixed. The combined influences affect the overall flight performance of the disc, including the range it covers when flown. For example, a putter has a rounder rim edge curvature, a higher camber and a larger thickness-to-diameter ratio, resulting in a larger frontal area compared to the other discs. This 'putter' geometry increases the drag of a disc but reduces its tendency to roll about the flight path.

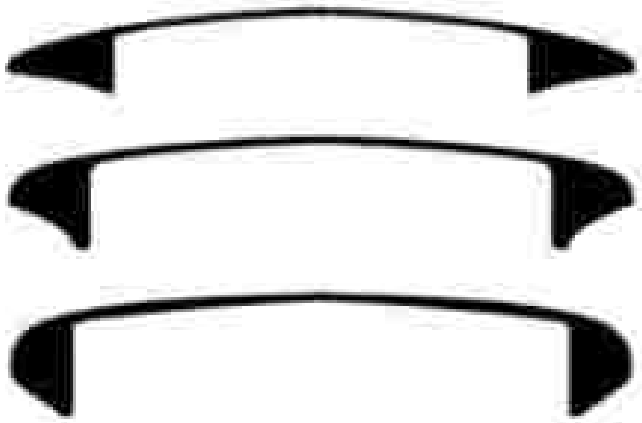

Figure 1.2: Schematic cross-sectional profiles of the driver (top), mid-range and putter (bottom) discs.

The flight characteristics of a putter are similar to those of a typical frisbee disc, which possesses shorter but straighter flight paths compared to long-range discs, i.e. discs designed to travel further distances. One such example of a long-range disc is a driver disc, which is designed with a smaller frontal area due to its smaller thickness-to-diameter ratio and a more aerodynamically streamlined shape to reduce drag. The improved flight performance is, however, at the expense of an increased tendency to roll about the flight path, which means that a player would need to have greater throwing skills to achieve the same accuracy achieved when throwing a putter disc. A mid-range disc is transitional in their design and performance characteristics between those of a putter and a driver discs.

A flying disc, also known as a disc-wing or a circular planform wing, has by definition an aspect ratio of 1.27 and thus can be generally classified as a low aspect ratio wing. It requires spinning about its centre axis to achieve stability during flight via the gyroscopic principle. The most recent and important work on the aerodynamics of one type of flying discs – the Frisbee disc – was performed by Potts (2005). His extensive experimental investigation with a secondary focus on flight dynamics using numerical simulations lead to the observation that the aerodynamic forces and moments acting on a disc are crucial to understanding its flight

characteristics. In addition, the spinning of a disc was observed by Potts to have negligible effects on its aerodynamic characteristics (further details of the work are described in the Chapter 2: Literature Review).

The work performed herein is motivated to investigate a variety of other discs with different designs to analyse how their geometrical properties affect their aerodynamic characteristics.

The earlier phase of the research reported herein focused on gathering experimental data via wind tunnel testing to investigate the aerodynamic forces and moments acting on the three different types of golf discs described above, i.e. the putter, the mid-range, and the driver discs. The three designs chosen for each of the category are based on existing commercially available golf discs (further details are provided in the Chapter 4: Method). Results show that each discs exhibit aerodynamic characteristics consistent with what was expected based on their generic flight performance. For example, the drag coefficient of a putter disc is larger than that of a driver disc at typical flight angles of attack. Wind tunnel experiments were also performed on a "control" disc, which is a flat-plate disc referred to hereafter as the baseline disc.

In addition to the use of a control disc, a more systematic approach of isolating various geometrical features of a disc was done. For this purpose, a large number of disc models were fabricated. These discs have simpler design features compared to those on the three golf discs experimented above; the design features of the simpler discs were varied parametrically to isolate the effect of one geometrical property while keeping other geometrical properties unchanged. These simpler disc models will be extensively referred to hereafter as the parametric discs. Design features that are particularly important to the aerodynamic characteristics of a disc in general are its thickness-to-diameter ratio, cavity (at the lower surface of the disc), camber shape and rim edge curvature; these features were isolated in this experimental study.

Analysis from this parametric study shows that the cavity of a disc fundamentally influences its aerodynamic characteristics.

The later phase of this research is concentrated on evaluating the flight performance and range of golf discs via numerical simulations of the complete six-degree-of-freedom equations of motion of the discs developed by Crowther and Potts (2007). These simulations allowed more detailed assessments on how the flight performance of a disc was influenced by its aerodynamic characteristics. The experimental data on the golf discs gathered in the first phase of study functioned as part of the input parameters into the simulation. Another important aspect that the numerical simulations allowed was how variations in the conditions of launching a disc (e.g. the launch pitch and roll angles, and the launch speed) affect its flight trajectory. Parametric variations of these launch conditions were performed to analyse their sensitivity toward the performance of a disc. Different types of discs were found in this study to have different sensitivity levels towards variations in the launch conditions; for example, a putter disc is less sensitive towards variations in the launch pitch angle compared to a driver disc. This sensitivity analysis was found to be an important tool to assess the throwing accuracy required of a player to achieve a certain target. The association between the sensitivity of a disc (towards a certain launch parameter) and the accuracy required of a player would allow one to assess the player's throwing skills. This analysis of this thesis, however, is not extended to include the player skill assessment because such an effort would require detailed study of the biomechanics of throwing.

1.2 Thesis aim

The aim of this thesis is to develop an understanding of the influence of disc geometry on the aerodynamic characteristics of golf discs and their subsequent flight performance in terms of range and accuracy.

1.3 Thesis objectives

The objectives of the thesis are sub-divided based on its chapters.

- To introduce the background on the characteristics and the dynamics of flying discs, describe the major phases of the investigation performed herein, and clarify the motivation and aim behind the work (Chapter 1).
- To provide a relevant literature review with a particular focus on the historical development of flying disc studies, and to describe studies investigating the flight range of sports projectiles (Chapter 2).
- To describe the theory relevant to the aerodynamics and the flight dynamics of discs and to present the derivation of range and sensitivity with respect to launch attitude (Chapter 3).
- To describe the experimental methods used in the work and to present the simulation methods implemented in the thesis (Chapter 4).
- To present and discuss results of the experimental work particularly on commercial golf discs and parametric discs (Chapter 5).
- To present and discuss results of the simulation work on flight performance, range and sensitivity of discs (Chapter 6).
- To present conclusions of the work and recommend potential studies for future research (Chapter 7).

Chapter 2

Literature Review

The first aim of this chapter is to review the development of fundamental research in the experimental and computational study of flying discs. Historical timelines of various works are provided to outline critical growth in this area. This outline tracks the previous interest and advancement in the field which leads to the identification of a need to develop and extend the work on geometry of the discs as well as their range. An overview of the content of this chapter is shown in Figure 2.1.

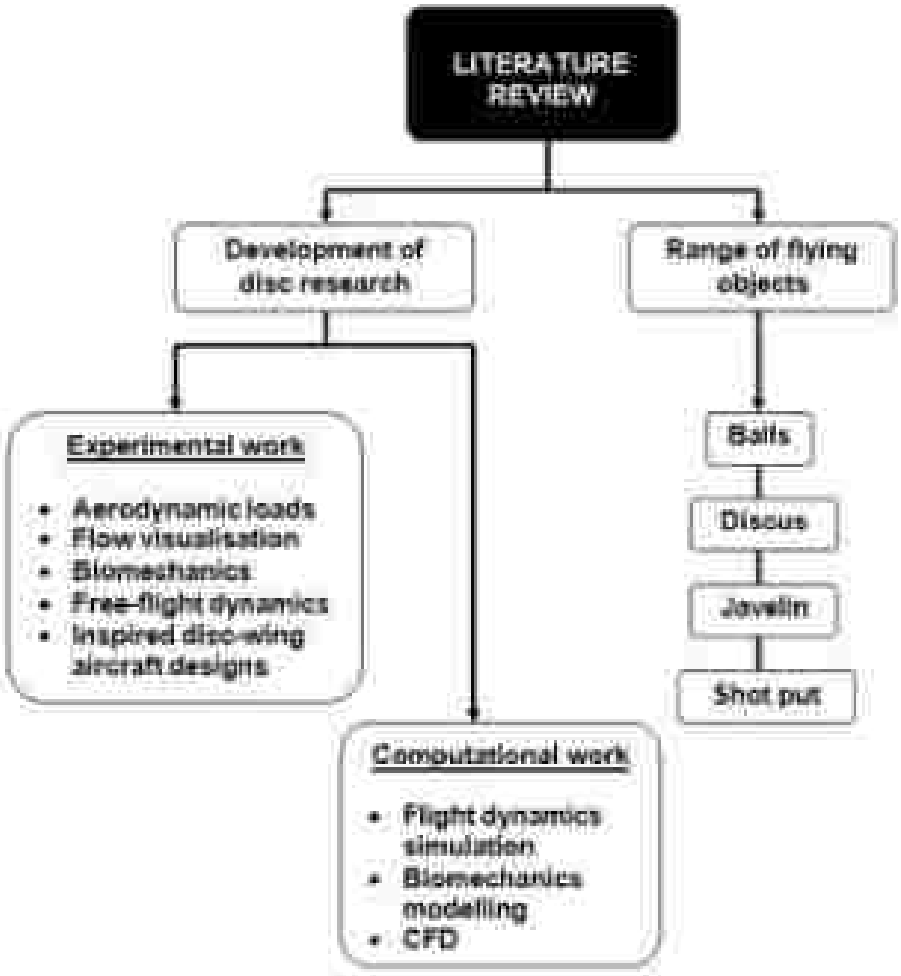

Figure 2.1: Outline of Chapter 2.

The second aim of this chapter is to provide a background on flying objects in sports with a focus on the factors influencing the range flown by the objects. Sports objects such as balls, discus, javelins, and shot puts rely on a number of factors critical for

the determination of their flight ranges. The range-influencing factors studied in these previous works are the aerodynamic forces, the biomechanics of launching techniques and most importantly the initial launch conditions, which is the subject of interest in this thesis. The review of the various sports objects highlights the similarity of the important factors influencing their flight despite the differences in the shapes of these objects. This similarity is extended for the study of flying discs to identify the main factors influencing their flight performances and ranges.

2.1 Development of disc research

2.1.1 Experimental work

There are significantly fewer experimental studies in the field of disc aerodynamics and flight dynamics compared to those on conventional prismatic-shaped wing planforms. One possible reason for the relative lack of research in this area could be due to their limited commercial applications. Some of the earlier works in this field, as will be described subsequently, are related to projects with military and sports applications.

Most experimental works carried out in disc research were mainly focused on understanding the aerodynamic characteristics. The earliest study on the aerodynamic characteristics of non-circular low aspect ratio wings were conducted by Zimmerman in 1935. The first study on the aerodynamics characteristics of discs, which can be classed as circular low aspect ratio wings, was performed almost four decades later by Stilley and Carsten in 1972. This experimental study was funded by the U.S. Navy whose practical interest was to develop self-suspended flares. Their models were tested in a wind tunnel and results for the lift, drag and pitching moment were gathered. The results produced by Stilley and Carsten exhibited some patterns that were similar to those obtained on the non-circular low aspect ratio wings. Specifically, the lift increased linearly with the angle of attack and the shape of the drag profile was parabolic. In addition to the flare configurations, they also

tested a hollow Frisbee-like model to observe the effect of cavity. They observed that the disc has a large nose-down (i.e. negative) pitching moment, which they speculated was due to the existence of a cavity at the lower surface of the disc. However, their study did not carefully investigate or isolate the effect of the cavity because they did not vary the cavity height nor compared with a control disc without a cavity. In contrast, the experimental work performed in this thesis tested the effect of varying the cavity height and found that the thickness of the disc also contributed towards the negative pitching moment although it was not as significant compared to the effect of the cavity.

A decade later, disc study was redefined with a new interest in the effect of spinning on aerodynamics by Lazzara et al. (1980). They measured aerodynamic loads of a Frisbee-shaped disc at various speeds and spin rates at angles of attack ranging from 0° to 10°. The study found that a small lift increment could be generated by spinning. However, it was not clearly stated how the spinning effect could generate the lift and recent experimental studies contradicted this finding – disc rotation at typically experienced spin rates does not generate any lift (Potts 2005).

The Reynolds number effect on discs was first investigated by Mitchell (1999). He measured lift and drag for three non-spinning discs and varied the flow speed to vary the Reynolds number. His results suggested that there were significant Reynolds number effects over the typical flight speed range. In contrast, Potts and Crowther (2000(a); 2001(a)) showed that Reynolds number effects are relatively insignificant for flight speed below 30 m s^{-1}. This contradiction is largely due to the different range of speeds tested. Potts and Crowther studied disc speeds typical to those measured for sports-related discs while Mitchell used discs with higher speeds. It is worth noting that besides Potts and Crowther's study, the measurement of disc rolling moments has never been performed in previous disc studies. They also complemented the Frisbee load measurement with pressure distribution analysis. They found that spinning has relatively little effect on disc aerodynamic loads as shown in Figure 2.2 (a)-(c). Note that there is a small rolling moment effect due to

spin that was attributed to the asymmetric lift distribution as a result of early separation on the advancing side and delayed separation on the retreating side. The advance ratio (AdvR) in their study is defined as the ratio of disc rim speed to flow speed (Potts and Crowther, 2000).

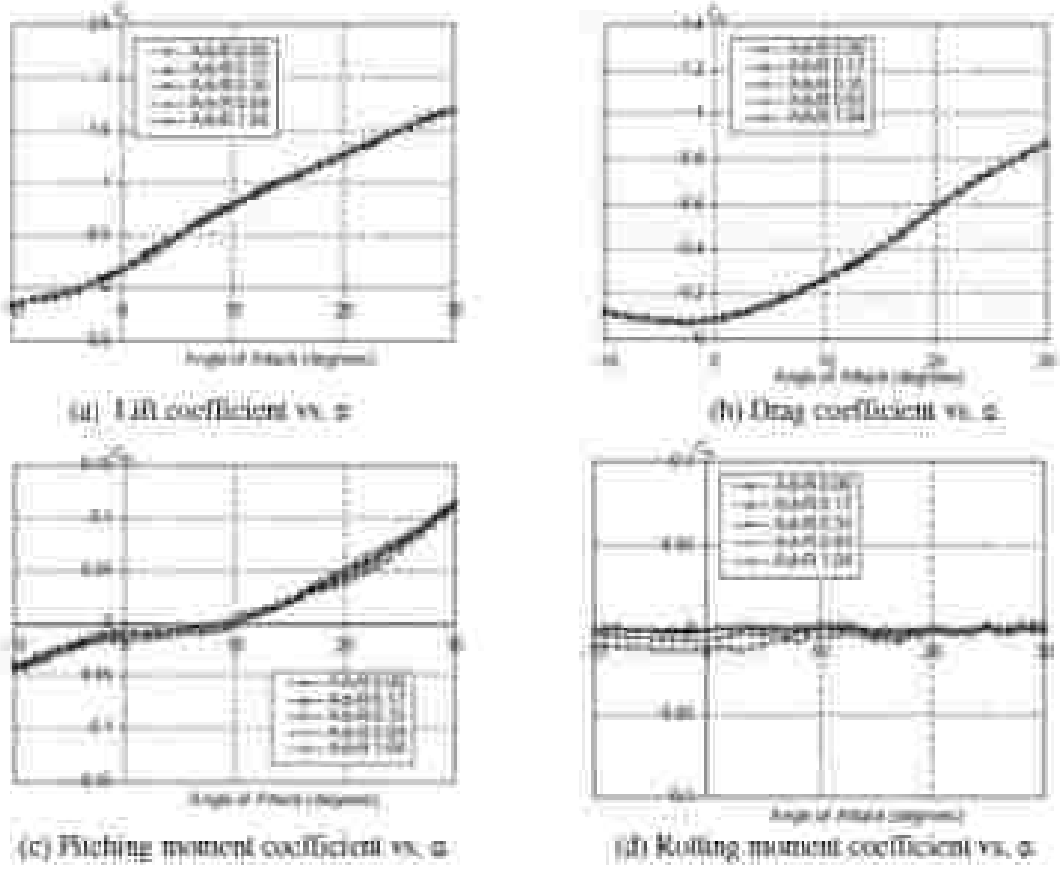

(a) Lift coefficient vs. α

(b) Drag coefficient vs. α

(c) Pitching moment coefficient vs. α

(d) Rolling moment coefficient vs. α

Figure 2.2: Effect of spin on the aerodynamic coefficients for Frisbee at V = 20 m s^{-1} for various spin rates of 0, 4, 8, 16, 24 Hz. Spin has very minimal effect on disc aerodynamic loads (Taken from Potts, 2005).

In addition to the experimental works on aerodynamic loads measurement, a number of disc studies focus on the flow visualisation technique to understand the flow behaviour around the disc. Nakamura and Fukamachi (1991) performed a flow visualisation study on a Frisbee disc by using a smoke wire technique. They observed that a strong downwash effect is generated by a pair of vortices (as would

be expected for a low aspect ratio wing). However, their results were for an advance ratio of 2.26, which did not match the typical flight value that is usually less than one (Potts, 2005). There was no clear justification of the reason how that advance ratio was higher than a typical flight value in their experiment, but this shows that limited disc literature could lead to unjustified method and misinterpretation of the experimental results.

A similar study was performed by Higuchi et al. (2000) to study flow over a spinning golf disc model complemented by particle image velocimetry measurement of its vortex strength. Their measurement shows that spinning did not affect the vortex strength at lower angles of attack. However, the vortex strength magnitude started to reduce as the angle of attack increases at higher angles of attack ($\alpha > 15^{o}$). Their observation suggests this was due to large areas of upper surface separation. In addition, they also discovered that the reattachment line on the golf disc moves further downstream as the angle of attack increases, consistent with the present golf disc flow visualisation study.

Potts and Crowther (2000(b), 2001(b)) also conducted a flow visualisation study on a spinning and non-spinning Frisbee disc model by using a similar technique as Nakamura and Fukumuchi (1991), coupled with a surface-paint flow visualisation technique. They found that a crescent-shaped separation bubble representing a boundary layer separation line occurred near the disc leading edge. A similar study by the author performed on a driver golf disc in this thesis confirmed Potts and Crowther's findings. However, the location of the boundary layer separation line occurrence varies between the Frisbee and the golf discs. At an angle of attack of α^{o}, the separation line of a Frisbee occurred at about 20% ahead of the leading edge while the driver golf disc's separation line is at approximately 5%. In addition, Potts (2002(a)) also discovered that the Frisbee wake flow is strongly influenced by the roll-up of the trailing vortex pair and revealed that spin causes an asymmetric vortex wake as shown in Figure 2.3. His results show that as the advance ratio increases

from 0 (i.e. non-spinning) to 0.7, the spin causes a slight asymmetry in the vortex wake which becomes more evident as the advance ratio increases to 1.6.

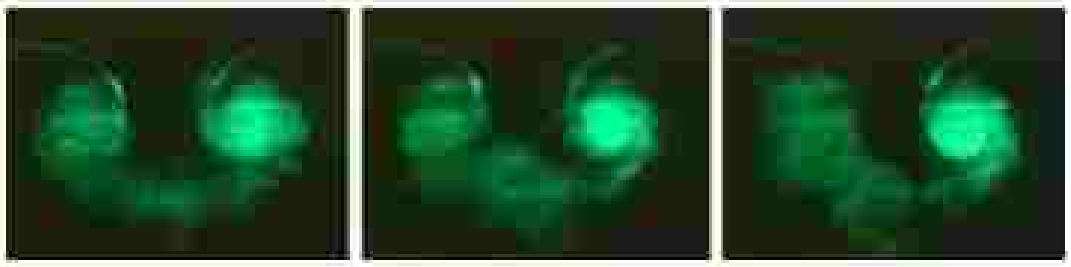

(a) Adv$R = 0$ (b) Adv$R = 0.7$ (c) Adv$R = 1.6$

Figure 2.3: The trailing vortex pair at various spin rates at Reynolds number of 5.67×10^4. Spin causes an asymmetric vortex wake (Taken from Potts, 2005).

Apart from the study of disc aerodynamics in the wind tunnel, there are several studies dedicated towards the biomechanics aspect with a focus on the throwing technique to achieve maximum range. Cotroneo (1980) proposed that range was not influenced by the back-hand or the side-arm throwing technique: the range remains approximately the same with both techniques. He also relates the launch speed and its association with respect to range to study the general trend between these parameters. He established that the launch speed was the most influential factor on determining the maximum range thrown. The study could have been improved if it had considered the effect of launch angles on disc range from the biomechanics point of view. This may be achieved by comparing the athlete's optimal launch angle and correlating their technique with maximum range.

In line with Cotroneo's work, Hummel (2003) also conducted a Frisbee biomechanics study, focusing on the backhand throws as shown in Figure 2.4. Although Cotroneo had already established that range remains unchanged despite having a different throwing style, Hummel's intention was to understand the Frisbee throwing technique for an individual. She developed a musculoskeletal Frisbee thrower's model with kinetic chains of seven rigid bodies (i.e. torso, scapula, clavicle, ulna, humerus, radius and hand) to study how these bodily movement can

be fully utilized to enhance the throwing technique. She reported that the humerus released the highest launch energy at about 100 W while the wrist flick contributed the least at only 8 W.

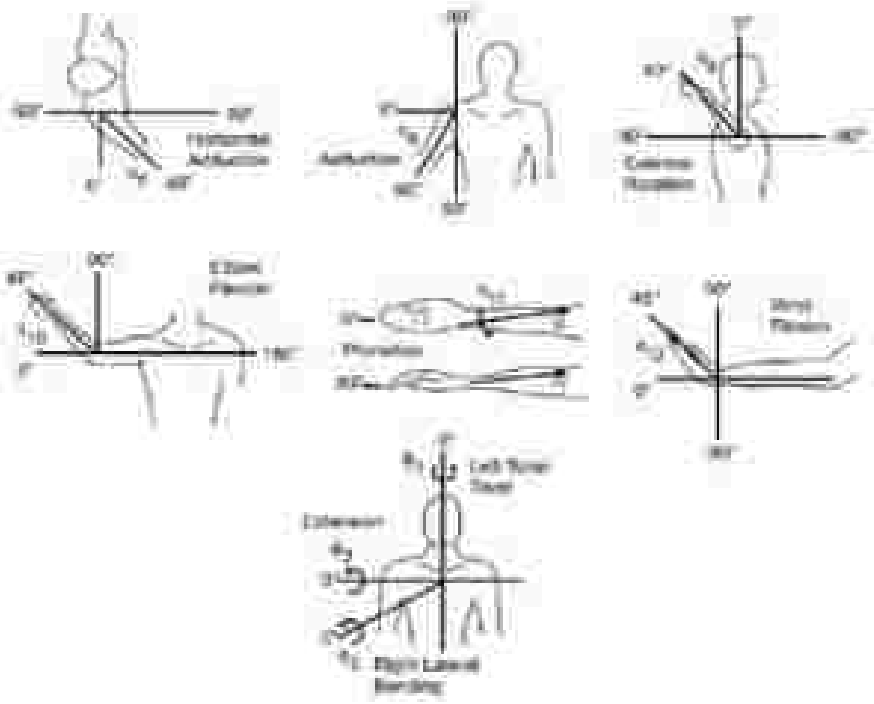

Figure 2.4: Frisbee throwing model to study the backhand throw. The humerus produces the highest source of launch energy at 100 W while the wrist flick only manages to produce 8 W (Taken from Hummel, 2003).

There have been a number of field studies on disc performance. Pozzy (2002) managed to record golf discs launch speed and the corresponding range made by golf disc players at sports events by using a radar gun. His data collection was considerably scattered but still manage to capture reasonable trend. The data suggested a linear relationship between the launch speed and range instead of quadratic (as would be expected for an ideal point mass projectile with negligible drag). The main reasons for this difference could be due to lift and drag on the discs. In addition, wind conditions or the altitude could also have some influence on the linear trend. Nevertheless, the results highlighted an important statistical pattern and

if combined with rigorous technique, the data could be used as estimations in disc flight simulations.

Lorenz (2005) measured free flight dynamics of a Frisbee disc by using on-board instrumentation as shown in Figure 2.5. He recorded a real-time Frisbee flight data by mounting a number of electronic devices (i.e. pressure sensor, infra-red sensor, accelerometer and magnetometer) underneath the cavity. His data generally were in well-agreement with Potts and Crowther (2003) although there were inconsistencies in drag and pitching moment, but the discrepancy could be due to the wobble effect of the disc following the launch but subsequently dampened afterward. (This wobble seems to be analogous to the phugoid effect experienced by an aircraft). The asymmetric distribution of the on-board instrumentation could have some influence on the flight wobble. This methodology is still in progress but the collected free flight data may potentially provide a significant contribution for comparison with wind tunnel data.

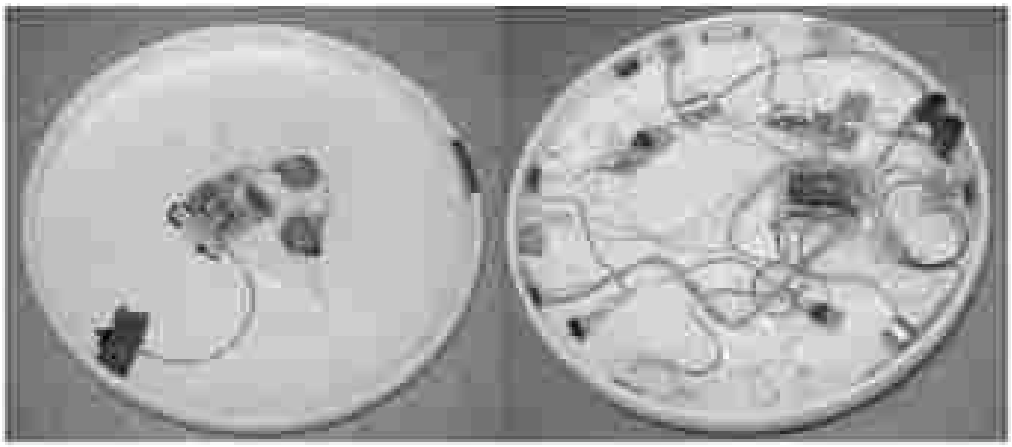

Figure 2.5: Frisbee free-flight data is obtained using on-board instrumentation. Electronic devices such as pressure sensor, infra-red sensor, accelerometer and magnetometer are mounted underneath the Frisbee cavity (Taken from Lorenz, 2006).

The development of disc research also witnesses a number of inspired disc-wing aircraft design such as Lee-Richards annular wings biplane, Zimmerman *'Vought V-173'* (Ginter, 1992), EC-2 Hawkeye and E-3 Sentry as shown in Figure 2.6.

However, the most historical disc-wing aircraft design achievement was 'Avrocar' designed by John Frost in 1959 (Lindenbaum and Blake, 1998). It was a circular vertical take-off (VTOL) aircraft as shown in Figure 2.6 (d). Unfortunately, apart from its spectacular design, Avrocar's performance was very disappointing as it failed to fly steadily due to an engine thrust problem. Amongst other issues, the exhaust air flow recirculated into the engine inlet causing the thrust performance to reduce significantly.

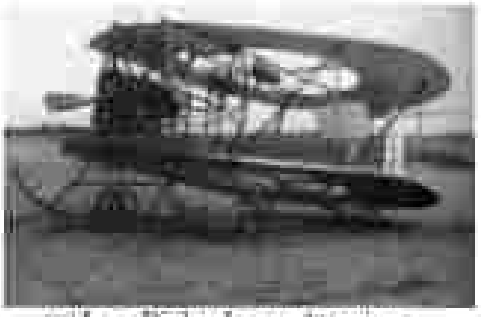

(a) Lee- Richards annular wings

(b) Vought V-173

(c) HC-2 Hawkeye

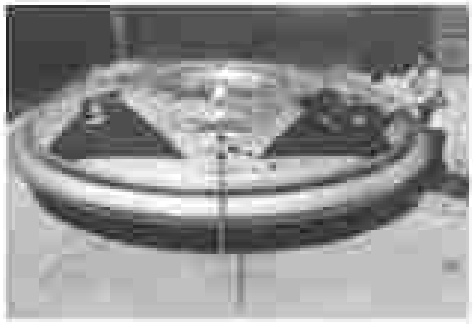

(d) Avrocar

Figure 2.6: Implied disc-wing aircraft designs. Photos of (a)-(c) are taken from Lorenz (2006) and (d) from Lindenbaum and Blake (1998).

2.1.2 Computational work

The development of disc research is complemented with the study in computational area. Most computational works on disc wings have focused on flight dynamics modelling and simulation. In 1968, Katz investigated flight trajectories and stability of a disc with the intention to replace ballistic artillery shells with discs rotating at

high speeds. He presented a mathematical model to calculate the disc flight trajectory in two-dimension with spin treated as an independent parameter.

Lissaman (1994) later improved disc flight dynamics modelling by analyzing dynamic models of spinning sports objects. He developed linearized flight dynamics equations of motion to produce longitudinal and lateral flight trajectories (Lissaman, 1996; 1998; 1999; 2001; 2003). These tasks were considered computationally at that time as they require small time-steps for convergence.

Along this line of research, Hubbard and Hummel (2000) conducted a disc study from the biomechanics aspect with, focus on investigating the effect of launch conditions and parameter identification from free-flight data. This data, captured with high speed video cameras, allowed them to derive the disc's aerodynamic coefficients from linear approximations. These coefficients were used to simulate Frisbee flight trajectories (Hummel and Hubbard, 2001; 2002; 2004). The results of their work compare well with Potts's wind tunnel data. Their work serves as an important input of disc free flight parameters for Crowther and Potts's (2007) numerical simulations of disc trajectories.

In 2002, Daniowsky and Cohanim (2002) also developed a model to simulate disc flight trajectories. In contrast to Hummel and Hubbard who uses free flight data, they applied potential flow theory to estimate the aerodynamic parameters in the simulation. This approach was not justified by the authors and the study is of limited value. They also ran experiments on disc aerodynamics to provide aerodynamics data required in the modelling. However, as the experimental disc model was made of plastic and would most likely deform during the wind tunnel test, the accuracy of the data obtained in the experiment might influenced the simulation results.

Although most computational studies focus on the flight dynamics simulation, Axel Rohde (2000) has performed a rigorous computational fluid dynamics (CFD) analysis around a rotating disc. He found that spinning did not affect the

aerodynamic forces, consistent with Potts's (2005) experimental results. The developed computational method was based on compressible Navier Stokes equations; however, the solutions were performed at a Mach number of 0.3. This is clearly impractical with respect to the typical throwing discs used in sports as they do not reach such a speed. Nonetheless, the solutions could still be potentially applicable for future studies with high speed flying discs, one such possibility is a ballistic projectile for military application.

In 2007, a six-degree-of-freedom disc flight simulation was developed by Crowther and Potts (2007), with the incorporation of actual Frisbee free flight data (Hummel and Hubbard, 2002) as well as wind tunnel aerodynamics data (Potts, 2005). The simulation estimates the disc flight trajectories and shows good agreement with experimental data. In the simulation, the effect of range on launch parameters was observed and the results highlight some important information. As expected, a disc with a high advance ratio (i.e. high spin rate) would result in a straighter flight trajectory but not necessarily lead to a greater range. Their simulation results revealed that range is very sensitive to launch pitch angle which agrees well with the golf disc study investigated in this thesis. However, their study did not include the effect of roll angle on range (Crowther and Potts 2007).

The review of computational works on discs research development in the computational area shows that although there have been a number of flight dynamics simulation studies, none have been used to thoroughly investigate the effect of launch parameters and disc aerodynamics on the range. The following sections aim to provide some insights to understand the range of flying sports objects (i.e. balls, discus, javelin, shot put) in general and to assist in the investigation of disc range in this thesis.

2.2 Range of Flying Objects

The study of ballistic projectiles has been relevant and practical in both military and sports fields. In one unique application of golf ball dynamics for a military purpose, Barnes Wallis developed "bouncing bombs" to breach the German Möhne dam in 1943 (Hutchings, 1976). The bombs were dropped with a back-spin at 500 rpm to cause them to bounce and skip on the water surface, much like spinning golf balls bouncing on fields. The bouncing bomb technique was necessary to skip over torpedo nets used to protect the dam wall (Figure 2.7). Important scientific collaborations in sports fields have also been noted, particularly to improve range of throwing and jumping events (Linthorne, 2006; Leigh et al., 2010).

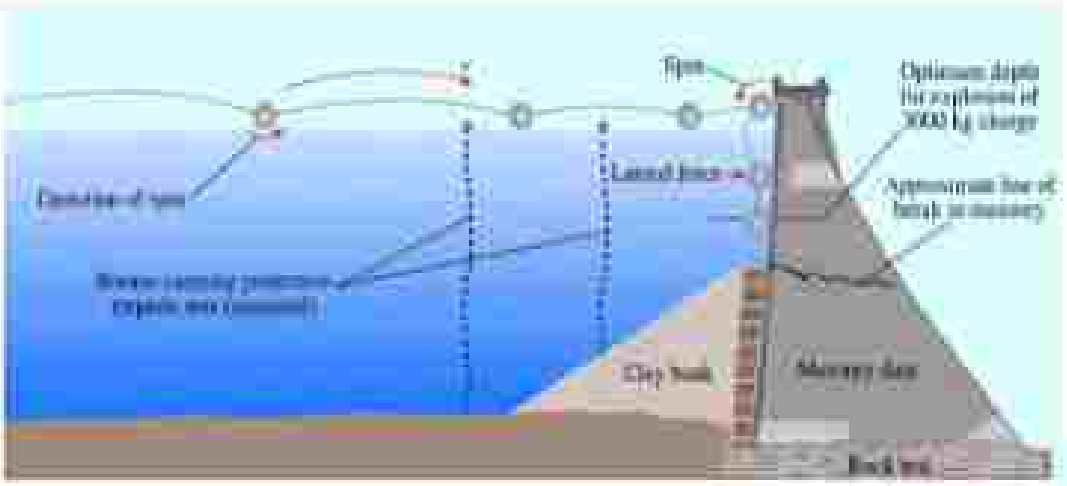

Figure 2.7: The "bouncing bomb" developed by Barnes Wallis used similar principle as a bouncing golf ball (Taken from Podesta, 2007).

2.2.1 Balls

This section briefly reviews study on golf balls, baseballs and footballs with a focus on factors influencing their range. The main launch parameters that affect range are the launch speed and the launch angle (Hubbard, 2000; Linthorne and Everett, 2006). The effect of launch speed on range is rather direct, as range is proportional

to the square of speed. It was more common for researchers in this field to investigate launch angles to determine optimum launch angles for maximum range (Hubbard, 1984; Linthorne, 2006; Hubbard and Cheng, 2007). This is due to the human difficulty to achieve the same speed at all launch angles. The common assumption is that launch angle is independent of launch speed. However, there are several studies dedicated to investigate the dependency of these parameters in sports objects that suggest the opposite, like in the case of javelin, shot put and discus (Bartlett, 2000; Leigh et al, 2010) but this topic will be discussed in brief in the following section.

The simple way to study the influence of range in principle is to understand the basic theory of projectile motion that was first discovered by Galileo in 1592. In addition to the basic understanding of projectiles, an extensive mathematical theory of sports projectiles can be referred to de Mestre (1990). Based from the projectile motion theory, for any given launch speed in idealized ball flight (zero air resistance), the maximum range would occur at 45°. According to Wesson (2009) who investigated golf balls, if the launch speed is fixed and the ball is launched at 30° or 60°, the range would be about 13% less than the maximum range obtained at 45°. In the case where the launch angle is fixed at 20°, the range of a golf ball with a launch speed of 72 m s^{-1} would extend four times further compared to that with a launch speed of 36 m s^{-1}. These results signify that the launch speed has more influence on range compared to the launch angle with both parameters independent of each other.

In reality, the range would be modified once the aerodynamic forces such as drag and lift are present. The effect of drag on the range of the golf ball launched with a high speed would result in nearly 50% reduction (Wesson, 2009). Lift also affects the trajectory of a golf ball by increasing its flight range and height. These effects are shown in Figure 2.8.

In general, the ball aerodynamic effects are complex as they depend on the Reynolds number and the spin rate. In addition, the surface roughness also contributes to the

complexity. There are many studies dedicated to investigate these parameters. The effect of the Reynolds number on the flight dynamics of a sphere was earlier investigated by Achenbach (1971). It is interesting to note that even though he did not directly conduct any experiments on sports balls, his experimental works on a generic sphere (Achenbach, 1972, 1974) were widely used by sports ball researchers for reference (Bearman and Harvey, 1976; Mehta, 1985; Smits and Smith, 1994). Although some of the researchers investigate the balls using different techniques, they found similar findings: increasing the spin rate consequently results in the increment of both the lift and drag coefficients.

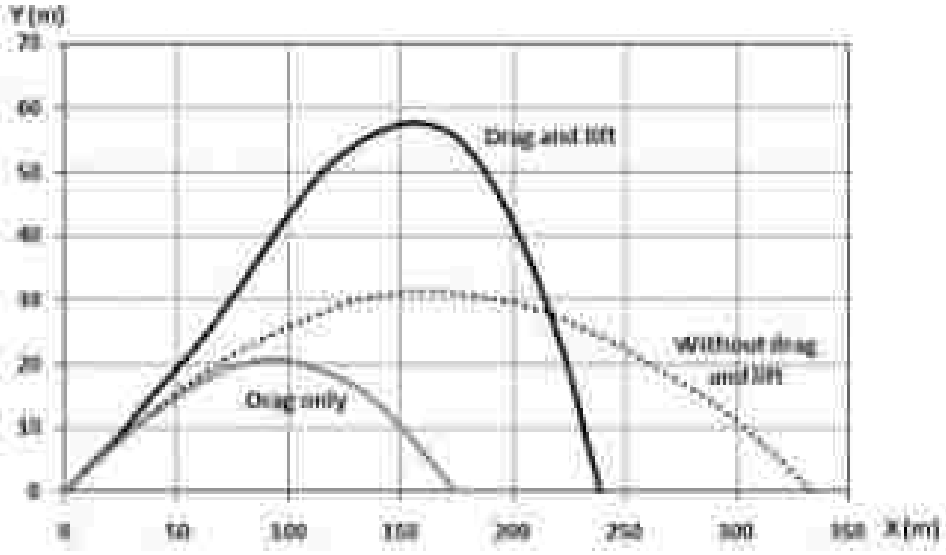

Figure 2.8: The effect of drag and lift on golf ball trajectories. Greater range occurs without the influence of aerodynamic forces. Drag has significant effect in reducing the range and lift modifies the trajectory shape (Taken from Wesson, 2009).

In 2001, Alaways and Hubbard made a compilation of sports ball data to study the influence of spin on the ball curves and lift by comparing the spin results of sphere and baseballs obtained in earlier by Maccoll (1928), Davies (1949), Bearman and Harvey (1976), Watts and Ferrer (1987). The results compare well with Watts and Ferrer (1987) which concluded that seam orientation at low spin had a significant influence on lift. However, the effect eventually decreases with increasing spin. Further study on the ball spin and lift was then conducted by Mehta and Pallis

(2001), James and Haake (2008), Carre et al (2002), Passmore et al. (2008) with extensive work on the surface roughness by Haake et al (2007). All these studies show all the parameters above (i.e. spin and roughness) have significant effect on the ball aerodynamic characteristics and subsequently influence the flight trajectory. The change in the flight trajectory ultimately modifies the range of the ball. Although most of the studies mentioned above did not relate directly the aerodynamic characteristics to the range of the balls, their results contribute to further understanding of the ball physics. This information is essential in the development of ball range study.

A study that investigates the ball range directly was conducted by Linthorne and Everett (2006). They reported that athlete musculoskeletal structure has more influence on range compared to the ball physical properties. They also found that the optimum launch angle for maximum range is lower than 45° as it is relatively easier for the athlete to launch the ball at lower launch angles. Their result agrees well with Wesson's findings (2002; 2009) on footballs and golf balls.

2.2.2 Discus

Discus is one of the oldest sports in the world that is still popular today. According to the International Association of Athletics Federation (IAAF), the men's World Record for the longest discus throw is held by Jürgen Schult in 1986 with a throw of 74.08 m, while the women's World Record is held by Gabriele Reinsch in 1988 with a throw of 76.80 m. Discus range is influenced by the release angles (Leigh et al, 2010), release speed and height (Soong, 1976; Bartlett, 1992).

Over the years, significant efforts have been made to estimate discus the optimal release conditions for maximum range (Hildebrand, 2001; Hubbard, 2002; Soodak, 2004). A comprehensive review of the discus literature is provided by Bartlett (1992). His compilation of nearly six decades of discus literature review has enabled optimization work to be accomplished in later years. In 2007, Hubbard and Cheng

successfully simulated a dynamic model for optimal discus trajectories for men and women. They found that discus range is more sensitive to the flight path angle rather than roll angle (for both genders). However, their findings did not consider the dependence of discus release speed and spin due to lack of experimental data available in the literature. This factor could possibly change the discus sensitivity result towards range. Nevertheless, their work provides substantial understanding of discus optimization.

Figure 2.9: Jürgen Schult hold the men's World Record in 1986 with a throw of 74.08 m. (Taken from German Federal Archive, 1988).

In terms of the influence of athlete throwing technique on range, Leigh and Yu (2007) correlated discus throwing performance and the technical parameters between men and women. They identified that men rely most on their physical strength to achieve the longest distance, while women depend on a specific throwing technique. Their result agrees well with Leigh et al. (2008) who found than men and women have different techniques to throw the discus effectively. Similar effort was also made by Chiu (2009) to estimate the optimal release conditions for men and women where he used a numerical simulation in different wind condition.

Recently, Leigh et al. (2010) discovered that the optimal release angle of a discus depend on each thrower. Their finding suggests that the optimal release angle of a

discus throw should be a combination of the discus aerodynamic characteristics and the thrower throwing technique. They also found that a relationship exists between the release angle and the release speed as these parameters are not independent. Based from the disc study investigated in this thesis, the author offers some insight to integrate the aerodynamics of the flying object and the athlete throwing technique with a method typically implemented in the uncertainty analysis (BSI, 2005). However, this potential method will be discussed for future work in Chapter 7 (Conclusion) as it is beyond the scope of this thesis and requires further investigations as well as interdisciplinary collaboration between the fields of aerodynamics and biomechanics for complete analysis.

2.2.3 Javelin

The javelin is another field sport with the aim to achieve the longest throwing distance. Unlike discus in which the throwing action involves a rotational motion, javelin throwing action involves over-arm throw (Bartlett, 2000). Based on the record by IAAF, the men's World Record for the longest javelin throw is held by Jan Železný in 1996 with a throw of 98.48 m, while the women's World Record is held by Barbora Špotáková in 2008 with a throw of 72.28 m.

Most research carried out to investigate the javelin and its association with maximum range is usually focused on the release speed and angle. Several studies were carried out to simulate javelin flight by using experimental data (Hubbard and Rust, 1984; Hubbard and Alaways, 1989). The results provide some important input parameters for optimal javelin trajectories (Hubbard, 1984). As anticipated, maximizing the release speed would increase the prospect of the javelin thrower to achieve maximum throwing distance. In a previous javelin study, Lichtenberg and Wills (1978) assumed that the release speed and angle is independent of each other. Although the assumption was made to simplify the mathematical analysis, it is found later on that these parameters are not independent as small deviations from one parameter leads to significant changes on another parameter and ultimately affect the

maximum range (Hubbard, 1984; Hubbard and Rust, 1984; Hubbard and Alaways, 1989; Best et al, 1995).

In parallel to the development of a javelin simulation to understand its flight characteristics and predict the optimal release angle previously, studies were also conducted to investigate the release conditions from a biomechanics perspective. This is due to the significant influence of javelin thrower technique in increasing the distance thrown. The biomechanics of javelin throw were studied comprehensively by Red and Zogaib (1977), Mero et al (1994), Zatsiorsky (1995), Morriss and Bartlett (1996) and Bartonicz (2000). Most recommendations from these studies suggest that in order to improve the throwing technique, thrower needs to focus on the muscular strength to increase the release speed. Young (2000) discovered that proximal-to-distal firing patterns and the body segments active acceleration-deceleration movement are important to increase the thrower success. He identified that this type of movement has the advantage to transfer the momentum from the lower body of a thrower to the upper body.

Recently, Chiu (2009) discovered that the javelin physical structure also plays an important role in maximizing the range. This is quite interesting as previous literature on javelin mostly focus on the release parameters, as well as the biomechanics aspect. According to Chiu (2009), the javelin throwing distance can be increased if the javelin centre of mass is located nearer to the javelin centre of pressure. This would eventually produce a smaller release angle and therefore, increases the range.

2.2.4 Shot Put

Shot-putting is another ancient sport with a similar aim to discus and javelin, but the throwing movement is confined within a circular base. In contrast to the discus or javelin, shot put is relatively heavy, with the male shot put weight at 7.26 kg and the female shot put weight at about 4.00 kg. Shot puts are heaviest compared to discus

and javelins. Therefore, the distance recorded for shot put throw is not as far as the discus or javelin. According to IAAF, the men's World Record for the longest shot put throw is held by Randy Barnes in 1990 with a throw of 23.12 m, while the women's World Record is held by Natalya Lisovskaya in 1987 with a throw of 22.63 m.

The development of shot put research mainly focuses on the biomechanics aspect particularly the shot-putting technique, as studies found that the implementation of appropriate techniques could enhance the athlete performance to throw as far as possible (Lichtenberg and Will, 1978; Hubbard, 1989; Maheras, 1995; Lanka, 2000). The focus of research in shot put literature is in biomechanics as shot put is mainly influenced by gravitational effects rather than aerodynamic drag and lift. The most common shot-putting techniques are the glide technique and the rotational technique as shown in Figure 2.10. If observed carefully, both techniques involve preliminary movements that are different but share similarity in the delivery phases.

In shot put, most studies were conducted to determine the optimal release angle. Although the effect of release angle on range is less significant compared to the effect of release speed, any deviation from the optimal release angle has significant effect on range. Shot put researchers found that the optimum release angle is usually less than 45° (McCoy et al, 1984; Bartonietz et al, 1995). Simulation models for shot put were widely developed to estimate the optimal release angle (de Mestre et al, 1998; Maheras, 1995; Hubbard et al, 2001; Linthorne, 2001). Recent shot put study by Linthorne shows similar result with Leigh et al. (2010) in discus. The study found that the optimal release angle varies with individual athlete as their decrement rate of release speed varies with increasing release angle.

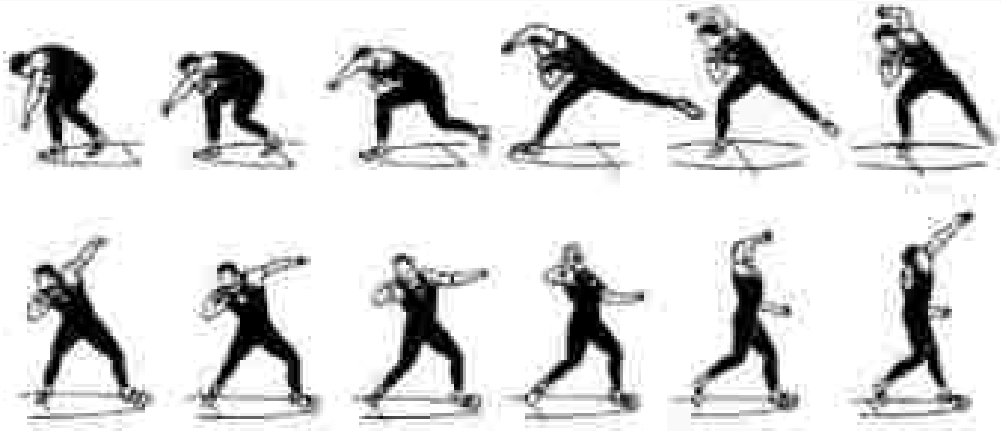

(a) The glide technique.

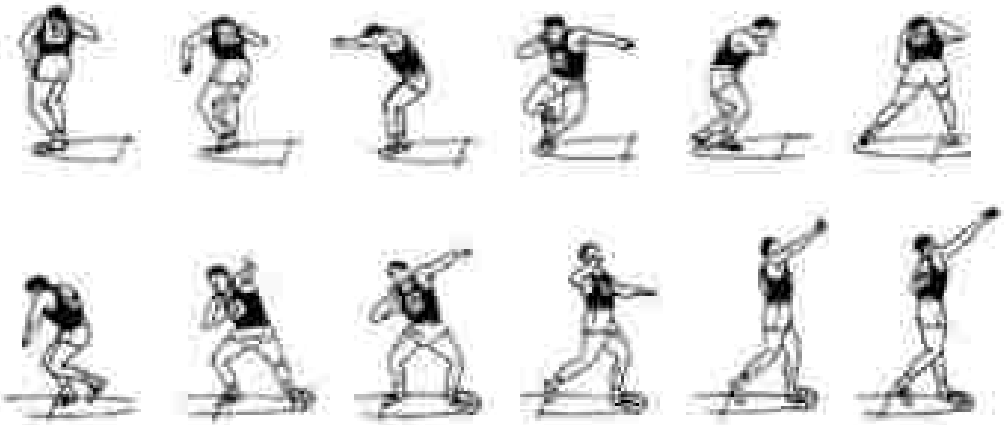

(b) The rotational technique.

Figure 2.10: The most common throwing techniques in shot-putting. The preliminary movements are different but the delivery phases are similar (Taken from Linthorne, 2001).

Chapter 3

Theoretical Background

This chapter establishes the theoretical principles relevant to disc dynamics and the fundamentals used to quantify the range and sensitivity of a flying disc. The first part lays out the background principles consist of the variables and equations used to analyse the aerodynamics and flight dynamics of a disc. Principles governing the trim and stability of the disc are given here. The second part introduces the general concept of range and sensitivity of a projectile applied on a point-mass sphere. The outline of this chapter is summarized in Figure 3.1.

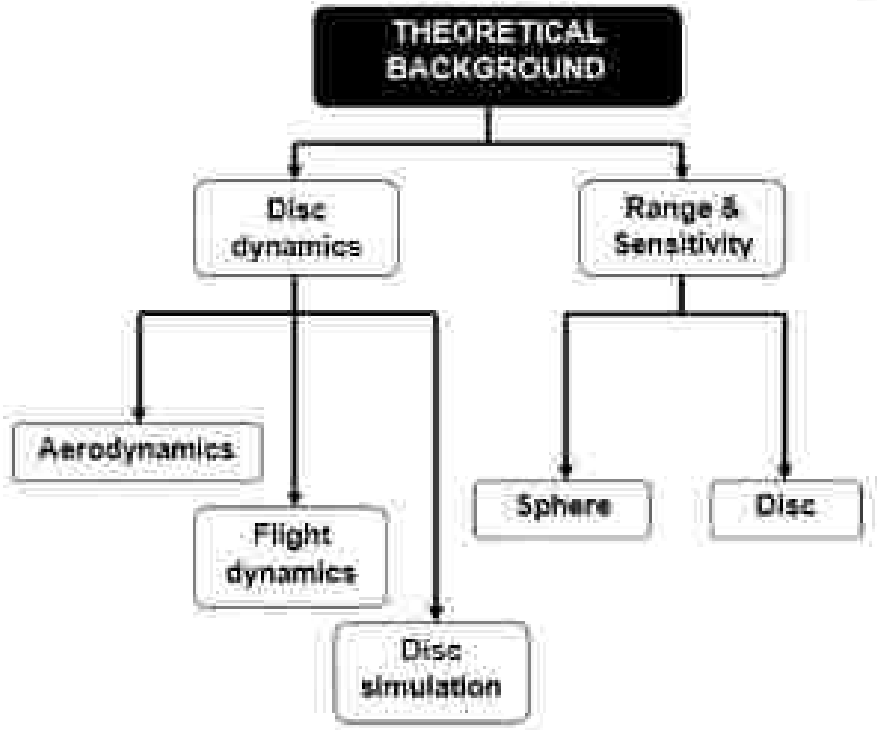

Figure 3.1: Outline of Chapter 3.

3.1 Disc dynamics

3.1.1 Aerodynamics

In a wind tunnel experiment to study the aerodynamic forces acting on a disc, the typical measured quantities are the axial (F_X), normal (F_Z), and side (F_Y) forces. The lift and drag forces on the disc are derived quantities. Figure 3.2 illustrates the aerodynamic forces acting on a disc and their relationships; α is the geometric angle of attack and V_∞ is the air speed. Coefficients of dimensionless aerodynamic forces are obtained by normalising the forces with the dynamic pressure q_∞ and surface planform area S.

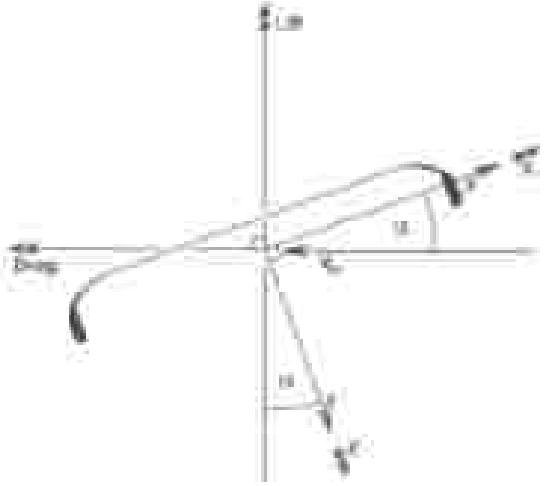

Figure 3.2: The aerodynamic forces acting on a disc (Taken from Petty, 2005).

The lift (L) and the drag(D) forces are derived from the axial and the normal forces as follows:

$$L = F_Z \cos\alpha - F_X \sin\alpha \tag{3.1}$$

$$D = F_Z \sin\alpha + F_X \cos\alpha \tag{3.2}$$

The dynamic pressure q_∞ is defined by:

$$q_\infty = \frac{1}{2}\rho_\infty V_\infty^2 \tag{3.3}$$

The coefficients for the lift, drag, axial, normal, and side forces are defined, respectively, as follows:

$$C_L = \frac{L}{q_\infty S} \tag{3.4}$$

$$C_D = \frac{D}{q_\infty S} \tag{3.5}$$

$$C_X = \frac{F_X}{q_\infty S} \tag{3.6}$$

$$C_Z = \frac{F_Z}{q_\infty S} \tag{3.7}$$

$$C_Y = \frac{F_Y}{q_\infty S} \tag{3.8}$$

The moments measured on the disc are the yaw (N), pitch (M), and roll (F_R) and their coefficients C_N, C_M, and C_R are defined as follows with d the disc diameter.

$$C_N = \frac{N}{q_\infty S d} \tag{3.9}$$

$$C_M = \frac{M}{q_\infty S d} \tag{3.10}$$

$$C_R = \frac{F_R}{q_\infty S d} \tag{3.11}$$

3.1.2 Flight dynamics

This section provides the background for the trim and stability of a flying disc. The full six-degree-of-freedom equations of motion for a flying disc based on the standard equations of motion of a rigid flight vehicle (Etkin and Reid, 1996) have been previously reported by Crowther and Potts (2007).

A disc in flight is in itself unstable in pitch without any spinning motion. Figure 3.3 illustrates the longitudinal forces and moments acting on generic tailless flight vehicles - i.e., hang gliders, delta winged aircrafts, which also includes flying discs. These types of vehicles only use a single aerodynamic surface to generate lift and provide balance and stability.

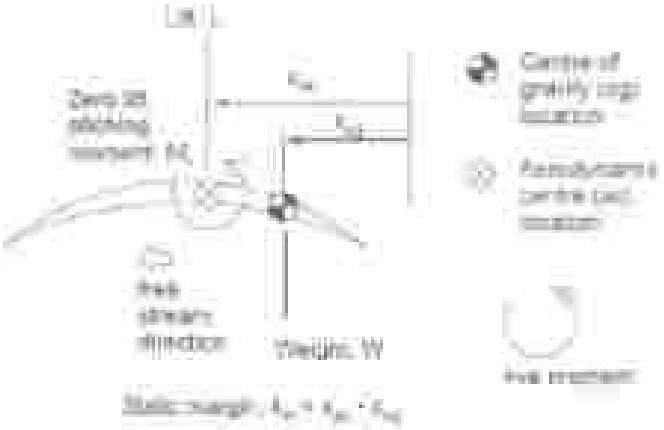

Figure 3.3: The longitudinal forces and moments acting on a generic tailless aircraft. The mass distribution is not necessarily centred at the geometric centre of this generic vehicle. (Taken from Potts, 2005).

The dimensionless balance equation for the pitching moment of the tailless configuration is given by:

$$C_{m_{cg}} = C_{m_{ac}} - C_L k_n \tag{3.12}$$

where k_n is the static margin obtained from the following relation:

$$k_n = \left(\frac{x_{ac} - x_{cg}}{d}\right). \tag{3.13}$$

The system is trimmed when $C_{M_{cg}} = 0$. In order to obtain the static margin in terms of the lift coefficient and the zero lift pitching moment coefficient, Equation (3.13) is substituted into Equation (3.12) to give:

$$k_n = \left(\frac{\frac{\partial C_M}{\partial \alpha}}{C_{L_\alpha}}\right) \tag{3.14}$$

The change in the pitching moment about the centre of gravity with respect to the lift coefficient must be negative for positive longitudinal stability. From differentiation of Equation (3.12), the static margin is given by

$$k_n = -\frac{\partial C_M}{\partial C_L} \tag{3.15}$$

Based on Equation (3.15), an unstable configuration such as that of a flying disc requires a negative C_{M_0} for balance as shown in Figure 3.4. Note that the disc centre of gravity is located at the centre of the disc. Thus, the static margin is negative as the disc aerodynamic centre is usually ahead of the centre of gravity (Potts, 2005).

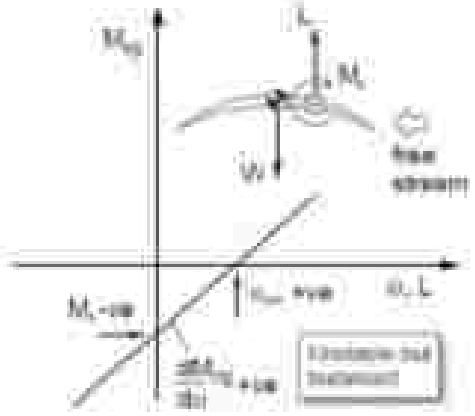

Figure 3.4: Trim characteristics of a disc as an example of a tailless flight vehicle. A disc must have a positive camber to provide balance (Taken from Potts, 2005).

3.1.3 Disc Simulation

The golf disc numerical simulation implemented in this thesis is derived from the work of Crowther and Potts (2007). Their numerical code was originally written in Matlab to simulate the flight of a Frisbee disc. In the work presented here, the Matlab program has been extended to include the capability of performing multiple simulations simultaneously; this extension allows optimization and sensitivity analyses on various flight parameters to be performed.

The core of the simulation uses a six degree-of-freedom mathematical model of a rotating disc. The gyroscopic motion associated with a spinning disc is incorporated into the model via the parameter called the Advance Ratio (*AdvR*), a dimensionless number derived from the spin rate, the disc geometry, and the flight velocity. The main assumptions built into the model are that the disc is a uniform circular cylinder of negligible height, that the disc does not wobble, and that the disc spin is constant during flight. These limitations definitely are not representative of the real situations, but do not introduce significant losses in the simulation accuracy according to Crowther and Potts (2007).

Disc Axes, Forces, and Moments

In this section, important steps in the model derivation are briefly described starting with the definitions of their axes systems (detailed mathematical formulations of these steps are referred to Crowther and Potts (2007)). Four axes systems are needed to derive the disc equations of motion. These axes are defined as follows:

1. Earth axes, $\{xyz\}_e$
2. Body axes, $\{xyz\}_b$
3. Zero sideslip body axes, $\{xyz\}_s$
4. Zero sideslip wind axes, $\{xyz\}_w$

The relationship between the earth and the body axes coordinate systems is illustrated in Figure 3.5; rotations from the earth axes into the body axes is achieved using the Euler roll (ϕ), pitch (θ) and yaw (ψ) angles. The zero sideslip body and the wind axes are illustrated in Figure 3.6. The angle of attack of the disc is achieved through a rotation from the zero sideslip body axes into the zero sideslip wind axes. The corresponding coordinate transformations between these different axes have been detailed in Crowther and Potts (2007).

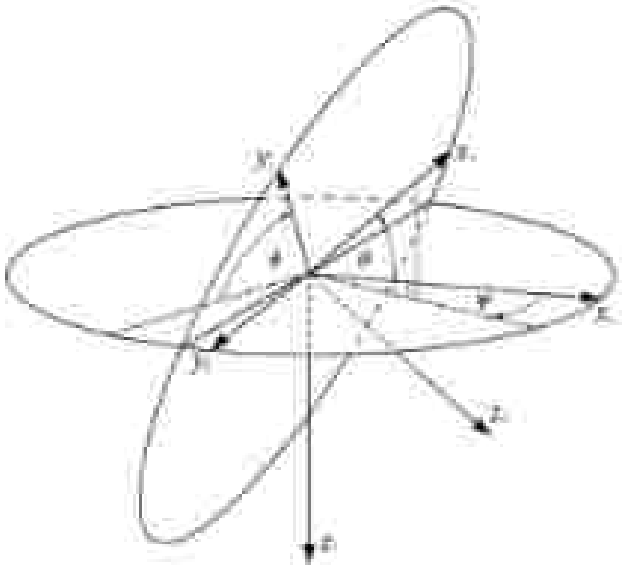

Figure 3.5: The relationship between earth axes $(xyz)_E$ and body axes $(xyz)_B$ coordinate systems defined in terms of the Euler roll (ϕ), pitch (θ) and yaw (ψ) angles (taken from Crowther and Potts, 2007).

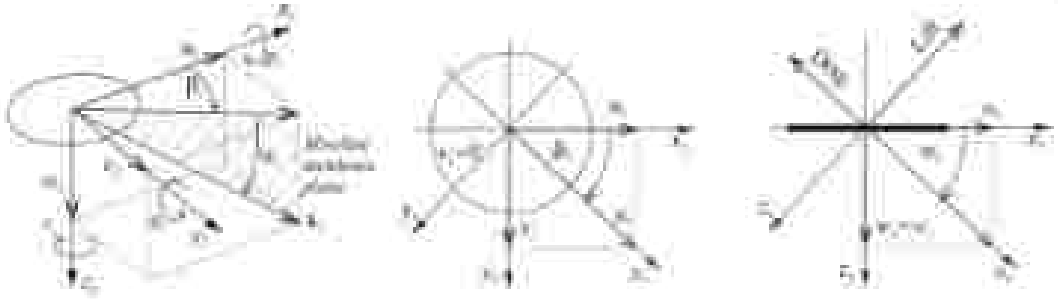

Figure 3.6: The zero sideslip body axes are obtained by rotating the body axes through the sideslip angle (β_d). The zero sideslip wind axes are obtained by rotating the body axes through the angle of attack (α_d) (taken from Crowther and Potts, 2007).

The system dynamics of the model is developed starting from the application of Newton's II Law on the disc in its body axes, where the disc linear and angular accelerations are related to the external forces and moments and its linear and angular velocities. The angular velocities, in the body axes, are the identical to the pitching (q), rolling (p), and yawing (r) rates. After transformation into the zero sideslip body axes, the aerodynamic forces and moments are rewritten as dimensionless coefficients. In this study, the values of these dimensionless aerodynamic coefficients are extracted from wind tunnel data.

The forces acting on the disc, in flight, are the gravitational force and the aerodynamic forces, which are the lift and the drag. The centre of pressure of the aerodynamic forces is located away from the geometric centre of the disc, thus resulting in a non-zero pitching moment. The aerodynamic rolling and yawing moments are negligible for the range of speeds tested in the experiments. After a simulation is performed, the main outputs are the coordinate, flight time, velocity, and acceleration of the disc centre of gravity in the earth axes system.

Gyroscopic Precession of Rotating Discs

An important aspect of the disc simulation is the coupling between the aerodynamic and the gyroscopic effects on the disc flight. This is achieved in the model by first setting the disc yaw rate (r) equal to the disc spin rate (Ω), which is assumed to be a constant. The spinning of the disc, in turn, causes the disc to precess via the gyroscopic principle whereby its pitching moment is translated into a rolling motion. The gyroscopic precession results when the spinning disc tries to resist the torque applied in a pitch (M) perpendicular to the spinning axis, but in turn manifested into a rolling motion at an angular rate p in the axis perpendicular to both the spinning and the pitching axes. This gyroscopic relation can be formally expressed in the mathematical form as

$$M = p \times I\Omega \tag{3.16}$$

where I is the moment of inertia of the disc. From the relationship in 3.16, the rolling rate is proportional to the pitching moment but inversely proportional to the spinning rate. Hence, the rolling rate can be reduced by increasing the spinning rate and/or decreasing the pitching moment. Increasing the moment of inertia of the disc can also reduce the rolling rate; one approach to achieve larger moment of inertia is by distributing the mass of the disc away from its geometric centre. Also, the spinning direction determines the direction of the rolling motion.

The entire flight dynamics of the disc are mainly governed by the aerodynamic and the gyroscopic effects, in addition to the gravitational influence. However, spinning does not affect the aerodynamics characteristics as has been investigated by Potts (2005). If one throws a disc without spinning (i.e., with zero spin rate), the nose-up pitching moment will destabilize the disc and cause it to tumble. Therefore, the disc needs to be spun to translate the pitching moment (which causes the instability) via gyroscopic precession into a rolling motion; this translation of pitch stabilizes the disc. The coupling between the pitching and rolling moments causes the disc to steer left or right depending on the spin direction. Throwing a disc in a clock-wise direction will cause the disc to bank left and vice versa.

Disc Aerodynamic Centre

The aerodynamic centre (ac) is defined as the location where the pitching moment is constant with respect to the angle of attack. For a typical airfoil, the aerodynamic centre is located at about 25% of the chord (i.e., the quarter-chord location) from the leading edge. The flow dynamics on a disc is not similar to those of a typical airfoil. As a result, the disc's aerodynamic centre is much closer to its geometric centre, or centre of gravity (cg), as opposed to its leading edge. Figure 3.5 shows the definition and a schematic location of the aerodynamic centre for a disc, which is measured with respect to the disc geometric centre.

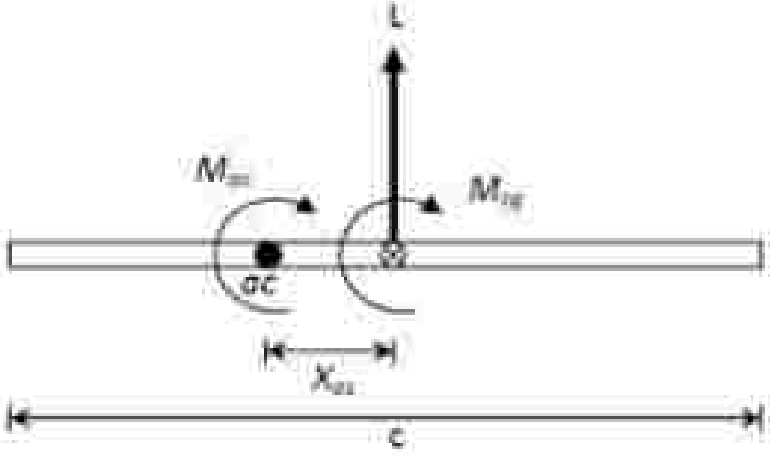

Figure 3.7: The location of the disc aerodynamic centre.

The moment acting on the disc, in its dimensionless form, is defined as below:

$$C_{M_{ac}} = C_L \frac{x_{ac}}{c} + C_{M_{cg}} \tag{3.17}$$

Differentiation of Equation 3.69 with respect to an angle of attack produces:

$$\frac{dC_{M_{ac}}}{d\alpha} = \frac{dC_L}{d\alpha}\frac{x_{ac}}{c} + \frac{dC_{M_{cg}}}{d\alpha} \tag{3.18}$$

The disc's aerodynamic centre can be calculated by recognizing that the moments at the aerodynamic centre, by definition, do not vary with respect to the angles of attack (i.e., $dC_{M_{ac}}/d\alpha = 0$); hence:

$$\frac{x_{ac}}{c} = -\left[\frac{dC_{M_{cg}}/d\alpha}{dC_L/d\alpha}\right] \tag{3.19}$$

Once obtained, the value of the aerodynamic centre is used to calculate the static margin k_n which is directly used in the simulation. In this work, the aerodynamic

centre is assumed not to vary with respect to the angles of attack (within the range studied). This assumption is supported by the experimental data of the commercial discs studied here, where the variations of their pitching moments with respect to the angles of attack are approximately linear.

On the other hand, there can be cases where different disc designs might produce pitching moments that do not exhibit linear variations with the angles of attack. For such a disc, the determination of its static margin is not as straight forward as described above as it will vary with the angles of attack. One impact of assuming a constant static margin for this disc could be a reduced accuracy in its flight simulation. However, the case of variable static margin is not explored in this thesis.

3.2 Range and sensitivity

Range is defined as the linear distance the disc travels from the launch position to the point of impact with the ground, i.e. the landing point. For the present work, it is assumed that disc is launched at ground level. The analysis in this thesis is mainly concerned with how the range is affected by the launch attitude rather than by the launch speed.

Sensitivity is defined as the partial derivative of range with respect to launch conditions (i.e. attitude and velocity). For the sensitivity analyses, this work is mainly focused on the range sensitivity with respect to launch attitude. A 'sensitive' disc will be harder to throw accurately than an "insensitive" disc because for the same level of precision in landing location, the tolerance towards a variation on launch attitude for an insensitive disc will be higher than the tolerance for sensitive disc. For example, a small variation of launch pitch angle would not affect the range travelled by a putter disc as much as compared to the range travelled by a driver disc. This behaviour may be translated into a requirement for a higher player skill level for a sensitive disc.

3.2.1 Sensitivity analysis of a spherical projectile

To introduce the concept of range and sensitivity on a disc, a theoretical formulation is devised for a simpler problem to allow us to arrive at an analytical solution; the problem is reduced to that of a flying point-mass spherical projectile under the influenced of the gravitational force only as shown in Figure 3.8. For a flying disc, the problem is less straight forward analytically due to the inclusion of the aerodynamic forces (lift and drag) acting on it. Due to this increased complexity, solutions from numerical simulations are used to calculate the sensitivity of discs analysed in this thesis.

The flight range of a point-mass sphere is a function of the launch speed V_0 and launch pitch angle θ_0, if all other launch variables (e.g. launch height and roll or yaw angles) remain fixed. The following analytical problem is simplified by assuming that the sphere trajectory is only influenced by the gravitational acceleration g.

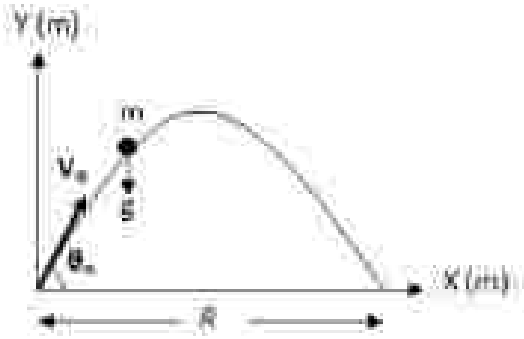

Figure 3.8. Motion of a sphere under uniform acceleration due to gravity and no aerodynamic forces.

The dimensional range R of the sphere is derived directly from Newton's 2nd Law that produce the relationship

$$R = \frac{V_0^2 \sin 2\theta_0}{g} \tag{3.20}$$

If the initial launch pitch angle is fixed and the initial launch speed is varied, the sensitivity of the range with respect to the change of initial launch speed $\frac{\partial x}{\partial v}$ derived from Equation (3.20) is given by

$$\frac{\partial x}{\partial v} = \frac{2v_0 \sin 2\theta_0}{g} \tag{3.21}$$

If the initial launch speed is fixed while the initial launch pitch angle is varied, the sensitivity of range with respect to the change of initial launch angle $\frac{\partial x}{\partial \theta}$ derived from Equation (3.20) becomes

$$\frac{\partial x}{\partial \theta} = \frac{2v_0^2 \cos 2\theta_0}{g} \tag{3.22}$$

Note that Equation (3.20) shows the dimensional sphere range. It is convenient to define a dimensionless range $\hat{R}$ by normalising the range with the gravitational acceleration and the initial launch speed as follows:

$$\hat{R} = \frac{g}{v_0^2} x = \sin 2\theta_0 \tag{3.23}$$

From Equation (3.23), it follows that the dimensionless range sensitivity of the disc with respect to the launch speed is zero while the dimensionless range sensitivity of the disc with respect to the launch pitch angle is given by

$$\frac{\partial \hat{R}}{\partial \theta_0} = 2\cos 2\theta_0 \tag{3.24}$$

A peak in the dimensionless range can be found by finding the maximum of Equation (3.23) which occurs at $\theta_0 = 45°$; this solution is universal for all point-mass projectile moving under the influence of gravity only. Simulations of the dimensional and dimensionless range and sensitivity of a sphere with respect to the

initial launch conditions are presented in Chapter 6 (Simulation Results and Discussions).

3.2.2 Disc range and sensitivity

The range of a flying disc is a function of its launch speed (V_L), its launch pitch angle (θ_L) and its launch roll angle (ϕ_L). The range could not be obtained directly as in the sphere case because analytical solutions to the disc governing equations (Crowther and Potts, 2005) are non-linear and can only be solved numerically.

The definitions of the range sensitivity with respect to changes in either the launch speed, the launch pitch angle, or the launch roll angles are defined as $\frac{\partial x}{\partial V_L}$, $\frac{\partial x}{\partial \theta_L}$, or $\frac{\partial x}{\partial \phi_L}$, respectively. If all of the launch parameters are allowed to vary within a small tolerance, then the resulting overall sensitivity of the disc range dR_{disc} can be combined as

$$dR_{disc} = \sqrt{\left(\frac{\partial x}{\partial V_L} dV_L\right)^2 + \left(\frac{\partial x}{\partial \theta_L} d\theta_L\right)^2 + \left(\frac{\partial x}{\partial \phi_L} d\phi_L\right)^2}. \qquad (3.25)$$

The relationship above is derived using the standard method for determining the overall uncertainty of a collection of independent variables, each having an uncertainty of its own (BSI, 2003).

Chapter 6 (Simulation Results and Discussions) presents the simulation results for the range sensitivities of two discs – putter and driver discs – to compare between the short and long range golf discs. The results are used to demonstrate the use of range sensitivities in determining the accuracy of a throw. Dimensionless launch speed V^* is used in Chapter 6 to compare discs with a fixed diameter d at varying launch speeds; V^* is obtained using the Buckingham Pi Theorem as

$$v^* = v_c / \sqrt{gR} \tag{3.26}$$

The disc flight time, t, is normalised by the total flight time, T_{max}, to provide a dimensionless comparator as each disc has a different flight time such that the non-dimensional time is given by:

$$t^* = \frac{t}{T_{max}} \tag{3.27}$$

Chapter 4

Methods

This chapter presents the experimental method performed on a generic set of parametric discs and commercial golf discs to measure aerodynamic loads in the wind tunnel. The experimental apparatus and disc model configurations are described including measurement techniques (i.e. surface flow visualisation) and uncertainties. This chapter also presents the computational method implemented to simulate flight trajectories and range of golf discs. The numerical simulation code, written in MATLAB and developed by Crowther and Potts (2007) uses wind tunnel data as the aerodynamic inputs. The outline to illustrate this chapter is shown in Figure 4.1.

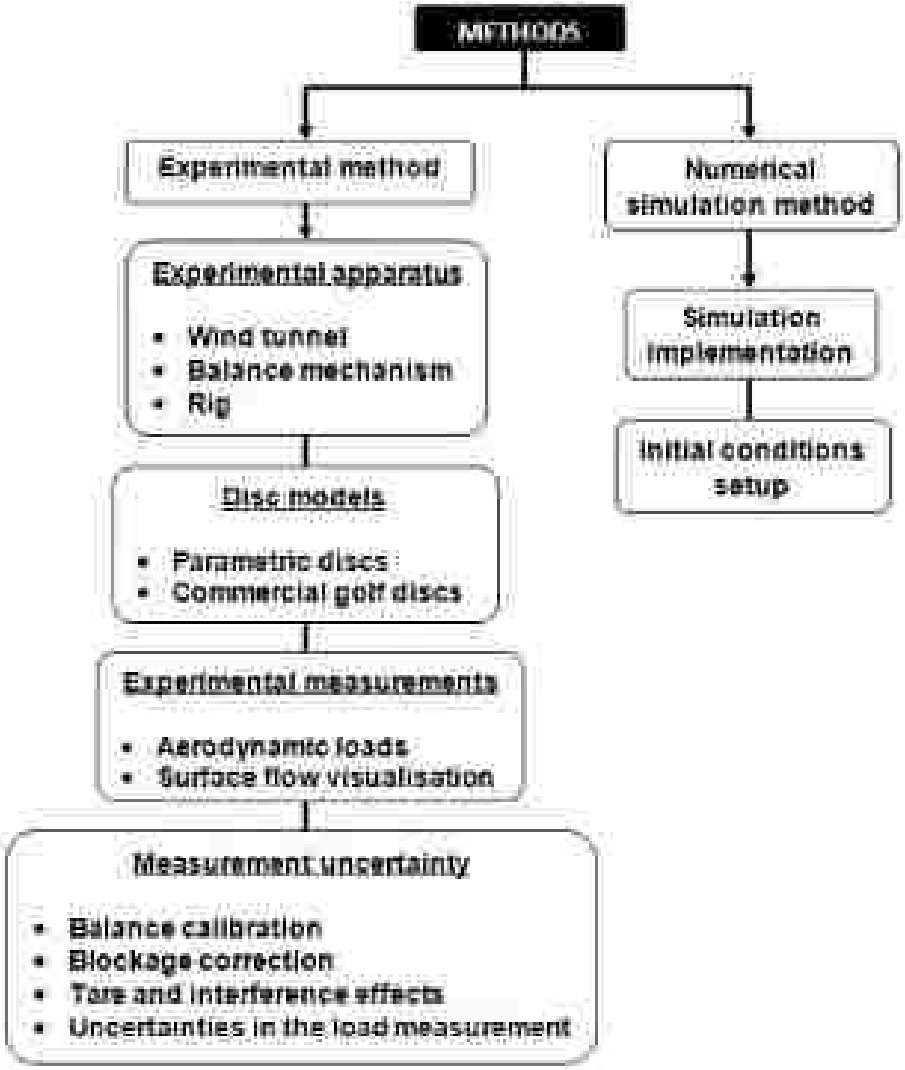

Figure 4.1: Outline of Chapter 4.

4.1 Experimental Method

4.1.1 Experimental Apparatus

Wind Tunnel

The experiments were performed in the 0.9 m x 1.1 m octagonal test section of the open circuit low speed Project Wind Tunnel at the University of Manchester's Goldstein Research Laboratory in Barton (this site is now closed and the tunnel moved to the main university campus). The wind tunnel has a top speed of 50 m s^{-1} with turbulence level of around 0.5%, and is equipped with a six component overhead balance. Preliminary tests suggest the load data for the disc model were independent of Reynolds number over a speed range of 10 m s^{-1} to 30 m s^{-1}. Therefore, in order to allow comparison with previous wind tunnel testing performed by Potts (2005), experiments were conducted at a fixed Reynolds number of 3.75×10^5 corresponding to a speed between 22 m s^{-1} to 27 m s^{-1} depending on the disc diameters. The wind tunnel operation was monitored from a control room. An overview of the wind tunnel facility with an illustration of the test section is shown in Figure 4.2 and Figure 4.3.

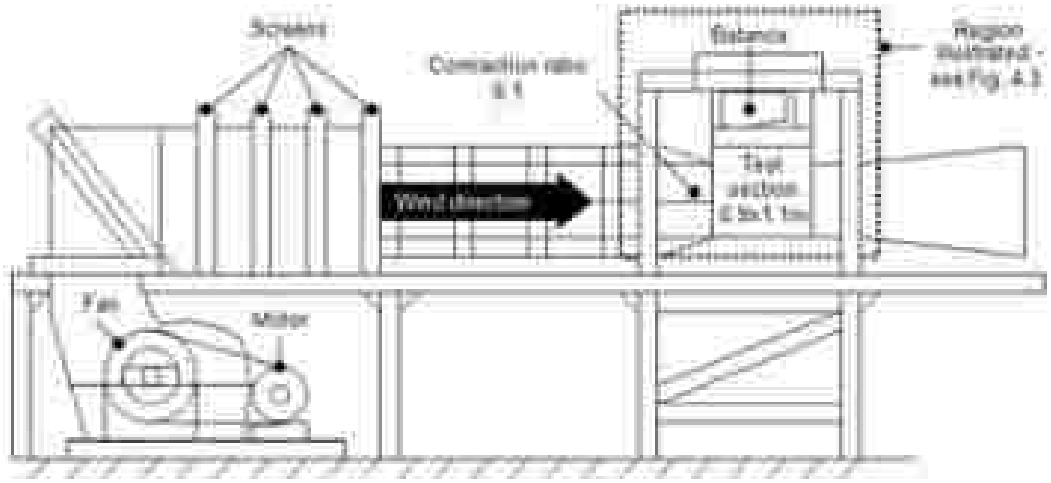

Figure 4.2: Diagram of the Project Wind Tunnel facility at the Goldstein Research Laboratory of the University of Manchester in Barton.

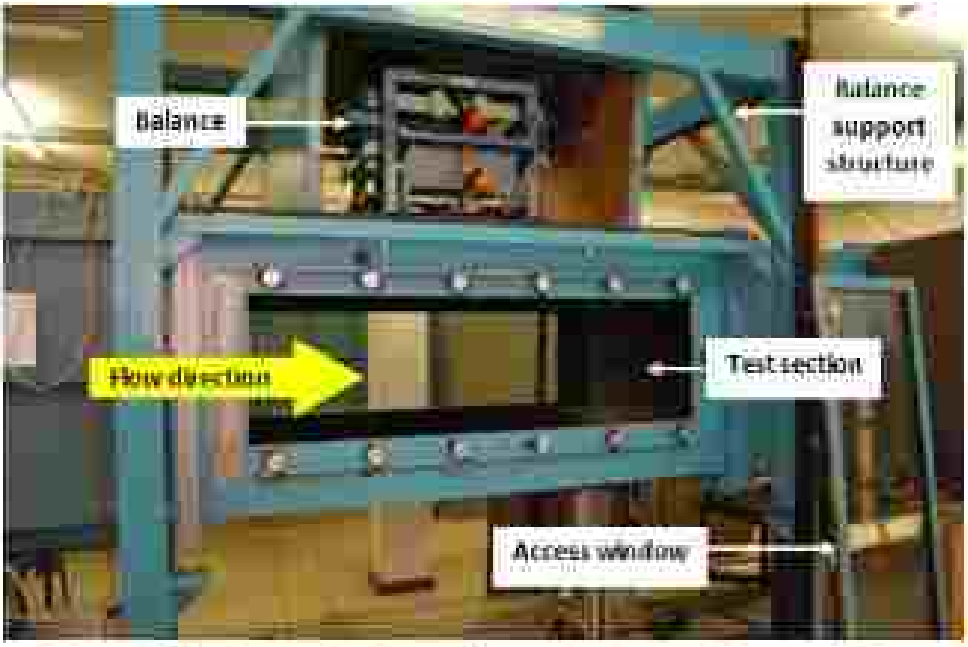

Figure 4.3: A photograph of the working section in the wind tunnel facility.

Balance mechanism

Images of the wind tunnel balance manufactured by Elven Precision Ltd (model 158) are shown in Figure 4.4. The overhead six component balance used in this study measured the forces and moments accurately. The balance consists of an earth frame mounted on a round turntable which allows it to yaw with respect to the vertical axis test section. Figure 4.4 illustrates the view of the balance frame bolted at the centre of the turntable. The turntable was built-in to the test section roof and can be rotated through 360°. The rotation was performed to allow strut adjustment to the balance 'T'-beam, particularly for load measurements. In order to avoid excessive loading due to the weight distribution of the model or rig, the moments and forces frame were locked to the earth frame when the disc was being fitted or adjusted to the balance. The loads should not exceed the maximum allowable loads on the balance as provided in Table 4.2 in Section 4.1.4. The detailed configuration of the balance frame bolted to the turntable is shown in Figure 4.4 (c).

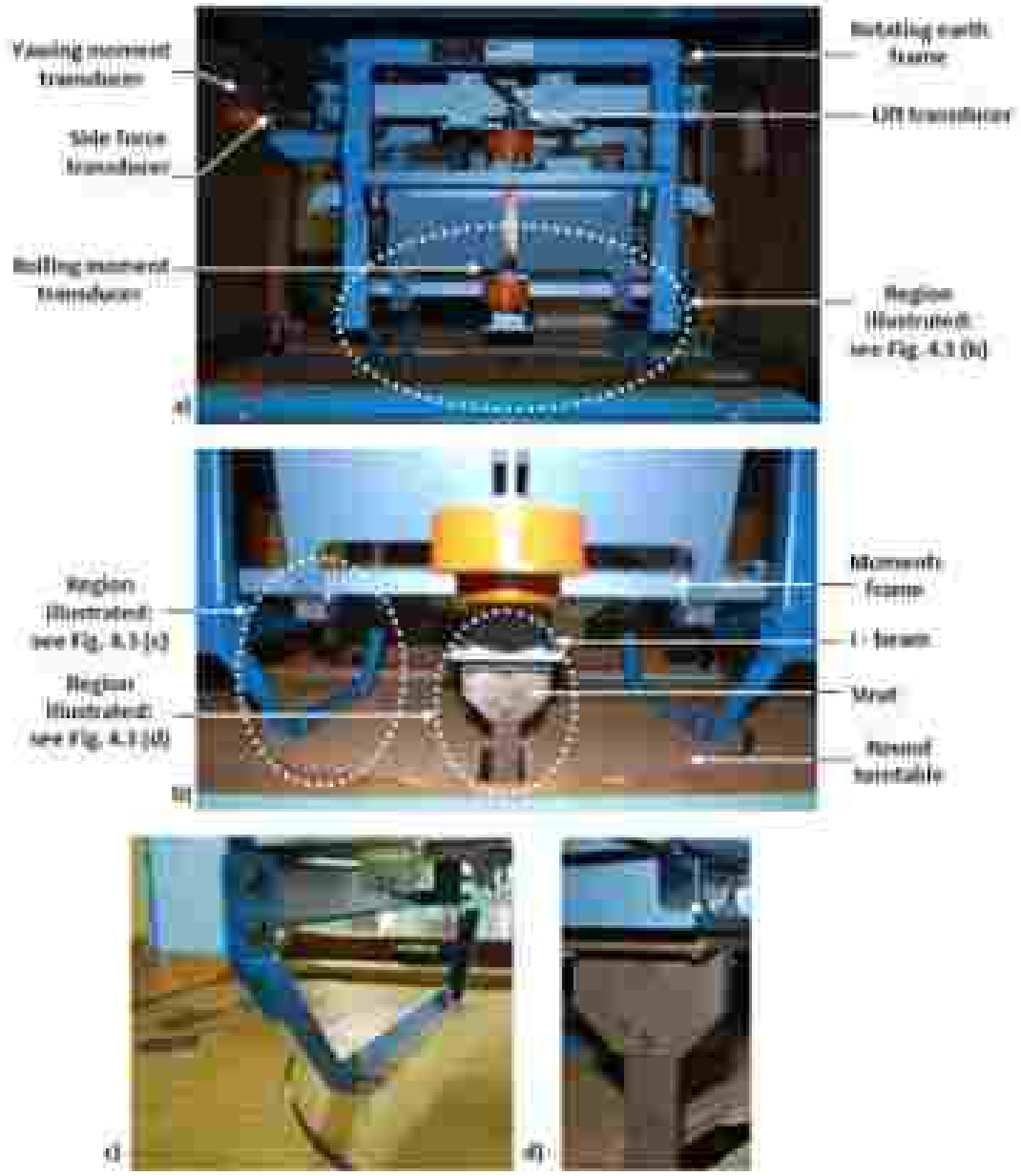

Figure 4.4: (a) Illustration of the wind tunnel balance from the side. Drag and pitch transducers are hidden on the other side. (b) Overview of the round turntable and strut bolted to the balance frame. (c) View of the round turntable connected to the balance. (d) View of the strut screwed to the balance I-beam.

Rig

There were two types of rig used in the experimental work: a primary rig for aerodynamic load measurements and a secondary rig for surface flow visualisation. These rigs were previously used by Potts and Crowther (2000) in their wind tunnel testing. For the primary rig, the disc models mounted in the wind tunnel test section were static and mounted vertically on a horizontal axle supported by a vertical strut as shown in Figure 4.3. The vertical strut was bolted onto the I-beam of the balance. Due to the unconventional mounting arrangement of the disc model, the disc pitch angle was varied by rotating the balance about its vertical (yaw) axis. An electric motor and gear box controlled the incidence and yaw angles as illustrated in Figure 4.5. The tunnel speed and the model incidence angle were slowly changed during testing to avoid overloading the balance. An image of the test section for aerodynamic load measurement setup is shown in Figure 4.6.

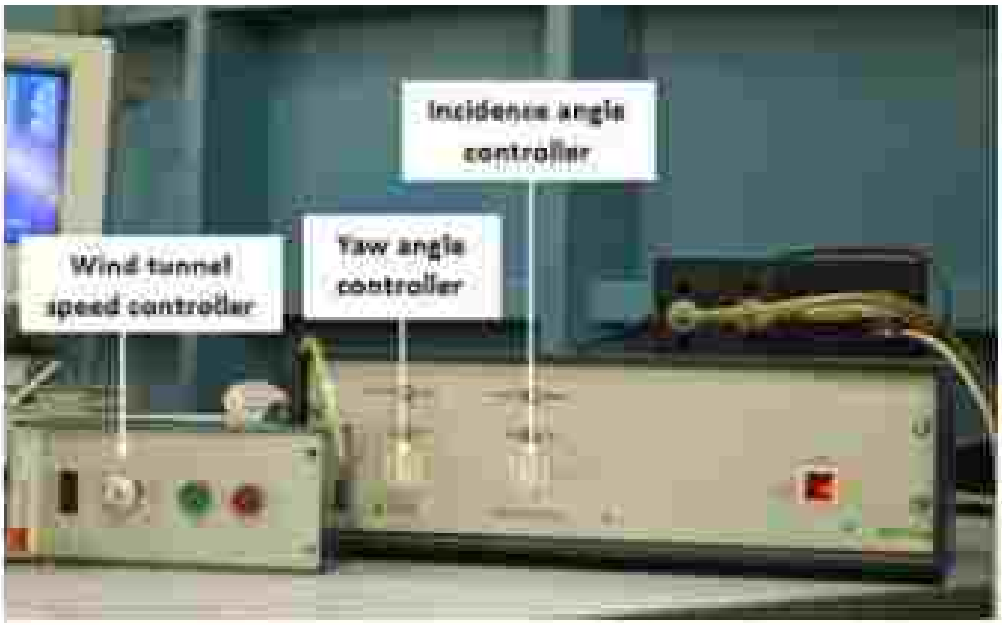

Figure 4.5: The balance yaw angle controller used to vary the disc pitch angle for aerodynamic load measurement and the balance incidence angle controller used to vary the disc incidence angle for surface flow visualisation.

Figure 4.6: Load measurement rig setup in the test section.

The secondary rig was used for surface flow visualisations as shown in Figure 4.7. The disc model was mounted in the horizontal between two vertical struts. An incidence arm was used to adjust the disc pitch angle. In addition, an inclinometer was placed on the model and balance to check the respective incidence angle. This was performed to reduce errors associated with misalignment when the model was attached to the strut and balance.

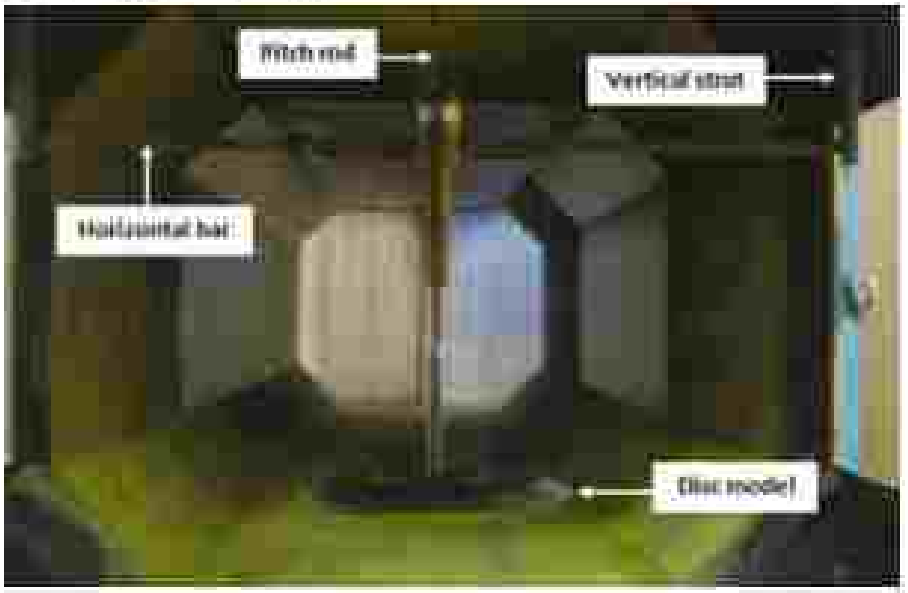

Figure 4.7: Flow visualisation rig setup in the test section.

4.1.2 Disc Models

Parametric Disc Models

The parametric disc configurations were designed using Solid Works 2007 and manufactured using ABS (*Acrylonitrile butadiene styrene*) plastic material with 0.2 m diameter and 0.02 m thickness (thickness-to-diameter ratio, $t/d = 0.1$). There were initially 17 disc models manufactured to investigate the disc geometric variation including 3 circular flat plate discs made from aluminium used to study the thickness variation (all others were ABS). However, only 12 selected disc models are presented in this thesis due to their significant results. The geometric variation was grouped into 4 categories:

- Thickness
- Rim edge curvature
- Camber
- Cavity

The geometric variations were categorized into four categories to serve two purposes; firstly, to isolate the disc design features in order to understand the effect of various design parameters, and secondly, to evaluate the design geometry and understand how the aerodynamic performance varies for different disc geometries.

The basic geometric definitions are shown in detail using schematic representations. The cross section view of the disc models are presented in Figure 4.8 to Figure 4.11. A circular flat disc with thickness-to-diameter ratio of 0.1 was used as a baseline for comparison in each test. In order to facilitate the load and surface flow visualisation investigation, careful attention was given to the surface finish. This was achieved by polishing the models with a minimum of 1000 grade wet and dry abrasive sheet, and spraying with matt black paint.

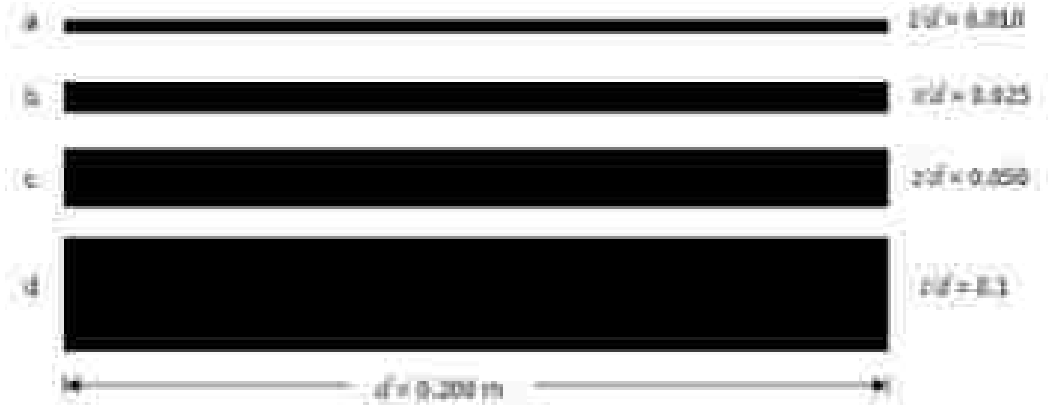

Figure 4.8: Parametric disc models constructed to study the effect of thickness.

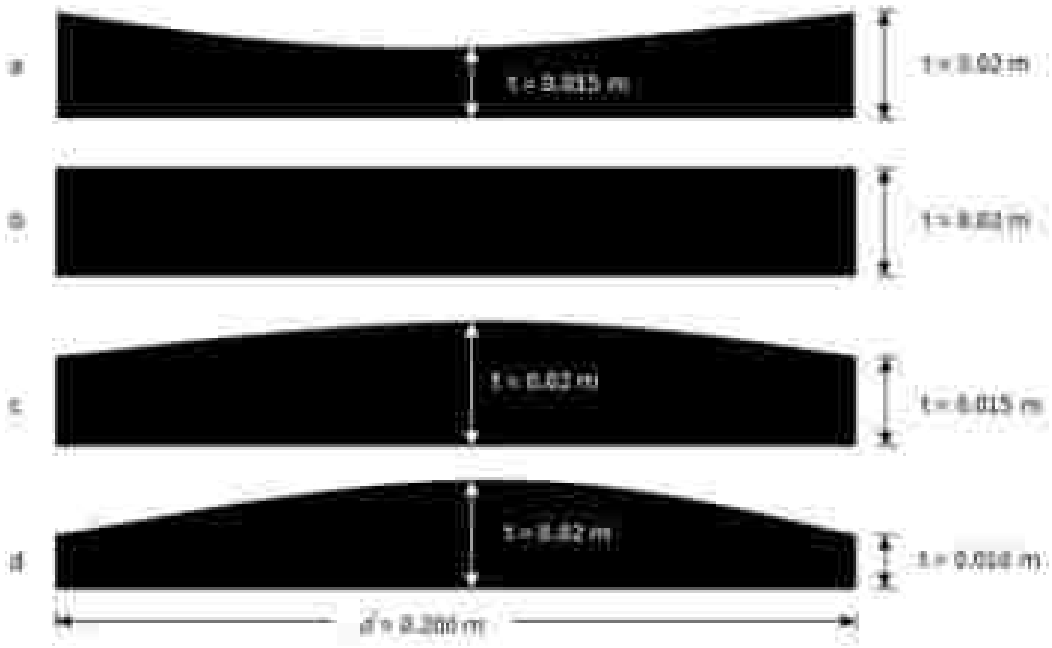

Figure 4.9: Parametric disc models constructed to study the effect of camber.

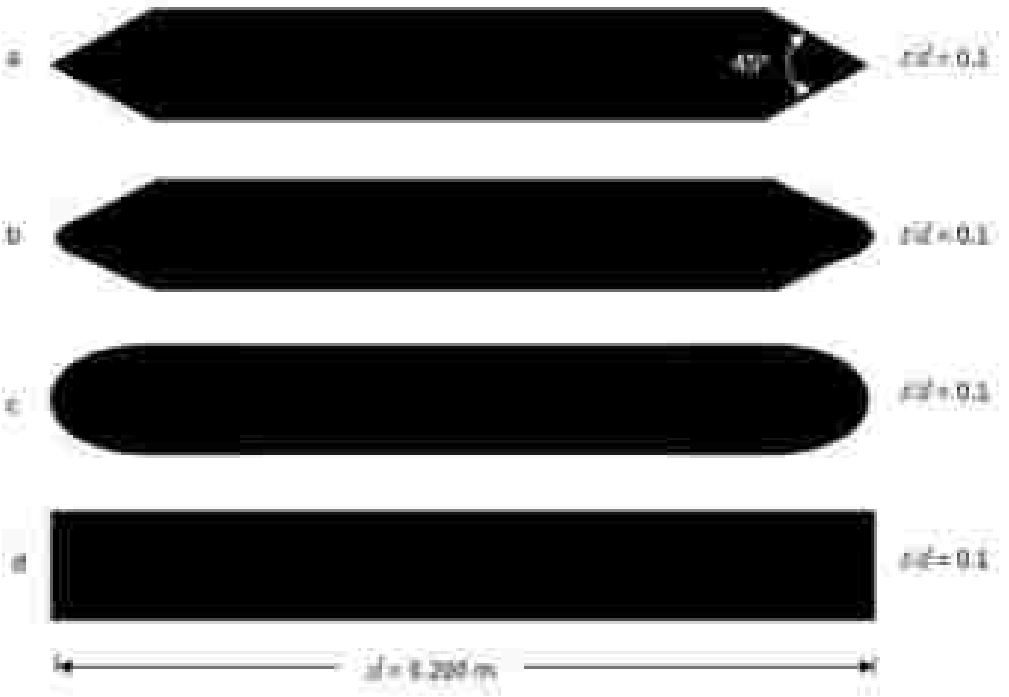

Figure 4.10: Parametric disc models constructed to study the effect of edges curvature.

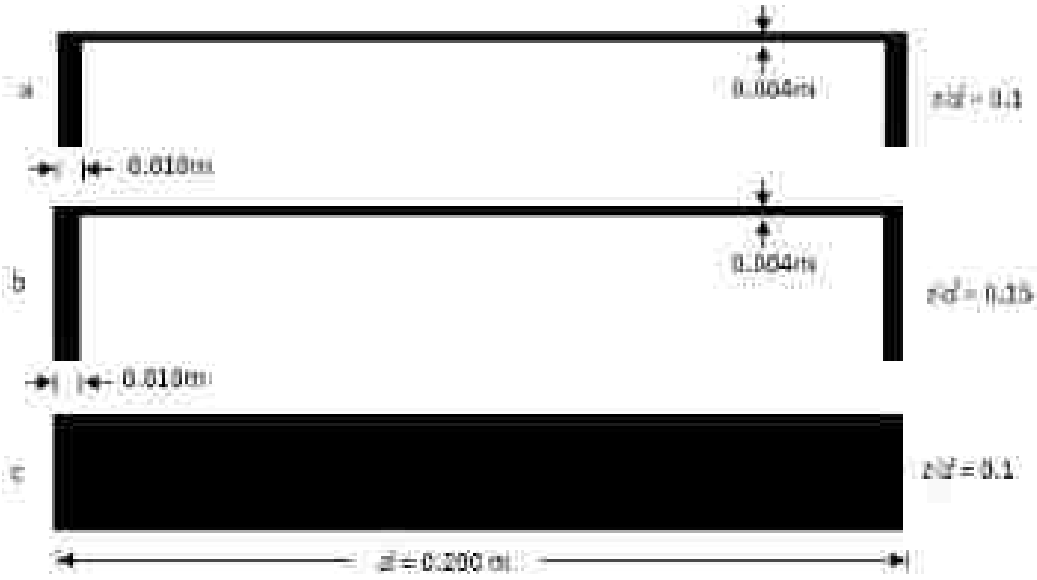

Figure 4.11: Parametric disc models constructed to study the effect of cavity.

Commercial Golf Disc Models

The commercial golf disc models used for the experiments were selected based on their distinctive geometric design to represent typical commercial golf disc models widely used in the sport of disc golf. The models were in their original form, except that the thin wall section of the central part of the plastic models was stiffened with carbon fibre underneath the cavity to prevent them from deforming during the wind tunnel testing. Note that a flat plate disc with thickness-to-diameter ratio of 0.01 was used as a baseline for comparison in this case. In general, typical golf disc geometry can be defined as follows:

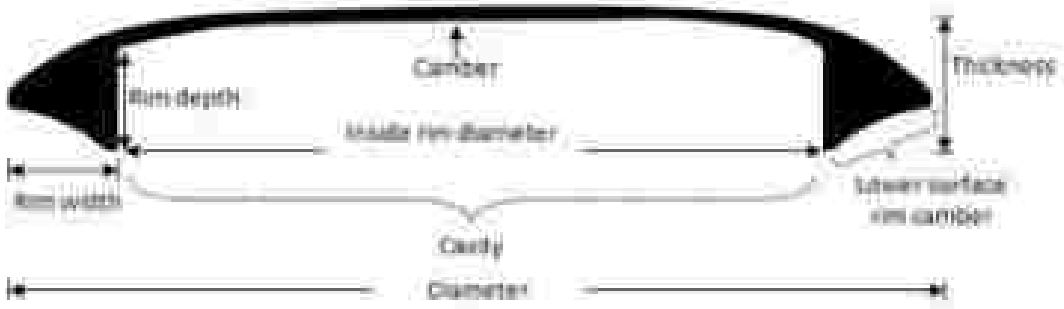

Figure 4.12: Schematic view of a typical golf disc profile geometry.

- **Diameter**: the distance through the disc centre from the leading edge to the trailing edge.
- **Thickness**: the maximum distance between the disc upper and lower surfaces.
- **Rim width**: the distance between the disc outer and inner edges of the rim.
- **Rim depth**: the distance between the disc inner edges of the rim.
- **Camber**: the curve that is halfway between the upper and lower surfaces of the aerofoil (in this case the disc cross-section).
- **Cavity**: the hollow area within the disc.
- **Inside rim diameter**: the distance across the disc cavity.
- **Lower surface rim camber**: the disc rim width curve camber.

The commercial golf disc models used for the experiments with their commercial company's name are shown in Table 4.1.The full cross-sectional profiles of the commercial golf discs are shown in Figure 4.13.

Model	Full cross-sectional profiles
Aviar	
Roc	
Buzz	
Wraith	
Flick	
Quarter K	

Figure 4.13: Schematic view of commercial golf discs full cross-sectional profiles focussing on the rim edge curvatures that vary in between discs.

Model	Manufacturer	Type	Diameter (m)	Thickness (m)	t/d	Inside rim diameter (m)	Rim width (m)	Rim depth (m)
Aviar	Innova Champion Discs Inc.	Putter	0.212	0.020	0.094	0.194	0.009	0.015
Roc	Innova Champion Discs Inc.	Mid-range	0.212	0.020	0.094	0.194	0.009	0.012
Buzz	Discraft Inc.	Mid-range	0.217	0.019	0.088	0.193	0.012	0.013
Wraith	Innova Champion Discs Inc.	Driver	0.211	0.014	0.066	0.169	0.021	0.012
Flick	Discraft Inc.	Driver	0.211	0.013	0.062	0.169	0.021	0.011
Quarter K	Discwing Ltd.	Driver	0.213	0.020	0.094	0.167	0.023	0.014

Table 4.1: The properties of commercial golf discs.

4.1.3 Experimental Measurements

Aerodynamic Loads

Load measurements were performed to analyse the disc aerodynamic characteristics, due to the large amount of disc models tested in the wind tunnel. The angle of attack for the load data was varied from -5° to 15° with 1° increments. These angles were chosen as from the simulation data for a typical disc throw, the percentage of trajectory for which the angles of attack is usually larger than 0° and less than 15° (with conventional higher aspect ratio wing, there is usually a clear stall and hence, it is more defined over the common angles of attack ranges the data should be plotted). The operating Reynolds number was fixed at 3.78×10^5 corresponding to a speed of 27.5 m s^{-1} for parametric discs and 22 m s^{-1} to 27 m s^{-1}depending on the commercial golf disc diameters unless stated otherwise. (Note that the disc pitching moment is measured as the torque about the half chord position, rather than the conventional quarter chord position as in the case of an aircraft).

The general procedure to run the wind tunnel to obtain the loads data is described as follows. The disc models were attached to the support strut and set at the required angle of attack by rotating the balance turntable. The turntable was locked safely and the balance was zeroed. The wind tunnel was run up to the required speed and the initial load data were acquired. The raw data from the balance transducers were passed through a 16-channel, analogue-to-digital (A/D) converter. The output from the converter was then fed into a computer. The load data is stored in three forms: pure forces and moments in N or Nm, aerodynamic coefficients and a sample average in counts. The tunnel speed and the disc incidence angles were also recorded. The wind tunnel was then stopped and the overall procedure was repeated for the next disc models.

All tests were repeated at least three times to ensure consistency of the results. In order to maintain good repeatability and avoid overloading the load transducers,

extra care was performed as the disc models were removed and during fitting of the disc model to the balance beam. A small movement or vibration could results in a large change of output volts and therefore, it is vital to ensure accurate load measurements. The load tolerance associated with the balance is carried out in Section 4.1.4.

Surface Flow Visualisation

Surface flow visualisation is a valuable method to support the aerodynamic load analysis, by providing information about the flow characteristics around the disc. However, in this thesis, the surface flow visualisation was only performed on selected parametric discs and commercial golf discs (the selection was based on the distinctive disc configurations focusing on the basic geometry).

The surface flow visualisation paint mixture consists of two parts of kerosene and one part fluorescent powder. The mixture was painted to the surface of the disc model using a paint brush as shown in Figure 4.14. In order to prevent any non-dissolved paint mixture particle from forming which could disrupt the flow, oleic acid was added to dilute the mixture. The paint mixture was then applied with brush strokes parallel to the flow direction to avoid any residual brush marks. To visualise the flow pattern, the painted disc model was mounted in the test section until the kerosene evaporated. Then, the disc model was removed from the wind tunnel test section and photographed. A pair of ultra violet strip lights were used to illuminate the flow pattern whilst a camera was positioned facing the centre of the disc model.

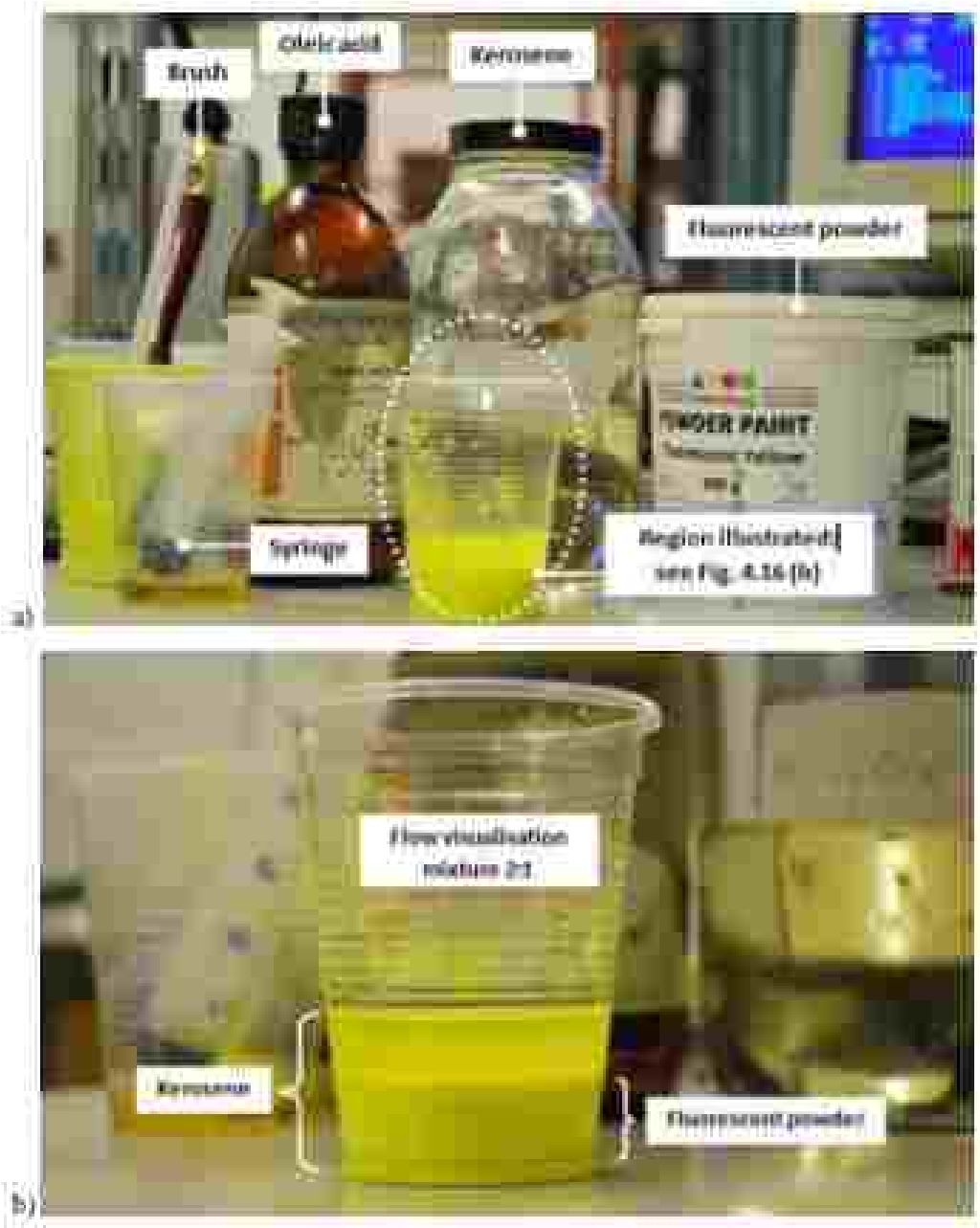

Figure 4.14: (a) Illustration of the flow visualisation chemicals. (b) Ratio of kerosene and fluorescent powder mixture.

4.1.4 Measurement Uncertainty

The results presented in this thesis had already taken into account the measurement uncertainty to ensure the accuracy of the experimental results. The wind tunnel measurement system was calibrated to ensure accurate and reliable experimental results. Uncertainty estimates for results presented in this thesis are made at a confidence level of 95% based on the British Standard Institutes - Guide to the Expression of Uncertainty in Measurement (2000).

Balance calibration

The balance was calibrated to ensure the load data obtained in the experiments was accurate. An 'X' calibration frame comprising a pair of calibration strut, pulley, weight hanger, pulley base and a calibrated weight set were used to perform the balance calibration. A tunnel centre line was scribed on the test section floor to ensure the pulley base was aligned precisely. In order to load the balance drag component, a pulley was aligned extending out from the 'X' frame as shown in Figure 4.15 (a). A calibrated weight was applied to the weight hanger lining vertically from the pulley. As more calibrated weights were applied, an inclinometer was placed on the tee frame centre to ensure the tee frame remain in the level position throughout the calibration process. The balance lift, yaw, pitch, roll and side component were loaded similarly in respective direction to the drag component as described above. This setup follows the standard procedure outlined by Barlow et al (1999). The maximum allowable loads on the balance, with the sensitivity of the system in each degree of freedom are shown in Table 4.2.

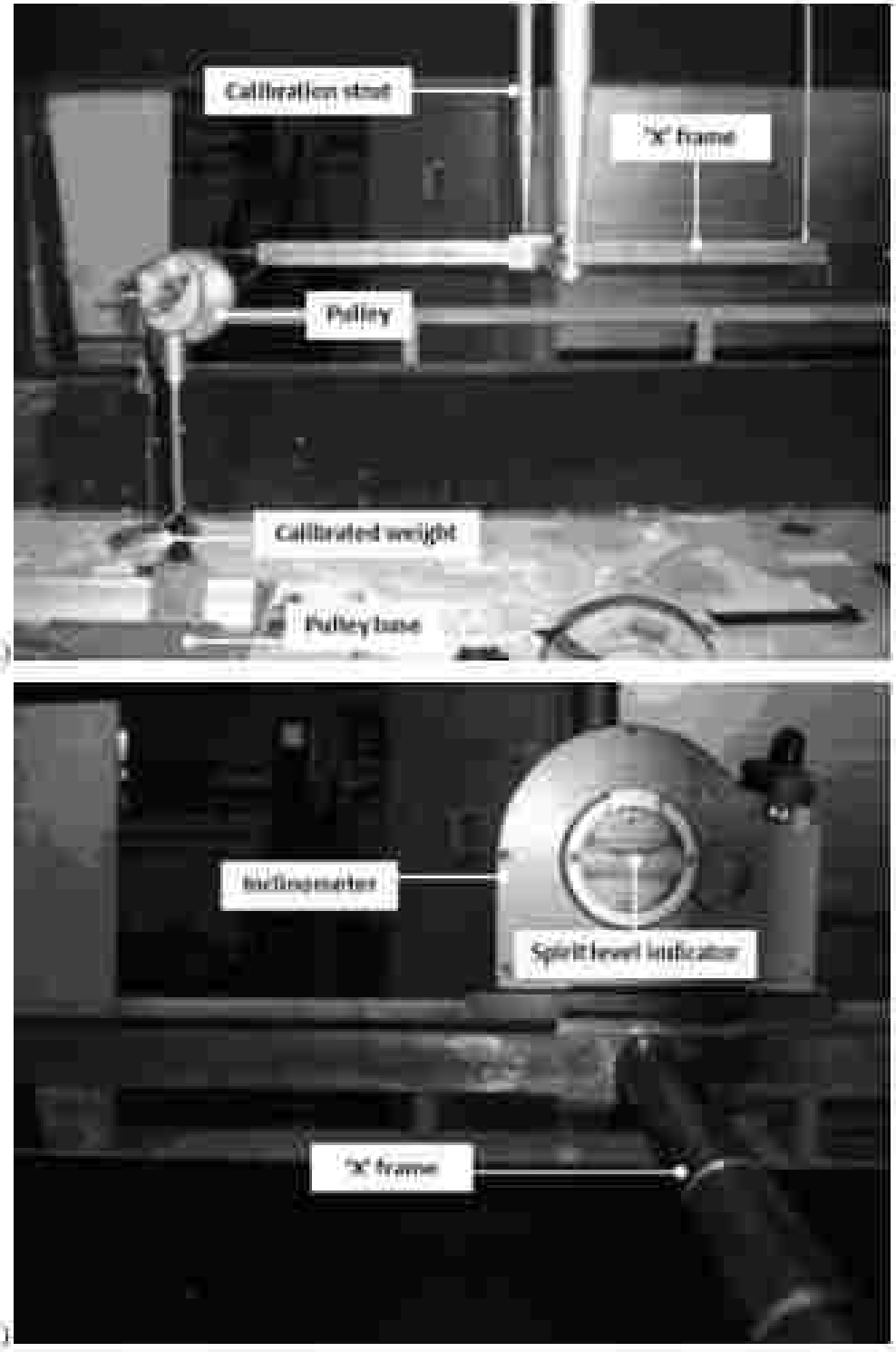

Figure 4.15: (a) Illustration of the drag calibration setup. (b) View of the inclinometer used to check the frame is level.

Force/Moment	Range	Accuracy (Percentage of full range)
Lift	0 to 200 N	± 0.10
Drag	0 to 67 N	± 0.10
Side force	± 135 N	± 0.25
Rolling moment	± 3.5 Nm	± 0.25
Pitching moment	± 11 Nm	± 0.10
Yawing moment	± 3.5 Nm	± 0.25
Incidence	±40°	± 0.08
Yaw angle	-115° to +225°	± 0.06

Table 4.2: Wind tunnel balance ranges and tolerances.

Blockage correction

This thesis applied the Maskell's method suggested by Barlow et al (1999) for blockage correction. The blockage for the range of angles of attack tested in the experiment is considered negligible, consistent with Potts (2005) who applied a similar method. Since it is negligible, corrections due to blockage effect have not been applied to the wind tunnel results.

Tare and interference effects

The strut tare and interference effects were measured using the method recommended by Barlow et al (1999). The strut tare is the direct drag resulting from the direct exposure of the support system to the flow. The interference is the result of the disturbance of the flow on the model cause by the presence of the support system. The dummy strut identical to Potts (2002 (b)) was attached to the balance turntable acting as a mirror image of the main support strut (Figure 4.16). Total tare and interference effects estimated for the experiment were approximately less than 2% change in the drag measured. Since the value is considerably small, corrections due to the strut tare and interference effects have not been applied in the wind tunnel results.

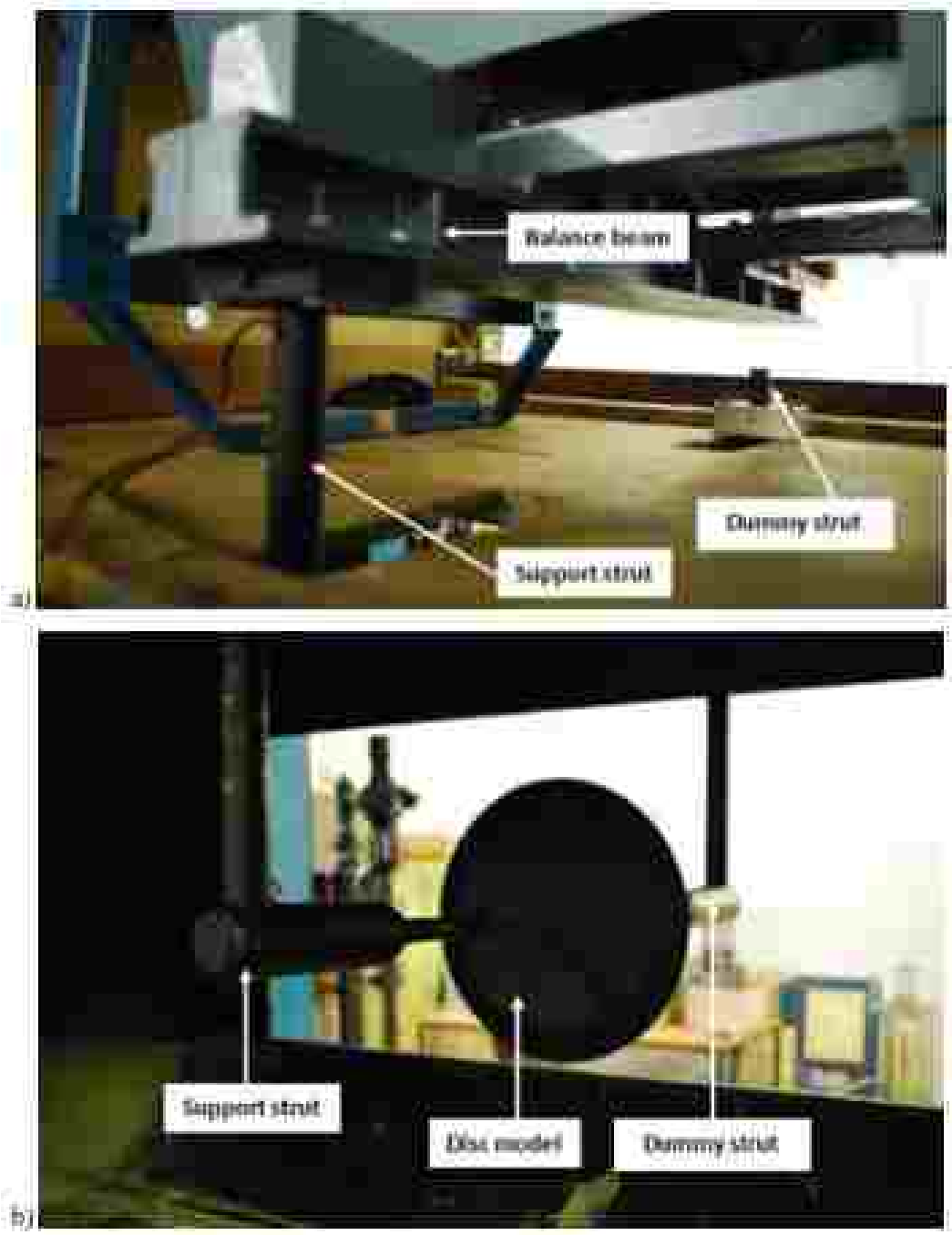

Figure 4.16: Illustration of the strut tare and interference effects. (a) View of the support strut bolted to the balance beam and dummy strut bolted to the turn table.

Uncertainties in the load measurement

The individual errors associated with the calibration process have been considered appropriately before the total uncertainty can be established. The total error for the measurement of load was ± 0.3%, which is an acceptable level of error.

4.2 Numerical Simulation Method

4.2.1 Simulation Implementation

The disc flight simulation was based on the standard equations of motion for a rigid flight vehicle (Etkin and Reid, 1996). Simulation code developed by Crowther and Potts (2007) was implemented with some modification to simulate different disc geometries simultaneously. The modified simulation code uses the ODE23s solver in MATLAB 7.11. For comparison, the modified simulation code uses the golf discs wind tunnel data as inputs to simulate the flight trajectories of short, medium and long range discs. Further reference on the derivation of the disc equations of motion can be referred to Crowther and Potts (2007).

4.2.2 Initial conditions setup

The flight trajectory simulation in this thesis only considers the range as a function of launch pitch angles (θ_L). The advance ratio (AdvR), defined as the ratio of the disc's rim speed to that of the free-stream, is fixed at 0.5. The value represents an approximate typical value widely used by player in real life (Potts, 2005; Nathan, 2008). For each disc, the mass and radius were set to 0.177 kg and 0.107 m, respectively. As range is proportional to the square of launch speed, and each player is assumed to have a maximum achievable launch speed, the launch speed in this analysis is fixed at $V_L = 20$ m s^{-1} with default initial conditions as follows: φ_L, α_L, ψ_L = $[0\ 0\ 0]^0$ unless stated otherwise. Note that the launch kinetic energy also was fixed since mass is approximately constant. The launch position was fixed at (0, 0).

Chapter 5

Experimental Results and Discussions

This chapter presents and discusses experimental results obtained from aerodynamic loads measurement performed on a set of generic parametric discs and a set of commercial golf discs. The main objective of the work is to understand the influence of disc geometric parameters on aerodynamic characteristics, particularly the effect of thickness, rim edge curvature, cavity and camber. A comparison of flat plate data with finite wing theory will also be presented to establish the fundamental understanding of low aspect ratio wings. The result gathered from this study has established the mapping between the disc geometry and aerodynamics (i.e. disc thickness is proportional to drag). The outline to illustrate this chapter is shown in Figure 5.1.

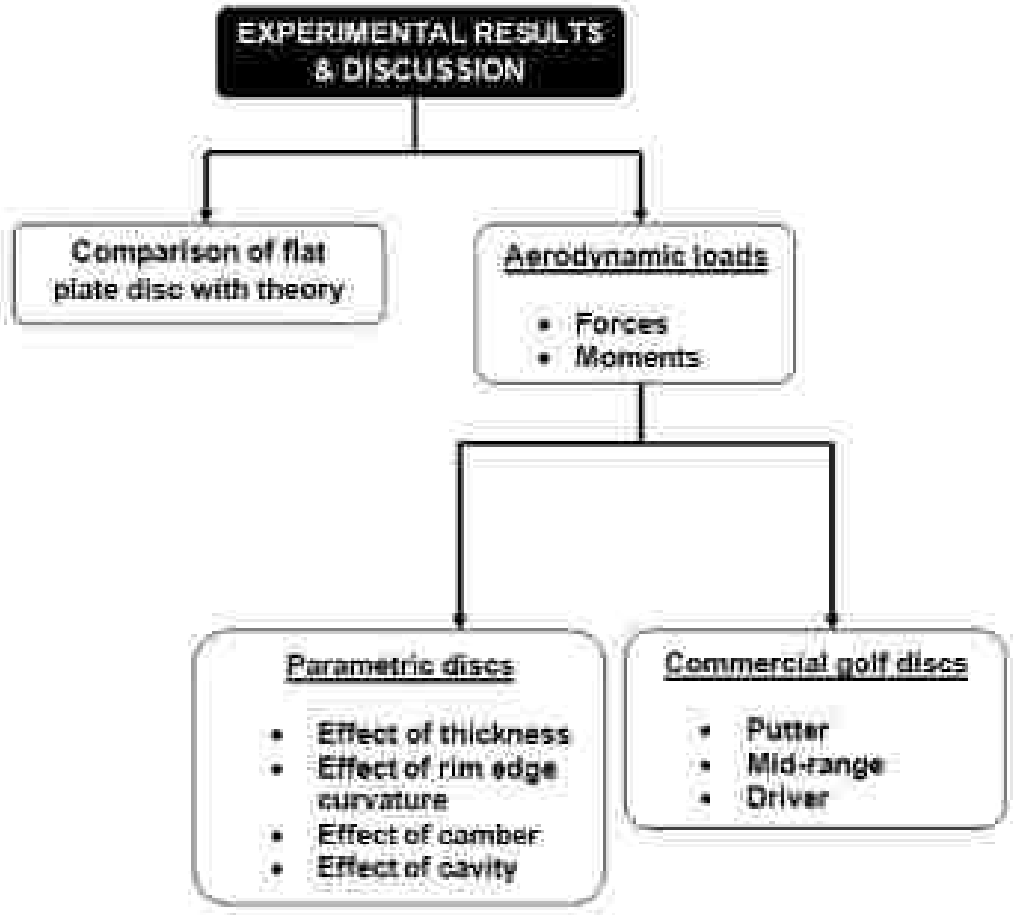

Figure 5.1: Outline of Chapter 5.

5.1 Finite wing theory and flat plate data

A comparison of lift and drag data for flat plate discs with finite wing theory (Potts, 2005) is shown in Figure 5.2. The flat plate data with thickness-to-diameter ratio (t/d) of 0.01 and 0.1 are chosen because they were used as a baseline comparison in the analysis of parametric discs ($t/d = 0.1$) and commercial golf discs ($t/d = 0.01$). Note that the aspect ratio of the disc is 1.27, whereas the finite wing theory is restricted to aspect ratio greater than 2 (the theoretical approximation to determine the lift and drag characteristics of a disc as an example of low aspect ratio wings can be referred to Potts (2005)). However, the comparison was made to establish the understanding of low aspect ratio wings before focussing on the discussion of various geometric variations that change the aerodynamic characteristics discussed subsequently.

Lift

The lift curve gradients of the flat plate discs are almost similar to that predicted from theory (~0.041 per degree) with flat plate disc of $t/d = 0.1$ has slightly lower gradient at higher angles of attack. The flat plate discs have zero lift at zero angle of attack due to their symmetrical profiles, whereas the theoretical curve has positive lift as a result of camber.

Drag

The theoretical drag curve is almost identical to the flat plate disc of $t/d = 0.1$ with slight disparity on the profile drag. However, the reduction in drag is significant for flat plate disc with $t/d = 0.01$. This is due to the small exposure of projected frontal area to the flow with increasing angles of attack.

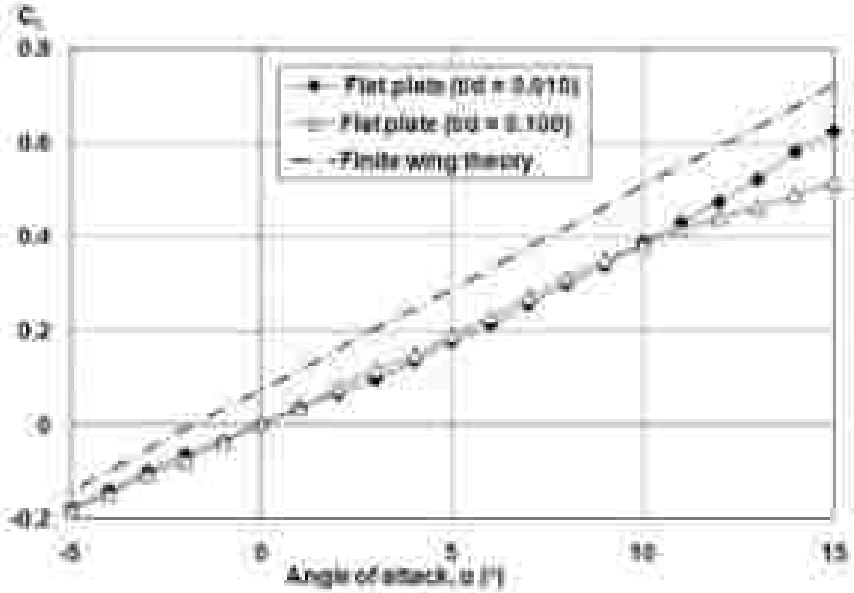

(a) Lift coefficient, C_L

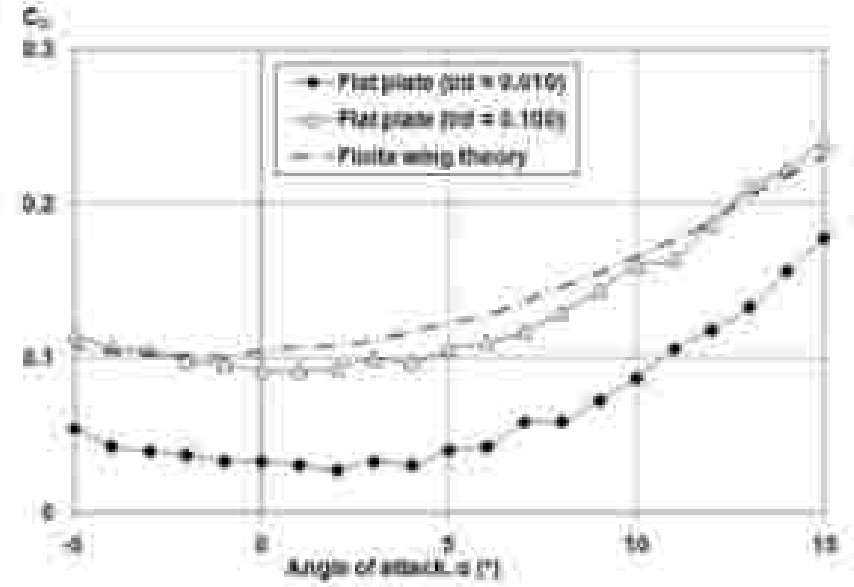

(b) Drag coefficient, C_D

Figure 5.2: Comparison of the flat plate data discs to finite wing theory.

5.2 Parametric discs

The geometry of a disc influences its aerodynamics. The following sub-sections discuss important features of disc geometry and their effect on the disc aerodynamic characteristics. Lift, drag and pitching moment about the half chord on non-spinning parametric discs were measured at angles of attack ranging from -5° to 15° with 1° increments. The operating Reynolds number was fixed at 3.78×10^5 corresponding to a speed of 27.5 m s^{-1} unless stated otherwise. A summary of the wind tunnel aerodynamic characteristics data for the parametric discs is presented in Table 5.1.

Geometric parameter	Aerodynamic characteristics					
	C_{L_0}	$\frac{dC_L}{d\alpha}$	C_{D_0}	C_{M_0}	$\frac{dC_M}{d\alpha}$	Trim angle
Thickness	0	0.039	0.032	0	0.008	0°
	0	0.038	0.042	0	0.006	0°
	0	0.037	0.052	0	0.005	0°
	0	0.036	0.092	0	0.004	0°
Edge curvature	0	0.027	0.041	0	0.006	0°
	0	0.035	0.049	0	0.007	0°
	0	0.032	0.047	0	0.005	0°
	0	0.036	0.092	0	0.004	0°
Cavity	0.054	0.049	0.124	-0.005	0.003	1°
	0.139	0.045	0.148	-0.004	0.001	1°
	0	0.036	0.092	0	0.004	0°
Camber shape	0	0.037	0.170	0.004	0.003	-1°
	0.057	0.034	0.068	-0.002	0.006	0°
	0.079	0.033	0.056	-0.001	0.007	0°
	0	0.036	0.092	0	0.004	0°

Table 5.1: Summary of parametric discs aerodynamic data.

Table 5.1 summarizes important parameters for the aerodynamic characteristics: these are the lift, drag and moment coefficients at zero angle of attack, C_{L0}, C_{D0}, and C_{M0}, respectively; the change of the lift and moment coefficients with respect to the angles of attack, or $dC_L/d\alpha$ and $dC_M/d\alpha$, respectively; and the trim angle, i.e., the angle of attack at which the disc's pitching moment is zero. The summary highlights that a symmetrical disc with a solid shape has zero lift and zero pitching moment at zero angle of attack ($C_{L0} = 0$ and $C_{M0} = 0$). The gradients of the pitching moment about the centre of gravity ($dC_M/d\alpha$) for all the discs are positive signifying that the discs are unstable in pitch. The profile drag (C_{D0}) for a disc with cavity is relatively higher compared to a solid disc. The trim angles of almost all the parametric discs studied are found to be zero.

Note that the aerodynamic centre of a disc is obtained by using Equation 3.19 in Chapter 3. However, the gradients of the pitching moment were averaged across the range of angles of attack from 0° to 15° (i.e., using linear variation). The impact of non-linearity on the position of aerodynamic centre of the disc is discussed in sub-section 5.1.3. It is important to highlight that the concept of steady-state flight in typical aircraft is not applicable in the context of a flying disc as it exhibits variable stability throughout its flight as the angle of attack varies.

5.2.1 Effect of thickness

A comparison of the force and moment data for various flat plate discs with thickness-to-diameter ratio of 0.01, 0.025, 0.05 and 0.1 is presented in Figure 5.3 (note: The thickness-to-diameter ratio will be referred to as the thickness only hereafter).

Lift

The data in Figure 5.3 (a) shows that all discs have zero lift at zero angle of attack, consistent with geometric symmetry of these profiles about the xy-plane. The gradients of the lift curves are almost identical (~0.04/ degree) but slight decrement

started to occur for $\alpha > 12^{\circ}$ as the thickness increases. From the literature (Ashley and Landahl, 1985; Pelletier and Mueller, 2000), it would be expected that increasing thickness reduces the lift curve gradient. However, in the present case, the disc aspect ratio is so low that the thickness effect is only apparent at relatively higher angles of attack and the lift curve is dominated by the 3d effects. Note that the stall is not evidenced in lift curves over the range of angles of attack tested. However, the surface flow visualisation result suggests that increasing thickness leads to a larger separation bubble on the upper surface leading edge. Hence, this behaviour could reduce the leading edge peak in the chordwise pressure distribution, but further investigation in the future is required to confirm this phenomenon.

Drag

Thickness has significant effect on drag through an increase in profile drag as shown in Figure 5.3 (b). This behaviour occurs due to the large exposure of projected frontal area to the flow. Since the lift is largely unchanged by thickness, the induced drag (lift dependent) component is similar between discs of different thickness. There is evidence from the surface flow visualisation that changing the thickness changes the extent of the upper surface leading edge separation bubble as shown in Figure 5.4. This behaviour is indicated by the formation of the crescent shape separation line as the angle of attack increases from $\alpha = 0^{\circ}$ to $\alpha = 5^{\circ}$. This phenomenon does make a significant contribution to the overall drag.

L/D

The lift-to-drag ratio (L/D or C_L/C_D) results in Figure 5.3 (c) shows that increasing thickness would increases the drag but has small effect on the lift (the term of L/D and C_L/C_D will be used interchangeably in this thesis). This result means that C_L/C_D reduces with increasing disc thickness for all angles of attack range tested. The C_L/C_D plot is commonly used to evaluate the aerodynamic efficiency and performance of an aircraft (Anderson, 2007); a higher value of maximum C_L/C_D usually indicates a better performance. However, the graph shown in Figure 5.3 (c) did not show a common trend of C_L/C_D plot which usually has a peak at the

maximum C_L/C_D. For discs, the C_L/C_D value increases with increasing angle of attack, then it reaches a plateau and remains relatively constant. The maximum C_L/C_D for the thinnest disc ($t/d = 0.01$) is around 5, whereas the peak C_L/C_D for the 10% thick disc is around 2.5 (50% reduction).

Pitching moment

The pitching moment result in Figure 5.3 (d) shows that all discs have zero pitching moment at zero angle of attack, consistent with all profiles that have zero camber. Pitching moment with angle of attack for different thicknesses is approximately similar for lower angles of attack. At higher angles, the effect of thickness is to flatten off the pitching moment curves, with increasing thickness leading to greater reduction in pitching moment. This is consistent with the stall behaviour of conventional wings in which stall shifts the aerodynamic centre aft and reduces the magnitude of nose up pitching moment.

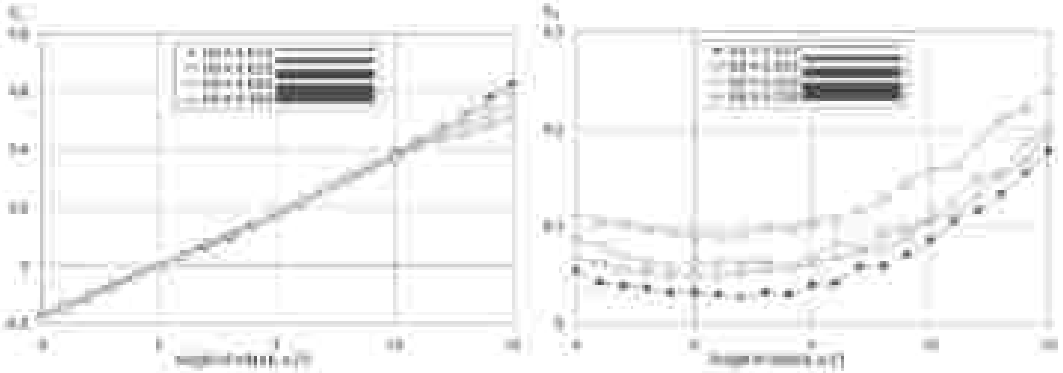

(a) Lift coefficient, C_L

(b) Drag coefficient, C_D

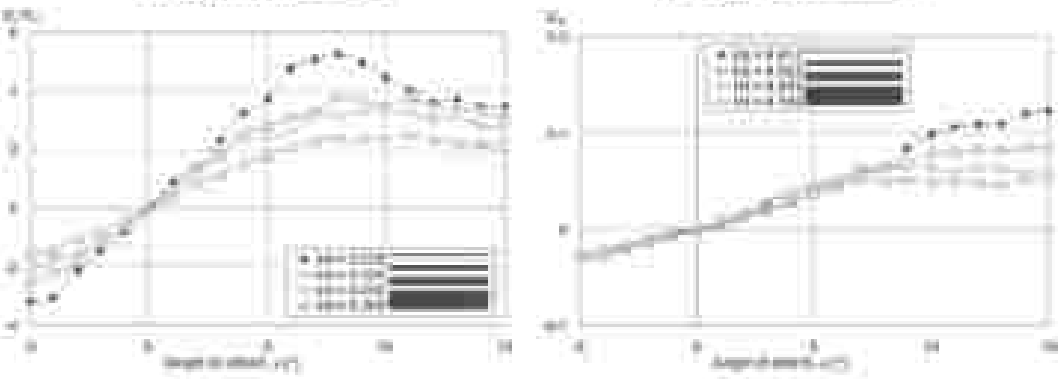

(c) Lift-to-drag ratio, C_L/C_D

(d) Pitching moment coefficient, C_M

Figure 5.3: Comparison of the influence of disc thickness on aerodynamic characteristics.

Aerodynamic centre position

The pitching moment gradients are positive, signifying that in free flight they are dynamically unstable in pitch. The gradients of the pitching moment curves generally increase with angle of attack and decrease with increasing thickness. The gradients can be associated with the position of the aerodynamic centre (x_{ac}) with respect to the disc centre of gravity (Etkin and Reid, 1996). A steeper gradient is associated with the location of the aerodynamic centre that is further from the disc centre, equivalent to a larger nose-up pitching moment. Based on the position of the disc aerodynamic centre (obtained from the experiment) presented in Table 5.2, it indicates that a disc with lower thickness ($t/d = 0.01$) produces a larger nose up pitching moment, as a result of the position of the aerodynamic centre located further from the disc centre of gravity (indicated by a steeper pitching moment gradient) at approximately 21% of the chord length ahead of the chord point (Note: the chord of a disc is equal to its diameter. The term chord is used here in keeping with standard practice in flight analysis). In contrast, a disc with a higher thickness ($t/d = 0.1$) produces a reduced nose down pitching moment resulting from the position of the aerodynamic centre that is located closer to the disc centre of gravity at approximately 12% of the chord length ahead of the chord point.

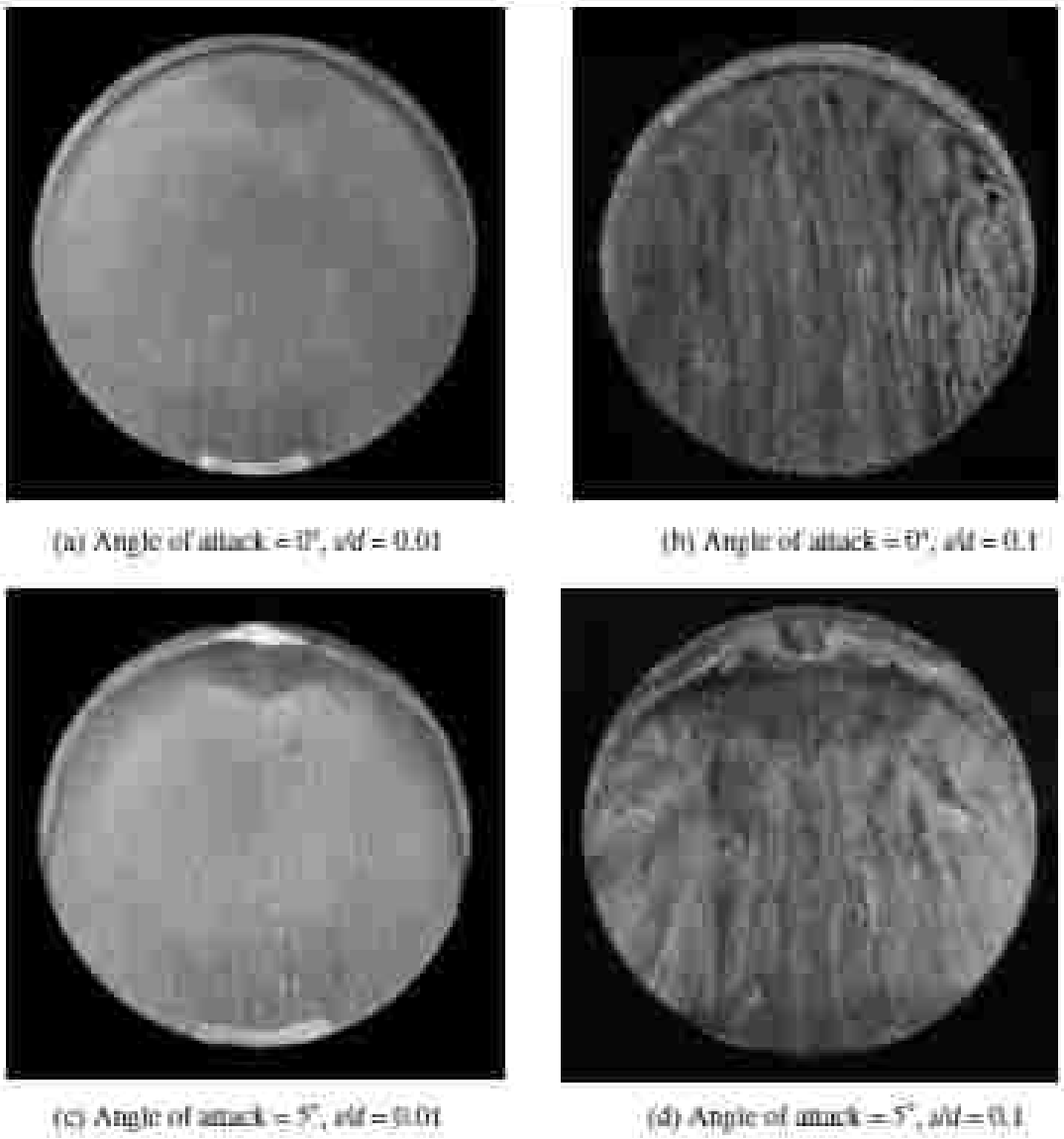

(a) Angle of attack = 0°, a/d = 0.01

(b) Angle of attack = 0°, a/d = 0.1

(c) Angle of attack = 5°, a/d = 0.01

(d) Angle of attack = 5°, a/d = 0.1

Figure 5.4: Surface flow visualisations performed on flat plate discs with a/d = 0.01 and 0.1 with increasing angle of attack. Regions of separated flow near the leading edge indicated by the crescent shape separation line increases with thickness. The flow direction is vertically from top to bottom of the image.

Thickness	Location of the aerodynamic centre
0.010	21% of the chord length ahead of the half chord point
0.025	18% of the chord length ahead of the half chord point
0.050	14% of the chord length ahead of the half chord point
0.100	12% of the chord length ahead of the half chord point

Table 5.2: Location of the aerodynamic centre with respect to the disc thickness. A thinner disc produces a larger nose up pitching moment, as a result of the position of the aerodynamic centre located further from the disc centre of gravity (indicated by a higher % of the chord length ahead of the half chord point).

5.2.2 Effect of rim edge curvature

A comparison of the force and moment data for various discs with rim edge curvature from sharp to blunt including a flat plate disc with $t/d = 0.1$ is presented in Figure 5.3.

Lift

All discs have zero lift at zero angle of attack due to their symmetrical design as shown in Figure 5.3 (a). The disc with square leading and trailing edge ($r/d = 0.1$) exhibits the highest lift gradient compared to all evaluated disc configurations. Interestingly, rounding off or tapering of a square leading or trailing edge leads to a reduction in lift for the range of angles of attack tested. This behaviour was not expected initially as the rounded edge shape is usually observed with a lower lift gradient compared to the sharp edge shape. The common observation in those cases is due to the large amount of trailing vortices produced by the rounded edge that create a large induced drag and results in the reduction of the lift gradient. As disc in

principle is classified as a very low aspect ratio wing. Prandtl Lifting Line Theory (Abbott and Von Doenhoff, 1959) could not be applied to estimate the lift as in the usual comparison of the rounded and sharp edge case. A reasonable explanation may be deduced from the investigation of Hoerner (1993) on sharp and rounded edges, which closely correspond to the present study. Apparently, a sharper edge disc has a lower effective aspect ratio compared to a rounded edge disc that has a higher effective aspect ratio. As a smaller effective aspect ratio leads to higher induced drag and therefore, causes the lift gradient to reduce. Note that given a non-square leading or trailing edge curvature, the difference in lift between the profiles is relatively slight, with the rounded edge profile producing higher lift gradient compared to the sharp edge profile.

Drag

The drag result illustrated in Figure 5.5 (b) shows that some degree of fairing of the leading or trailing edge significantly reduces the drag compared to the non-fairing case (square edge) over the range of angles of attack tested. Between the faired cases, the two tapered profiles (sharp edges) perform better than the rounded profile particularly at higher angles of attack. In addition, qualitative flow visualisation conducted to observe the flow behaviour between sharp and rounded edge support the load results. It reveals that a sharp edge shape has lower drag because they generate a small amount of wake compared to the rounded edge. This is indicated by the size of a pair of nodes produced close to the trailing edge as shown in Figure 5.6, It shows the stagnation points that suggest trailing vortices detach from the surface. This behaviour is expected as Hoerner (1993) data compilation of drag for sharp and rounded edge shapes, which closely correspond to the present investigations, also shows similar aerodynamic characteristics. However, Pelletier and Mueller (2000) who conducted a study on a low aspect ratio flat plate wing (with sharp and elliptical trailing edge only) observed that the edge curvature does not have significant influence on drag. The difference between their observation and the present investigation is believed due to the influence of Reynolds number. Their investigation was conducted at Reynolds number of 8×10^4, lower than the present

study. According to Laitone (1997), the effect of edge curvature is not apparent at this low Reynolds number and therefore, explained the discrepancy.

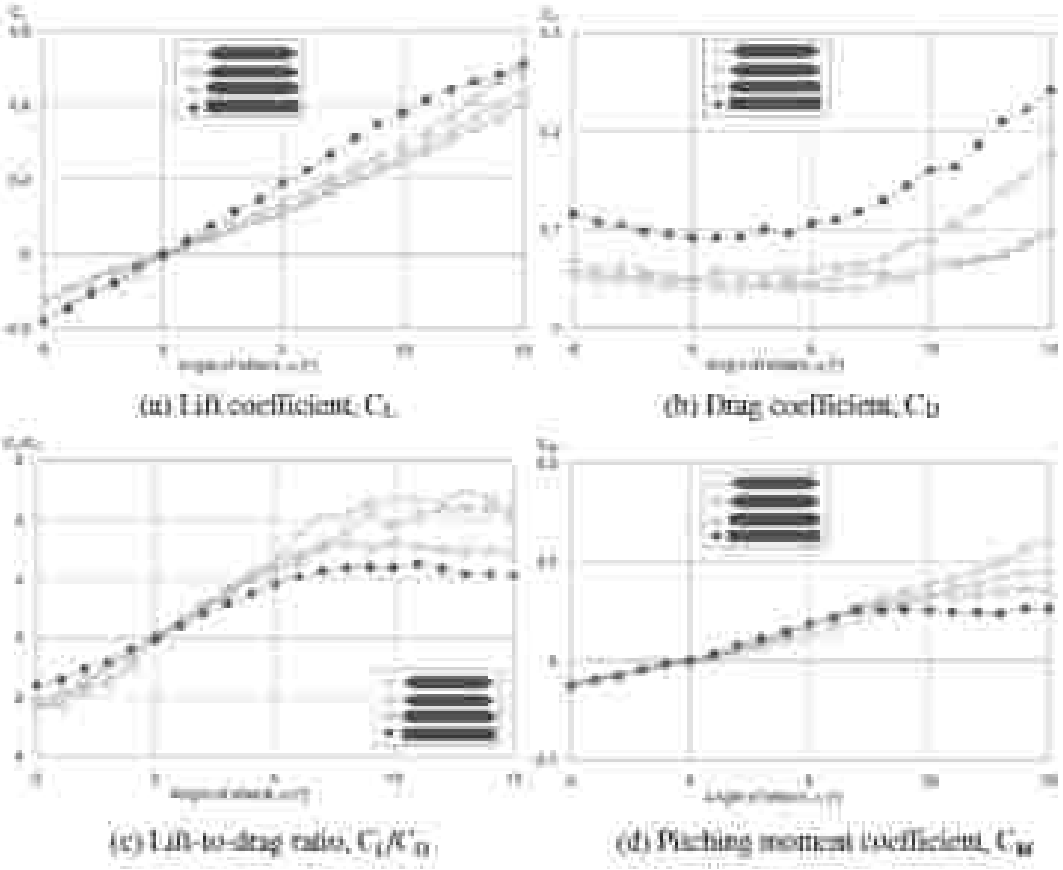

(a) Lift coefficient, C_L (b) Drag coefficient, C_D

(c) Lift-to-drag ratio, C_L/C_D (d) Pitching moment coefficient, C_M

Figure 5.5: Influence of disc rim edge curvature on aerodynamic characteristics

L/D

The overall effect of fairing the leading or trailing edge as shown in Figure 5.5 (c) is to increase the C_L/C_D of the disc for the range of angles of attack tested, compared to the non-fairing case (square edge). In particular, the sharp edge profile produces a peak C_L/C_D of around 5, similar to that of the flat plate disc ($t/d = 0.01$), compared to a C_L/C_D of around 2.5 for the square profile (50% reduction).

Pitching moment

Figure 5.5 (d) shows that all discs have zero pitching moment at zero angle of attack due to their symmetrical profile as expected. Pitching moment with angle of attack

for different rim edge curvature is approximately similar for lower angles of attack. At higher angles of attack particularly at $\alpha > 9^{\circ}$, the effect of non-fairing (square edge) is to flatten off the pitching moment curves. However, tapering the disc edge leads to greater increment in pitching moment.

Aerodynamic centre position

Table 5.3 indicates that the sharp edge discs produce a large nose-up pitching moment as the angles of attack increases, corresponds to the distance of the disc aerodynamic centre that is located further from the disc centre of gravity (between 22% to 28% of the chord length ahead of the half chord point). In contrast, the square edge discs produce a small magnitude of nose-up pitching moment as the angle of attack increases at around 12% of the chord length ahead of the half chord point, corresponds to the distance of the disc aerodynamic centre located near to the disc centre of gravity.

(a) Disc with rounded edge (b) Disc with sharp edge

Figure 5.6: Surface flow visualisations performed on rounded and sharp edge discs at angle of attack = 0°. Regions of separated flow edge indicated by the crescent shape separation line can be seen near the leading edge for rounded edge disc. The line moves downstream nearly 25% of the disc diameter for sharp edge disc. A pair of nodes was produced which indicate the detachment of trailing vortices from the surface. The flow direction is vertical from top to bottom of the image.

Rim edge curvature	Location of the aerodynamic centre
	28% of the chord length ahead of the half chord point
	22% of the chord length ahead of the half chord point
	17% of the chord length ahead of the half chord point
	12% of the chord length ahead of the half chord point

Table 5.3: Location of the aerodynamic centre with respect to the disc rim edge curvature. A square edge disc produces a reduced nose up pitching moment, as a result of the position of the aerodynamic centre located closer to the disc centre of gravity (indicated by a lower % of the chord length ahead of the half chord point).

5.2.3 Effect of camber

Four disc geometries with varying camber including a flat plate disc with $t/d = 0.1$ were studied to investigate the effect of camber as shown in Figure 5.7. Camber is introduced to generate lift at zero angle of attack.

Lift

Comparisons of the results for the effect of camber in Figure 5.7 (a) show that disc with a negative and zero camber produce zero lift at zero angle of attack ($C_{L\theta} = 0$). Disc with 25% and 50% camber produce a slight increase of $C_{L\theta}$ at 0.06 and 0.08, respectively. The difference in pressure distribution over the upper and lower surface when a disc is cambered increased due to the asymmetry and therefore, leads to the increment in lift. The gradients of the lift curves are almost identical (~0.03/degree) but the baseline flat plate disc gradient is slightly higher (~0.04/degree). The development of disc camber and subsequent interaction with the aerodynamic

characteristics for each case shows that camber has the advantage to increase the positive lift at zero angle of attack as expected.

Drag

Camber has significant effect on drag as shown in Figure 5.7 (b), with the reduction in profile drag as a result of increased camber. The discs with positive camber have lower profile drag at around 0.05 compared to the disc with negative and zero camber which have a profile drag around 0.1. Comparisons of the results with Gordon and Rom (1985) investigations of low aspect ratio delta wing planform leads to a conclusion that a disc designed with positive camber produce a small wake compared to a disc with zero camber. Hence, the small wake results in a small drag.

L/D

The C_L/C_D results in Figure 5.7 (c) shows that discs with positive camber have a significantly higher C_L/C_D compared to the discs with negative and zero camber. This is expected due to the small amount of drag produced by the positive camber. The results imply that disc with a positive camber has the advantage to increase the lift at zero angle of attack as well as to reduce the drag quite significantly.

Pitching moment

Discs with positive camber have approximately zero pitching moment at zero angle of attack as shown in Figure 5.7 (d). At higher angles of attack, the effect of camber is to elevate the pitching moment curves, with increasing camber leading to greater increment in pitching moment gradient. The result indicates that there is a limit beyond which the pitching moment becomes more destabilized if the camber is increased more than a disc requires as this would result in a large nose-up pitching moment. As the effect of camber allows the aerodynamic characteristics of the disc to be changed in flight, this may explain why a commercial golf disc driver is usually designed with a moderate camber to reduce the large nose-up pitching moment as the angle of attack increases while flying.

Aerodynamic centre position

Table 5.4 shows that disc with 50% camber produces a large nose-up pitching moment, corresponds to the distance of the disc aerodynamic centre that is located further from the disc centre of gravity (at about 23% of the chord length ahead of the half chord point). Disc with zero camber produce almost less than half of the amount of nose-up pitching moment produces by disc with 50% camber, as indicated by the location of the aerodynamic centre at about 12% of the chord length ahead of the half chord point.

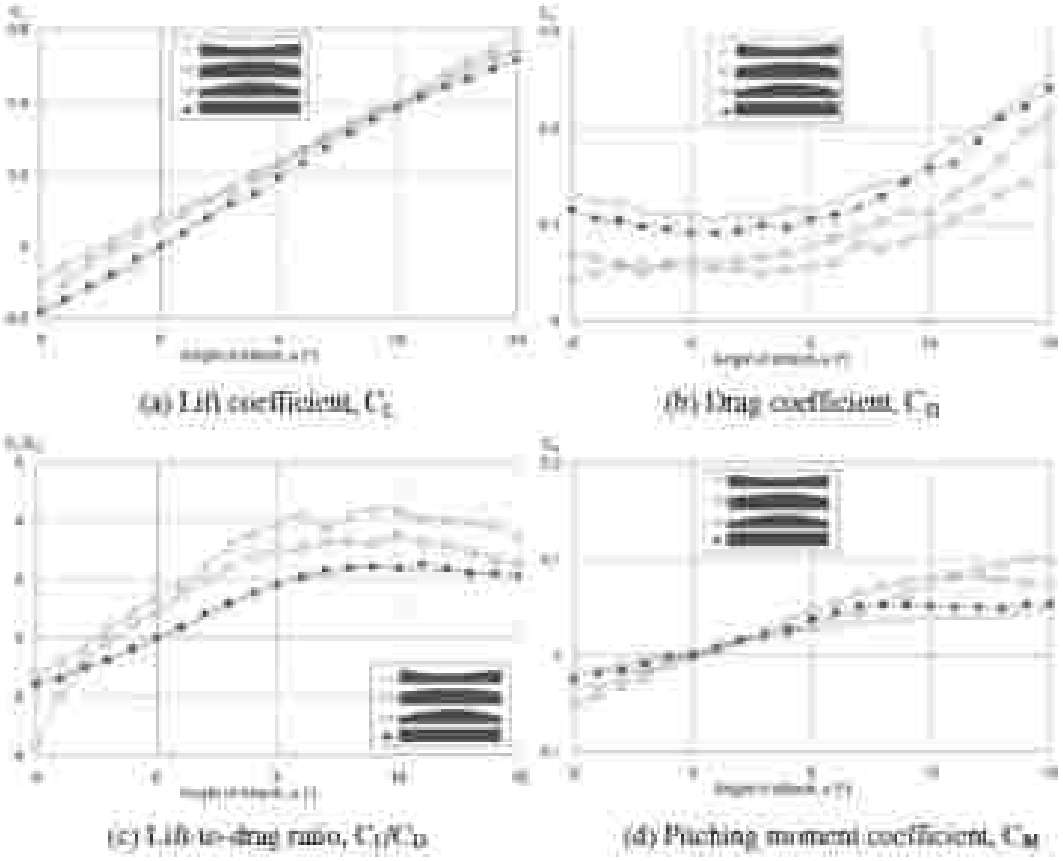

(a) Lift coefficient, C_L (b) Drag coefficient, C_D

(c) Lift-to-drag ratio, C_L/C_D (d) Pitching moment coefficient, C_M

Figure 5.7: Influence of disc camber on aerodynamic characteristics.

Camber	Location of the aerodynamic centre
Negative	9% of the chord length ahead of the half chord point
Zero	12% of the chord length ahead of the half chord point
26%	19% of the chord length ahead of the half chord point
50%	23% of the chord length ahead of the half chord point

Table 5.4: Location of the aerodynamic centre with respect to the disc camber. A disc with higher camber produces a larger nose up pitching moment, as a result of the position of the aerodynamic centre located further from the disc centre of gravity (indicated by a higher % of the chord length ahead of the half chord point).

5.2.4 Effect of cavity

Two variations of disc geometric shape with cavity height-to-thickness ratio c_d/t of 0.8 (square symbol) and 0.9 (triangle symbol) were compared with the flat plate disc of $Ad = 0.1$ to study the effect of cavity on aerodynamic loads as shown in Figure 5.8. Note that the disc with c_d/t of 0.8 has Ad equivalent to the flat plate disc.

Lift

The gradients of the lift curves shown in Figure 5.8 (a) are almost identical for the discs with cavity regardless of the cavity height, with a constant offset in lift consistent with the difference in C_{L0}. However, the flat plate disc (with zero cavity height) has a lower lift gradient. Comparison of the discs with same thickness, but with and without cavity (square and circle symbol) at zero angle of attack shows that introduction of a cavity on the lower surface produces a positive increase in lift. The result exhibits similar behaviour to a disc with positive camber. However, increasing the disc cavity depth further (means thickness is also increasing at the same time)

produces a negative change in C_{l_α}, inconsistent with the effect of increasing camber. It is believed that beyond a certain cavity depth the camber analogy is inappropriate due to the nature of flow topology inside deep cavities.

Drag

The results in Figure 5.8: (b) show that introduction of a cavity increases drag compared to a cavity free profile of the same thickness. This is consistent with the increased effective frontal area of the cavity profile due to the projection of the rear inner face of the cavity in the free stream direction. However, for increased cavity depth disc, the drag is largely unchanged over the range of angles of attack tested.

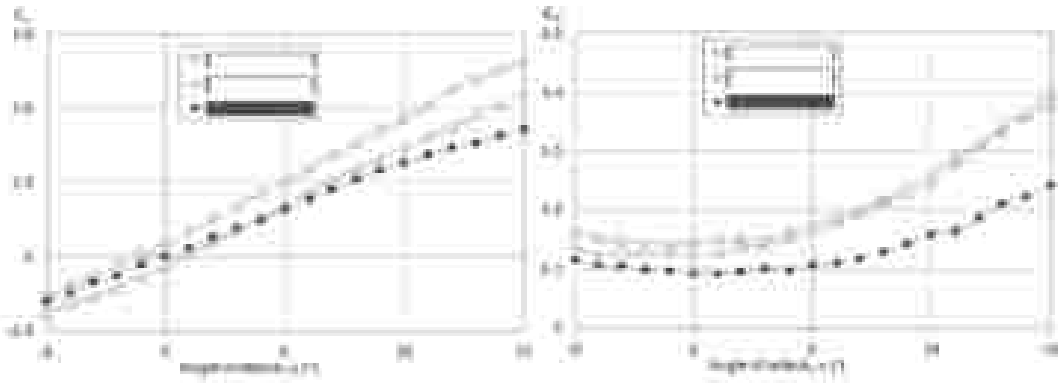

(a) Lift coefficient, C_L (b) Drag coefficient, C_D

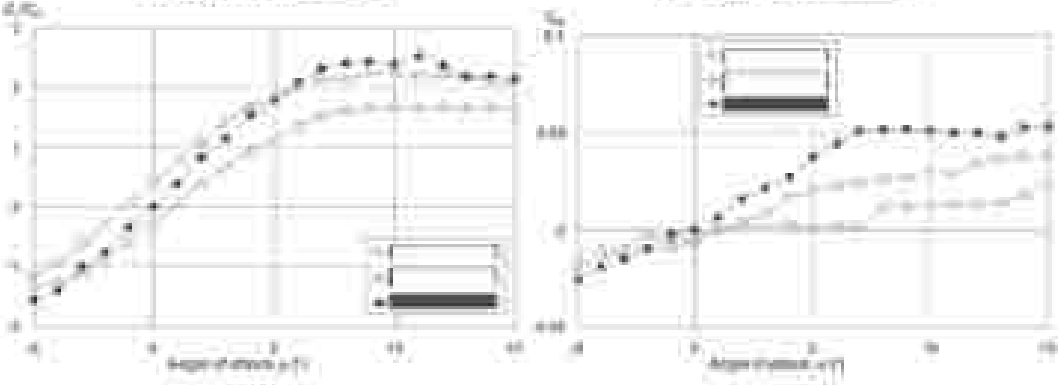

(c) Lift-to-drag ratio, C_L/C_D (d) Pitching moment coefficient, C_M

Figure 5.8: Influence of disc cavity on aerodynamic characteristics.

L/D

The results in Figure 5.8 (c) shows that changes in lift and drag as a result of the introduction of the cavity means that the C_L/C_D for the same thickness disc with and without cavity is approximately similar. The increased cavity depth disc (triangle symbol) has significantly reduced C_L/C_D compared to the other discs.

Pitching moment

The pitching moment result in Figure 5.8 (d) demonstrates the reason why all practical discs need to have a cavity in the lower surface. The presence of this cavity produces a significant afterwards shift in the aerodynamic centre position (x_{ac}) such that the pitching moment about the centre of the disc is substantially zero particularly for the angles of attack ranging from 0° to 7°. This means that the disc will have minimal tendency to roll about the flight axis and hence, require less skill to throw towards a given target and achieve a greater range compared to a disc with the same C_L/C_D but strong roll divergence. Note that the introduction of cavity produces a reversed flow on the lower surface which subsequently causes negative C_{M0} at zero angle of attack.

Aerodynamic centre position

Data in Table 5.5 shows that a disc with a higher cavity depth produces a significant reduced nose-down pitching moment as indicated by the aerodynamic centre at approximately 4% of the chord length ahead of the half chord point. The introduction of cavity reduces the magnitude of nose-down pitching moment by almost 50% compared to a cavity free profile of the same thickness.

Cavity height	Location of the aerodynamic centre
zero	12% of the chord length ahead of the half chord point
0.8	8% of the chord length ahead of the half chord point
0.9	4% of the chord length ahead of the half chord point

Table 5.5: Location of the aerodynamic centre with respect to the disc cavity height. A disc with higher cavity height produces a reduced nose up pitching moment, as a result of the position of the aerodynamic centre located closer to the disc centre of gravity.

5.3 Commercial Golf Discs

The aerodynamic loads on non-spinning commercial golf discs were measured at angles of attack ranging from -5° to 15° with 1° increments. The operating Reynolds number was fixed at 3.78×10^5 corresponding to a speed between 22 m s^{-1} to 25 m s^{-1} depending on the golf disc diameter. The Reynolds number was fixed to ensure the viscous effects were accurately modelled for all discs as the diameter for short and long range disc vary. A flat plate disc with thickness-to-diameter ratio of 0.01 was used as a baseline disc to provide reference data to which the commercial golf discs can be compared. A summary of the wind tunnel aerodynamic characteristics data for the commercial golf discs for short (putter), medium (mid-range) and long range (driver) disc is presented in Table 5.6.

The results in Figure 5.9 show a comparison of the force and moment data for flat plate and frisbee with putter *'Aviar'*, mid-range *'Roc'* and driver *'Wraith'* discs. These discs were representative of the typical shape of commercial golf discs that are widely used in disc golf game. A comparison of the force and moment data for all putter discs and all driver discs is presented in Figure 5.10 and Figure 5.11, respectively, in order to demonstrate the aerodynamic characteristics for short and

long range disc. For completeness, all commercial golf discs aerodynamic data obtained in the experiment is shown in Figure 5.12. The results for the side force and rolling moments are also shown in Figure 5.12 and they were approximately zero throughout the range of angle of attack tested, as expected for symmetrical discs.

Lift

The data in Figure 5.9 (a) shows the typical shape of linear lift with all golf discs including frisbee have positive lift at zero angle of attack, consistent with cavity geometry of these profiles. The gradients of the lift curves are similar but frisbee has a slight increment at higher angles of attack. Although frisbee thickness is relatively higher than the golf discs tested, however, the effect of thickness is not dominant to influence the lift curve gradient. Based from the observation on the results of parametric discs study, the disc rounded edge curvature has significant influence on the gradient of the lift curves. This is indicated by the gradient decrement as the edge curvature varies from rounded edge frisbee disc to sharp edge driver disc.

Drag

Thickness has a significant effect on flying discs drag as shown in Figure 5.9 (b). This is indicated by the increment of drag with respect to increasing thickness by the flat plate disc followed by driver, mid-range, putter and frisbee. This may explain the reason frisbee (t/d = 0.14) has the largest drag over the range of angles of attack tested compared to the golf discs (t/d < 0.1). In addition, the drag increment might also be influenced by the rim edge curvature as it varies from sharp edge driver disc to rounded edge putter disc.

LD

A comparison of the C_L/C_D for the discs in Figure 5.9 (c) indicates that the minimal thickness of the flat plate disc minimizes its profile drag compared to other discs, and therefore, results in relatively the highest value of maximum C_L/C_D, followed by that of the driver disc. The introduction of camber to the commercial golf discs and

the frisbee disc, on the other hand, increases the lift and the corresponding C_L/C_D is positive at $\alpha = 0$.

Pitching moment

The pitching moment gradients result for the discs are positive, signifying that they are dynamically unstable in pitch. As expected, the effect of cavity in golf discs is significant that it reduces the gradient of pitching moment particularly for frisbee, putter and mid-range disc. Note that the pitching moment gradient increases from short range disc to long range disc.

Evaluating disc performance using the C_L/C_D curves above would conclude that the flat plate disc is superior. However, the performance of a free flying disc does not depend on maximizing its lift and minimizing its drag alone. Based on the results, it shows that the pitching moment has significant influence on the disc performance. The pitching moment is translated into rolling rate as a disc spins. A minimal $C_{M\alpha}$ means that the rolling motion is minimized and this behaviour could improve the disc performance.

Aerodynamic centre position

The disc aerodynamic centre data shown in Table 5.7 indicates that driver disc *'Flick'* produces a large nose-up pitching moment, as a result of the position of the aerodynamic centre which is further from the disc centre of gravity (at approximately 21% of the chord length ahead of the half chord point). In contrast, putter disc *'Aviar'* produces a reduced nose-down pitching moment due to the position of the aerodynamic centre that is located closer to the disc centre of gravity (at about 5% of the chord length ahead of the half chord point).

Flow visualisation

In addition, qualitative flow visualisation conducted to investigate the behaviour of three long range discs (Flick, Wraith and Quarter K) presented in Figure 5.13 and 5.14 found that the boundary layer separates near the leading edge to form a

separation bubble that produces a crescent shape separation line at $\alpha = 0^{\circ}$ on the upper surface. As the angle of attack increases to 5°, the separation line move further downstream closer to the trailing edge and the shear layer at the trailing edge separates from the separation line. This indicates that trailing vortices detach from the surface. The separation line movement is influenced by the disc thickness as the driver disc thickness increasing from Flick, Wraith to Quarter K (properties of commercial golf discs can be referred in Chapter 4 Method). The separation and reattachment of reversed flows underneath the lower surface shows that the shear layer that separates off the trailing edge reattaches to the surface inside the trailing edge rim and is predominantly influenced by the cavity.

Golf discs	Aerodynamic characteristics					
	C_{L_0}	$\frac{dC_L}{d\alpha}$	C_{D_0}	C_{M_0}	$\frac{dC_M}{d\alpha}$	Trim angle
Aviar	0.152	0.044	0.083	-0.018	0.002	8°
Buzz	0.089	0.041	0.061	-0.033	0.004	8°
Roc	0.053	0.043	0.067	-0.015	0.003	8°
Flick	0.100	0.038	0.078	-0.007	0.008	1°
Storm	0.107	0.045	0.057	-0.026	0.004	7°
Wraith	0.143	0.040	0.055	-0.020	0.008	4°
Quarter K	0.138	0.039	0.065	-0.038	0.005	7°

Table 5.6: A summary of the wind tunnel aerodynamic characteristics data for the commercial golf discs.

Model	Location of the aerodynamic centre
Aviar	5% of the chord length ahead of the half chord point
Roc	7% of the chord length ahead of the half chord point
Buzz	10% of the chord length ahead of the half chord point
Storm	9% of the chord length ahead of the half chord point
Quarter K	13% of the chord length ahead of the half chord point
Wraith	15% of the chord length ahead of the half chord point
Flick	21% of the chord length ahead of the half chord point

Table 5.7: Location of the aerodynamic centre for commercial golf discs. A putter disc generally produces a reduced nose up pitching moment as a result of the position of the aerodynamic centre located closer to the disc centre of gravity (indicated by a lower % of the chord length ahead of the half chord point). The result is in contrast with a driver disc which generally produces a larger nose up pitching moment.

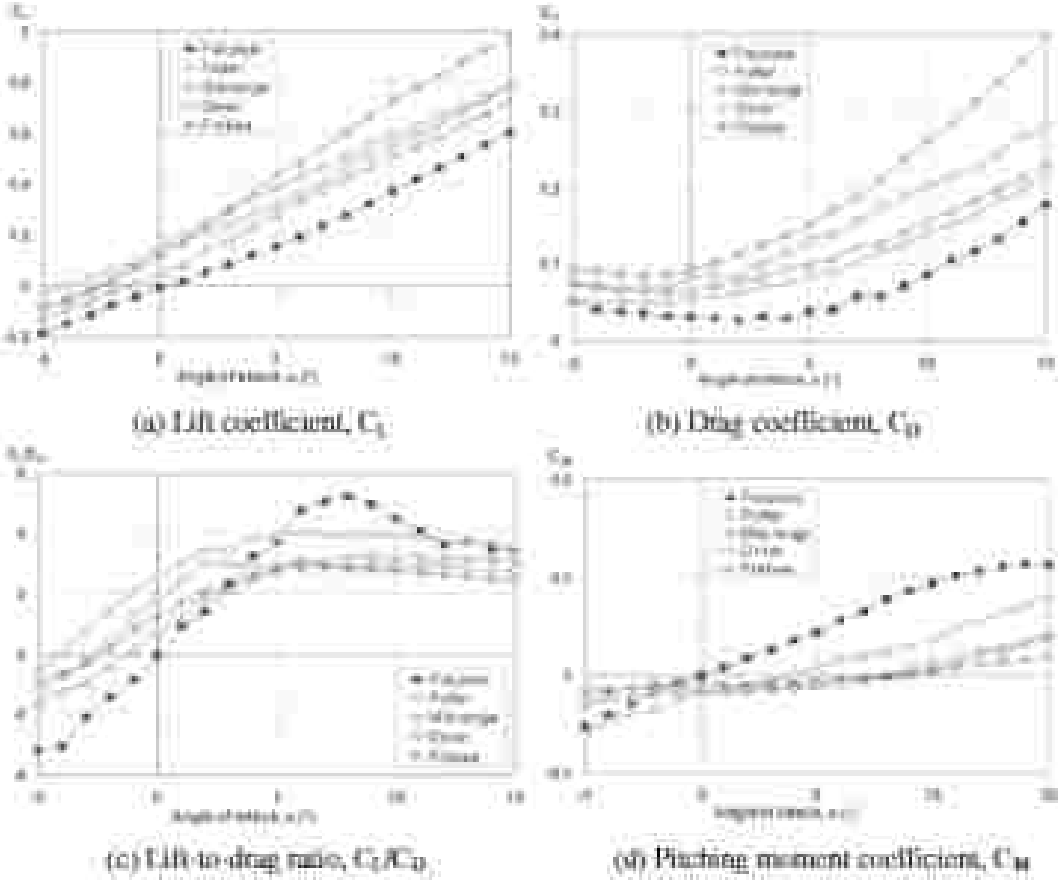

(a) Lift coefficient, C_L (b) Drag coefficient, C_D

(c) Lift-to-drag ratio, C_L/C_D (d) Pitching moment coefficient, C_M

Figure 5.9: Comparison of the aerodynamic forces and moment data for typical putter, mid-range and driver discs with a flat plate disc $\alpha_0 = 0.01$ and a Frisbee (Potts, 2005).

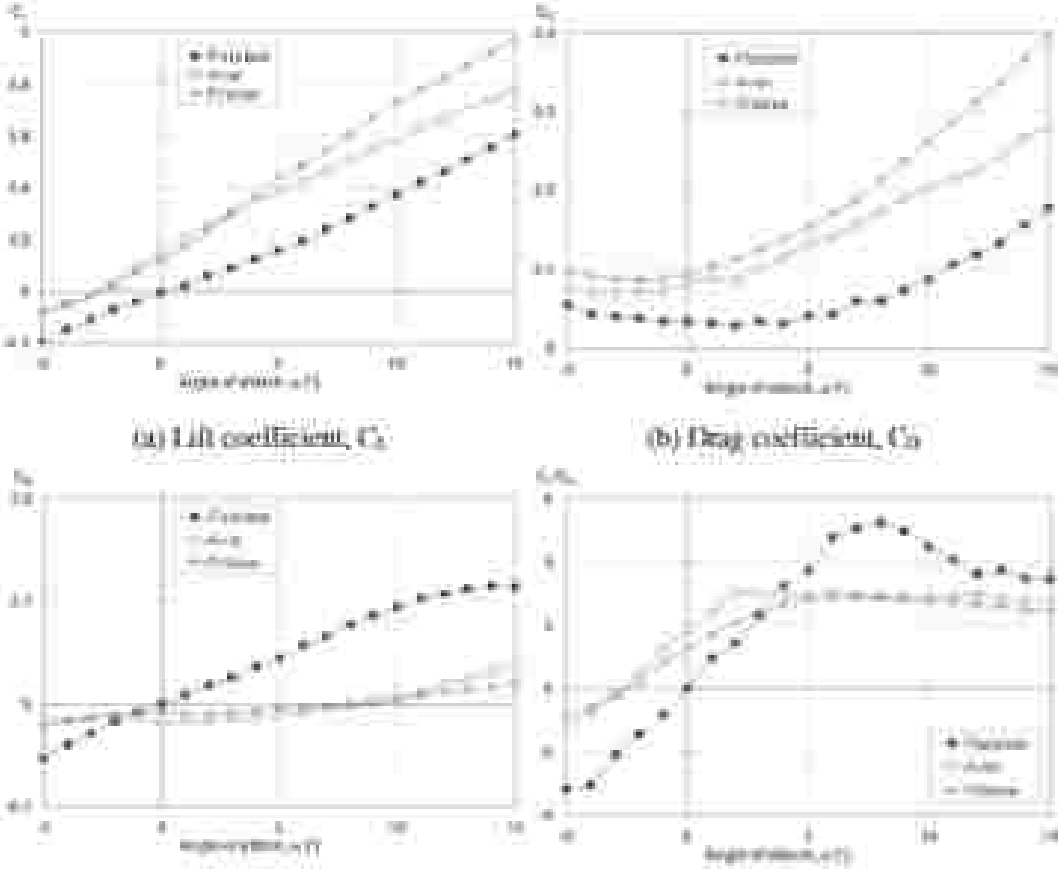

(a) Lift coefficient, C_L

(b) Drag coefficient, C_D

(c) Pitching moment coefficient, C_M

(d) Lift-to-drag ratio, C_L/C_D

Figure 5.10: Comparison of the aerodynamic forces and moment data for a paper disc "Aviar" with a flat plate disc $s/r = 0.01$ and a Frisbee (Potts, 2005) disc.

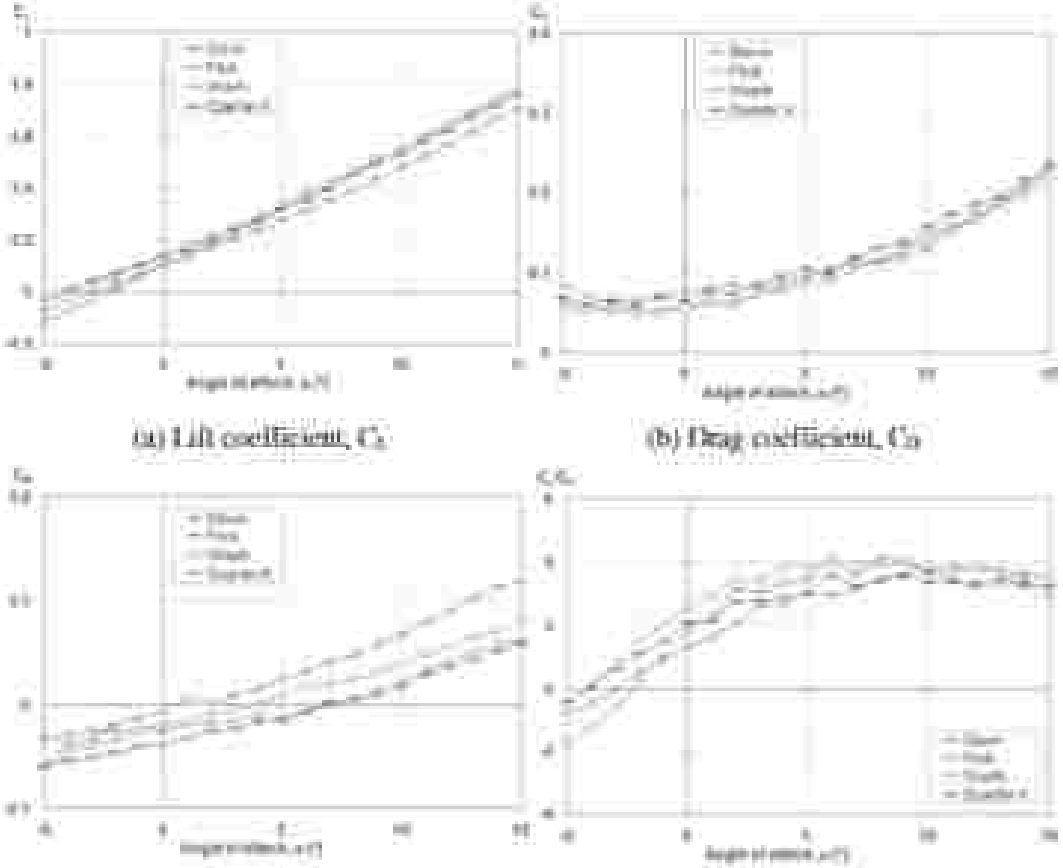

(a) Lift coefficient, C_L

(b) Drag coefficient, C_D

(c) Pitching moment coefficient, C_M

(d) Lift-to-drag ratio, C_L/C_D

Figure 5.11: Comparison of the aerodynamic forces and moment data for the commercial "driver" golf discs.

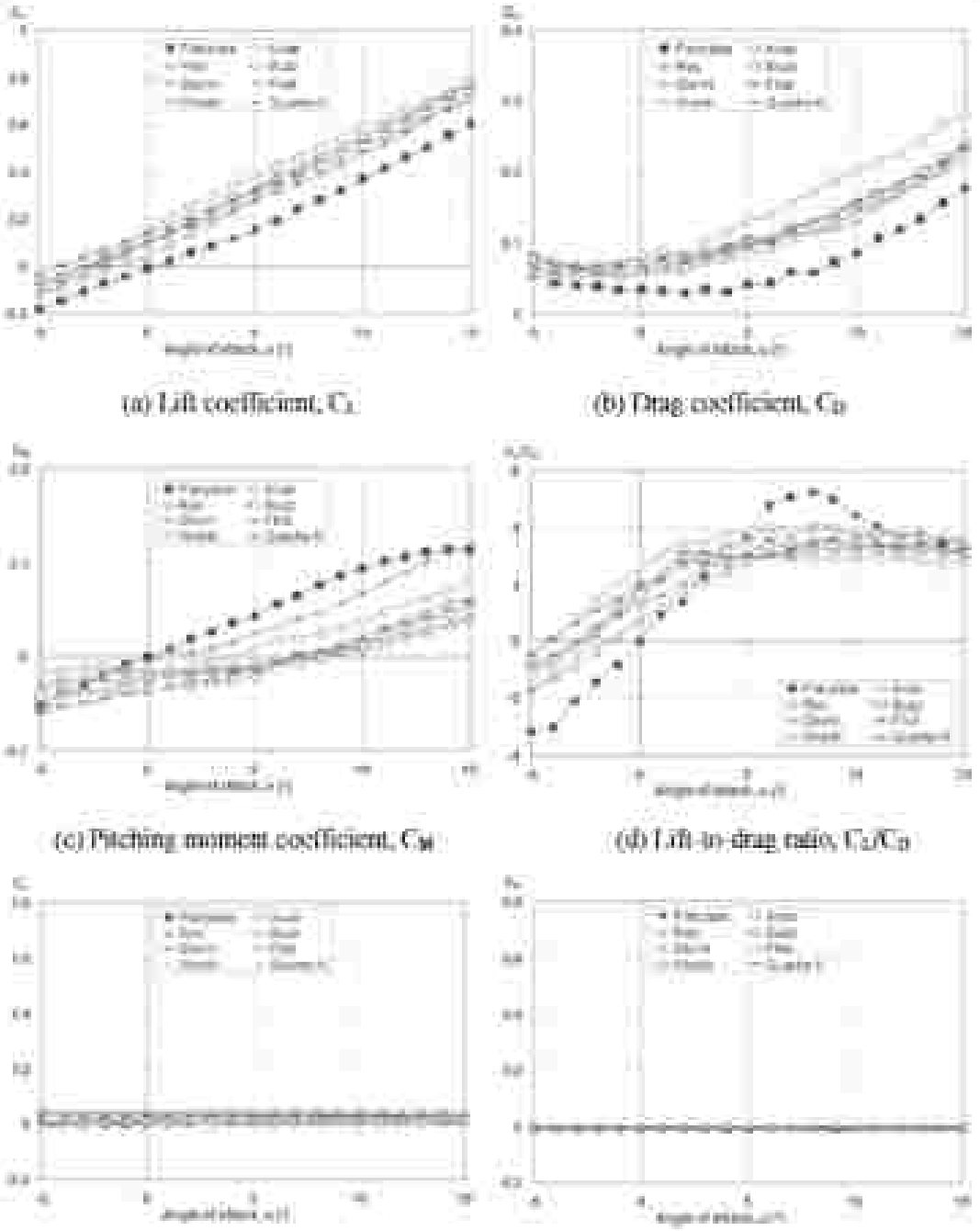

(a) Lift coefficient, C_L

(b) Drag coefficient, C_D

(c) Pitching moment coefficient, C_M

(d) Lift-to-drag ratio, C_L/C_D

(e) Side force coefficient, C_Y

(f) Lift coefficient, C_L

Figure 5.12: Comparison of the aerodynamic forces and moments data for all commercial golf discs with a flat plate disc $\mu V = 0.01$.

(a) Quarter K, $\alpha = 0°$

(b) Quarter K, $\alpha = 5°$

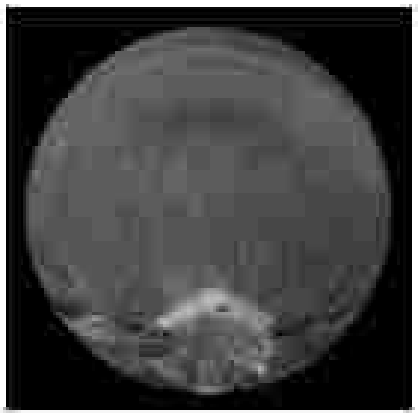

(c) Wraith, $\alpha = 0°$

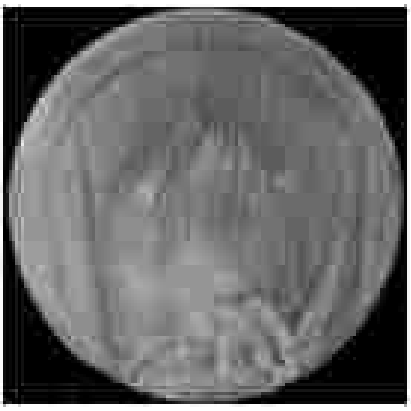

(d) Wraith, $\alpha = 5°$

(e) Flick, $\alpha = 0°$

(f) Flick, $\alpha = 5°$

Figure 5.13: Comparison of the upper surface flow visualisation for commercial driver discs at $\alpha = 0°$ and $\alpha = 5°$. The flow direction is vertically from top to bottom of the image.

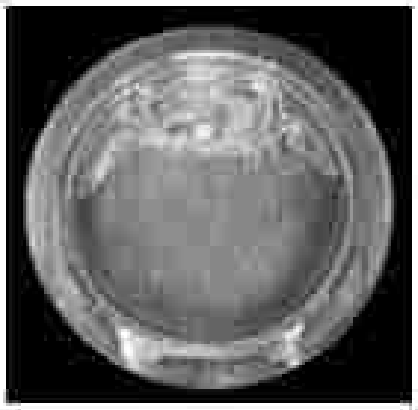

(a) Quarter K, $\alpha = 0°$

(b) Quarter K, $\alpha = 5°$

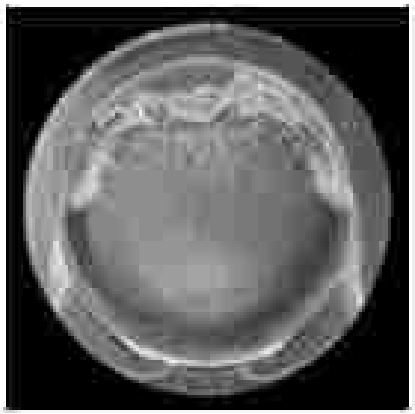

(c) Wraith, $\alpha = 0°$

(d) Wraith, $\alpha = 5°$

(e) Flick, $\alpha = 0°$

(f) Flick, $\alpha = 5°$

Figure 5.14: Comparison of the lower surface flow visualisation for commercial driver discs at $\alpha = 0°$ and $\alpha = 5°$. The flow direction is vertically from top to bottom of the image.

Chapter 6

Simulation Results and Discussions

This chapter presents and discusses simulation results for commercial golf discs particularly the putter and driver discs. The main objective of the work is to understand the flight trajectories of short and long range discs, with focus on the range and sensitivity. A comparison of sphere with other flying objects is presented in the beginning to establish the concept of range and sensitivity analysis. Then, the golf discs flight trajectories are discussed, as well as the effect of launch attitude on achievable range. A range and sensitivity analysis will finally be employed to assess the throwing skill level required of a player with respect to the golf discs categories. The outline to illustrate this chapter is shown in Figure 6.1.

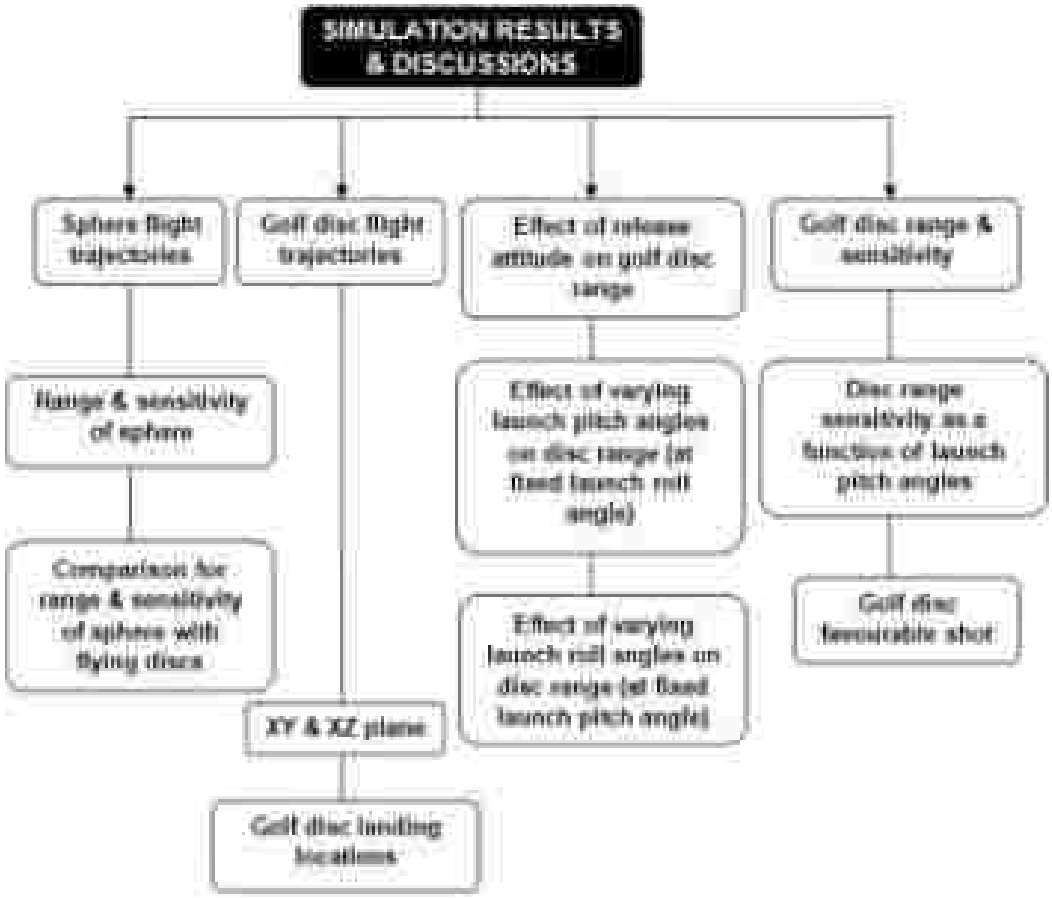

Figure 6.1: Outline of Chapter 6.

6.1 Sphere flight trajectories

A comparison of sphere flight trajectories with respect to launch angles as a function of launch speeds is presented in Figure 6.2. (Note that the sphere in the simulation is analogous to a baseball with a diameter = 0.073 m, mass = 0.145 kg and C_D = 0.5).

6.1.1 Range and sensitivity of sphere

Range as a function of launch angles at varying launch speeds

The data in Figure 6.2 (a) shows that dimensional sphere range at varying launch angles from 0° to 90° have parabolic shapes. The maximum range occurs at around 43°, lower than the angle predicted by projectile theory because the sphere is under the influenced of the drag force. Sphere has zero sensitivity ($dR/d\theta = 0$) at the maximum range with launch angle of 43° as shown in Figure 6.2 (b). It means a change of sphere range with respect to the changes of launch angle is zero at this point.

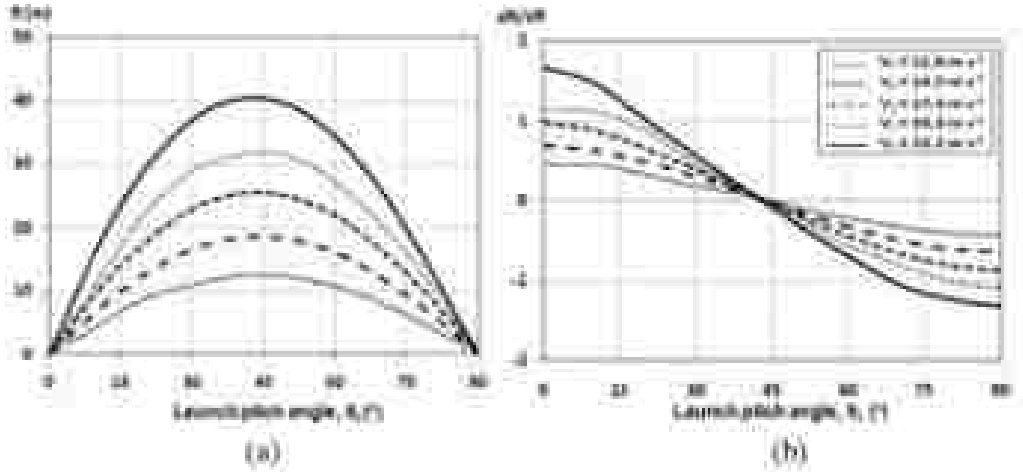

(a) (b)

Figure 6.2: Comparison of sphere with drag at varying launch speed for dimensional range.

6.1.2 Comparison for dimensionless range and sensitivity of sphere with flying discs

A comparison of dimensionless range and sensitivity analysis for spheres (with and without drag) and golf discs (putter 'Aviar', mid-range 'Roc' and driver 'Wraith') including Frisbee (simulated by using Potts (2005) data) is shown in Figure 6.3. Note that for ease of comparison, the legend displays sphere as a 'baseball' to illustrate the physical size of the sphere.

Sphere with and without drag

Figure 6.3 (a) shows that both spheres with and without drag curves have a parabolic shape as expected. The maximum range for sphere without drag occurs at 45° while sphere with drag occurs at approximately 43°. As drag is introduced in the sphere case, maximum sphere range substantially reduces to 25%. This suggests that drag has significant impact on reducing the maximum range.

Flying discs

There is significant dissimilarity between the spheres and the flying discs results as shown in Figure 6.3 (b). The flying disc curves generally skewed to the left with zero sensitivity occurs at lower launch angles between 10° to 13°. This is mainly due to the influence of lift as Weston (2009) also observes similar phenomenon in a ball (his works indicate that as the lift is introduced in the ball case, the symmetrical parabolic curve started to skew to the left and the optimal launch angle value becomes lower). The level of difficulty in throw is quantified by the width of the "peak bucket", with wider width can be associated with a less sensitive disc. Figure 6.3 (b) shows that flying discs are generally more sensitive than spheres as indicated by the narrow width of the peak bucket. This means that flying discs are more difficult to be thrown at launch and generally requires greater skill to throw than spheres.

(a)

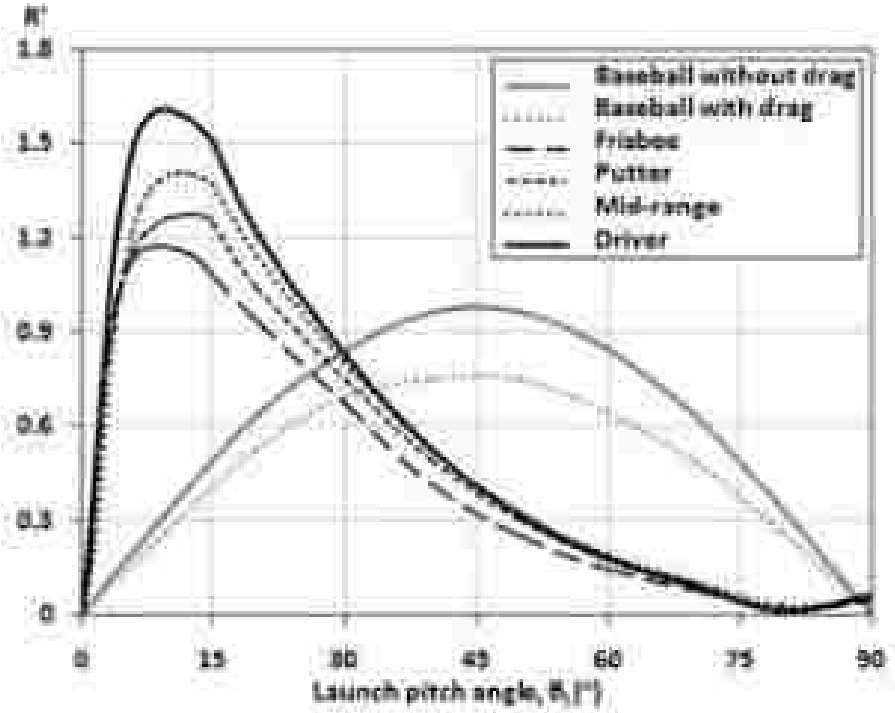

(b)

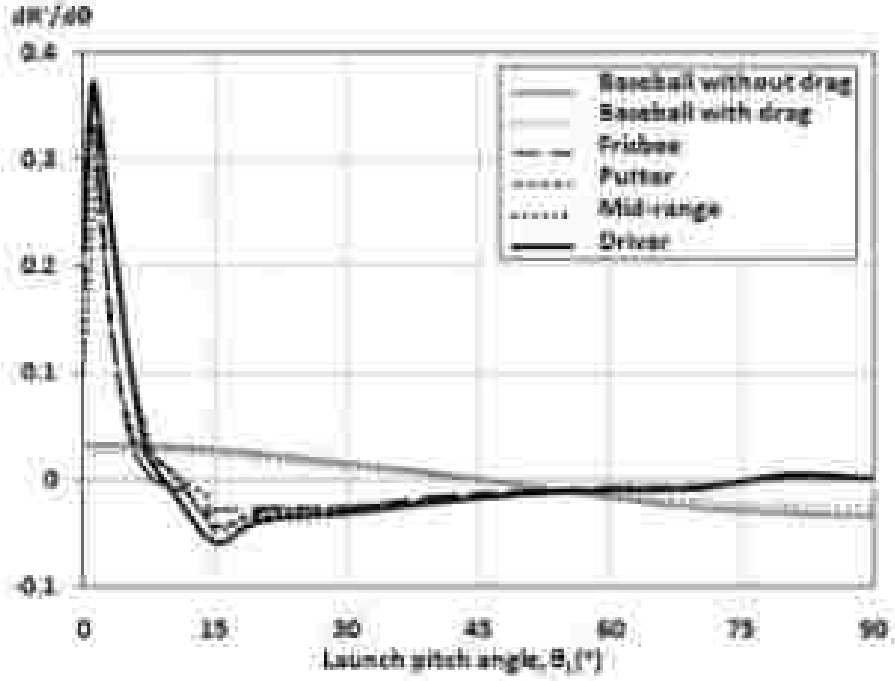

Figure 6.3: Comparison between flying discs with spheres at launch speed 20 m s^{-1}. The flying disc curves generally skewed to the left mainly due to the influence of lift and causes the optimal launch pitch angle to occur at lower values.

6.2 Golf disc flight trajectories

The results in this section only consider the golf disc flight trajectories as a function of launch pitch angles (θ_{I_2}). Each disc was launched with a clockwise direction and the launch pitch angles (θ_{I_2}) vary from 5° to 30°. The remaining initial conditions were as follows: V_I = 20 m s^{-1}, ϕ_I = 0°, α_I = 0°, ψ_I = 0° and AdvR = 0.5. The commercial golf disc models used throughout the simulation to represent the short, medium and long range discs are putter *'Aviar'*, mid-range *'Roc'* and driver *'Wraith'* unless stated otherwise.

The advance ratio in the simulation is fixed at 0.5 as it represents the typical value widely used by players in practice (Potts, 2005; Nathan, 2008). The effect of the advance ratio is briefly explored in the study; it was found that increasing the advance ratio to 1.0 reduces the roll rate but this produces negligible effect on the disc flight range for typical flight trajectories.

6.2.1 XY and XZ plane

Trajectories at varying launch pitch angles (with fixed roll angle)

The golf discs flight trajectories as a function of launch pitch angles in the XY and XZ plane are plotted in Figure 6.4 and Figure 6.5. The golf discs generally have a tendency to bank right (positive roll) initially before banking left for the remainder of the flight as the discs fly through their trim condition. The reason that causes the changes is due to the following. The disc has a negative pitching moment when launched at low angle of attack. As the angle of attack throughout the flight steadily increases due to the incremental value of vertical velocity and reaches its trim angle, the pitching moment becomes positive leading to a negative roll rate with increasing magnitude as shown in the attitude time history in Figure 6.8.

Driver disc then banks sharply to the left followed by the mid-range and putter discs. The results show that for a fixed launch speed, the driver disc produces the greatest range, followed by the mid-range disc and the putter disc. The optimal launch pitch angle for maximum range for the putter, mid-range and driver discs occur approximately at 15°, 10° and 10°, respectively, giving ranges of 51 m, 54 m, and 61 m. Note that the symbols are at fixed time intervals so the disc relative velocity can be inferred by the symbol spacing.

The simulation result agrees well with Potts (2005) findings in which similar behaviour was also observed in the frisbee disc simulation. The golf discs comparison implies that the optimal launch pitch angle is unique to the disc. This means that the optimal launch pitch angle values for other golf disc models would be different; which depends on the disc geometrical shape and their aerodynamic characteristics.

Trajectories at varying launch roll angles (with fixed pitch angle)

Note that the results discussed previously were obtained when the disc launch roll angle (ϕ_0) is fixed at zero (Chapter 4 has stated the default initial conditions for the simulation). It assumes that the launch pitch angle is independent of launch roll angle. If the disc launch roll angle is not fixed at zero, the disc flight direction change more abrupt due to increasing roll rate. Therefore, another case study was simulated to understand the disc behaviour when the launch roll angles were varied from -30° to 30°. The golf disc flight trajectories as a function of launch roll angle in the XY and XZ plane are plotted in Figure 6.6 and Figure 6.7. All parameters remain the same as the previous case study except that the launch pitch angle was fixed at $\theta_0 = 15^0$. The results show that the optimal launch roll angle for the putter, mid-range and driver discs occur approximately at 0°, 5° and 10°, respectively, giving maximum ranges of 50 m, 53 m, and 60 m, respectively. The general trend of increased optimum launch roll angle values from putter to driver disc indicates that the driver roll rate is higher than putter and therefore results in greater range.

In summary, the trajectories result highlights that:

- The disc aerodynamics is a function of disc geometry.
- The disc dynamics is a function of the aerodynamics and disc inertial properties.

The parameter values for maximum range depend on the geometry of the disc and hence, each disc categories have to be thrown with particular initial conditions to achieve maximum range.

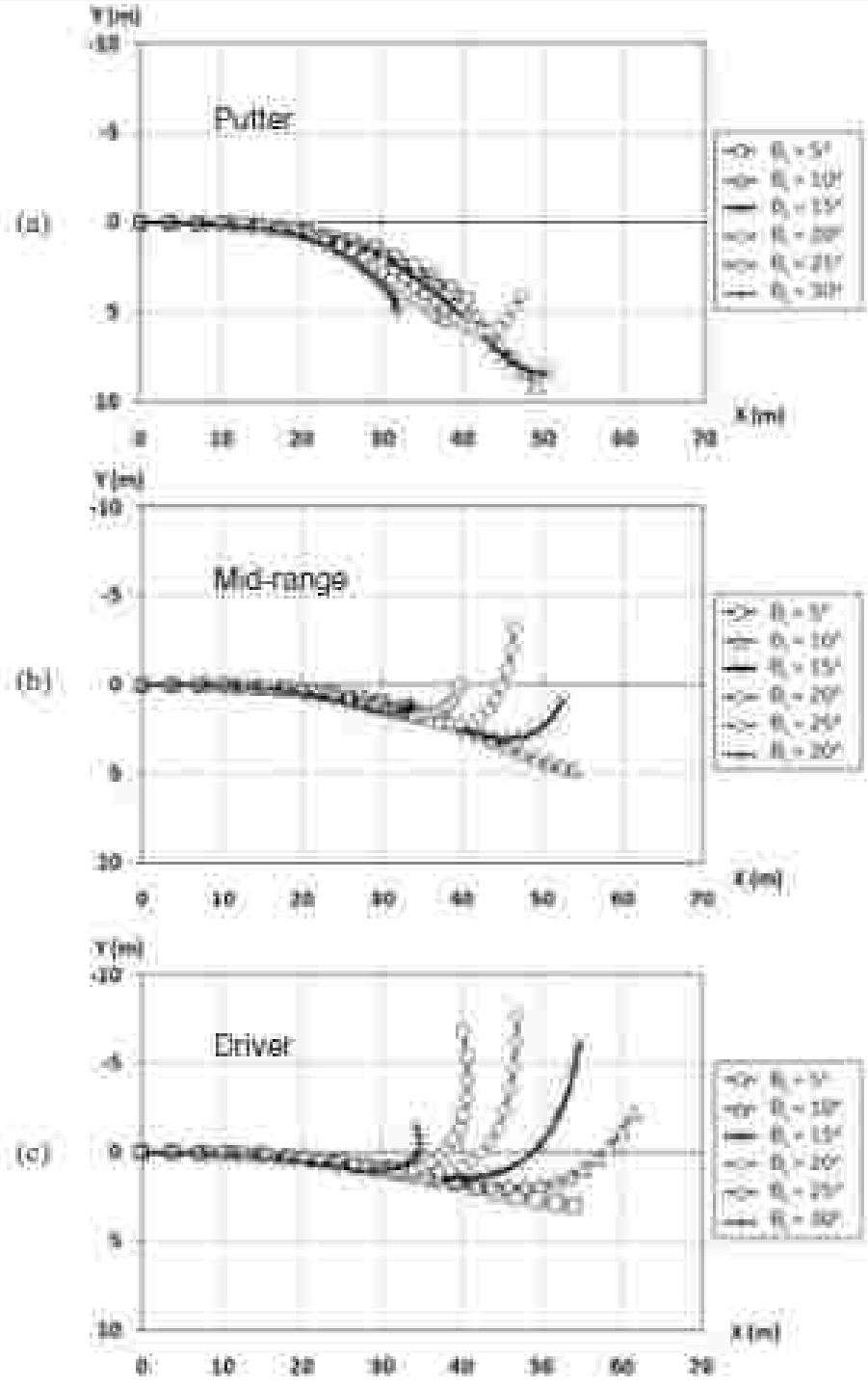

Figure 6.4: Comparison of the (a) putter, (b) mid-range and (c) driver disc in plan view as the launch pitch angles vary from 5° to 30°. The initial conditions are: $V_0 = 20$ m s^{-1}, $\psi_0 = 0°$, $\omega_0 = 0°$, $\gamma_0 = 0°$.

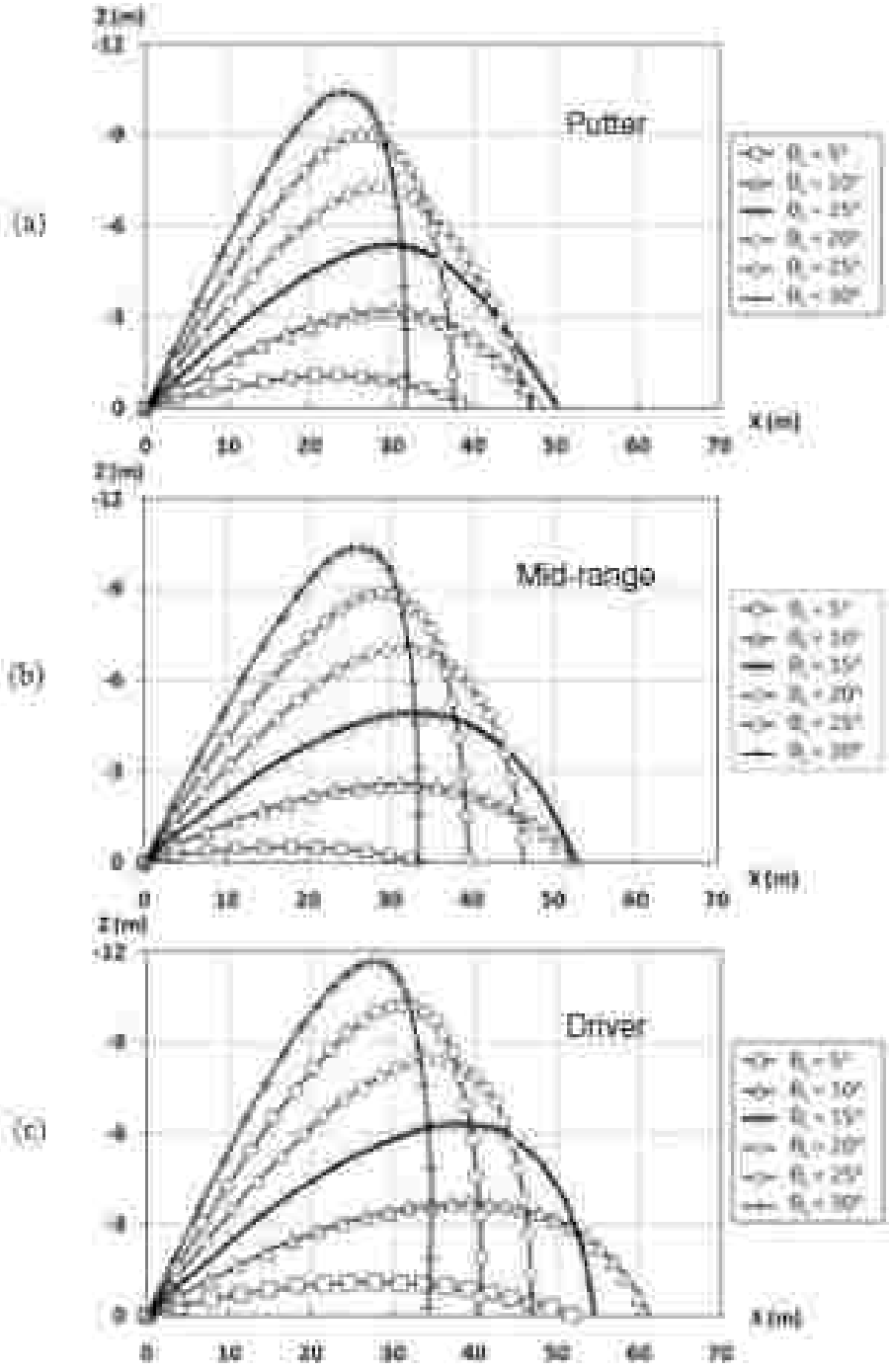

Figure 6.5: Comparison of the (a) putter, (b) mid-range and (c) driver disc in side view as the launch pitch angles vary from 5° to 30°. The initial conditions are: $V_{0,i} = 20\ m\ s^{-1}$, $\varphi_{0,i} = 0°$, $\omega_{0,i} = 0°$, $v_{0,i} = 0°$.

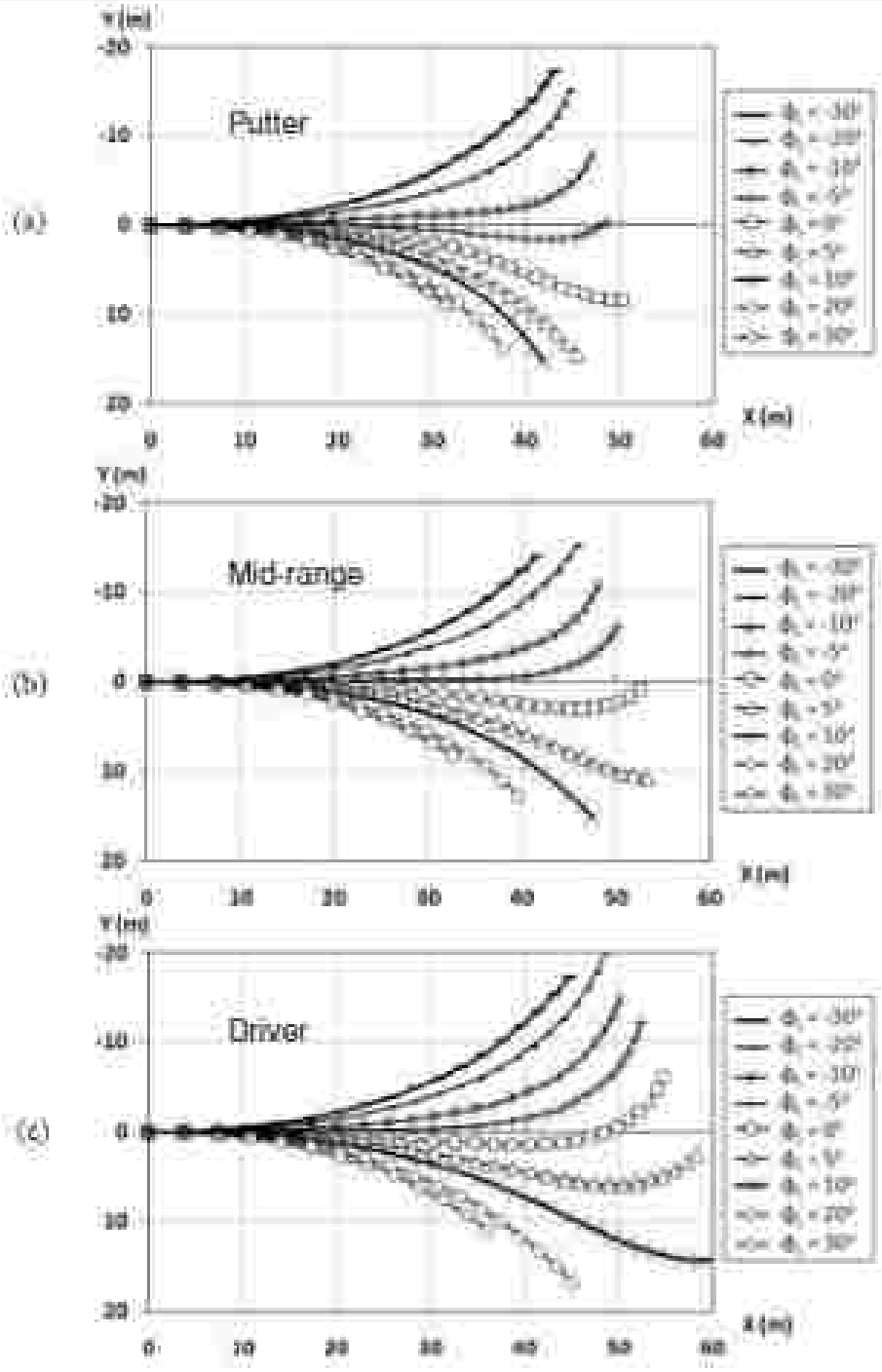

Figure 6.6: Comparison of the (a) putter, (b) mid-range and (c) driver disc in plan view as the launch roll angles vary from -30° to 30°. The initial conditions are: $V_i = 20$ m s^{-1}, $\theta_i = 15°$, $\omega_i = 0°$, $\psi_i = 0°$.

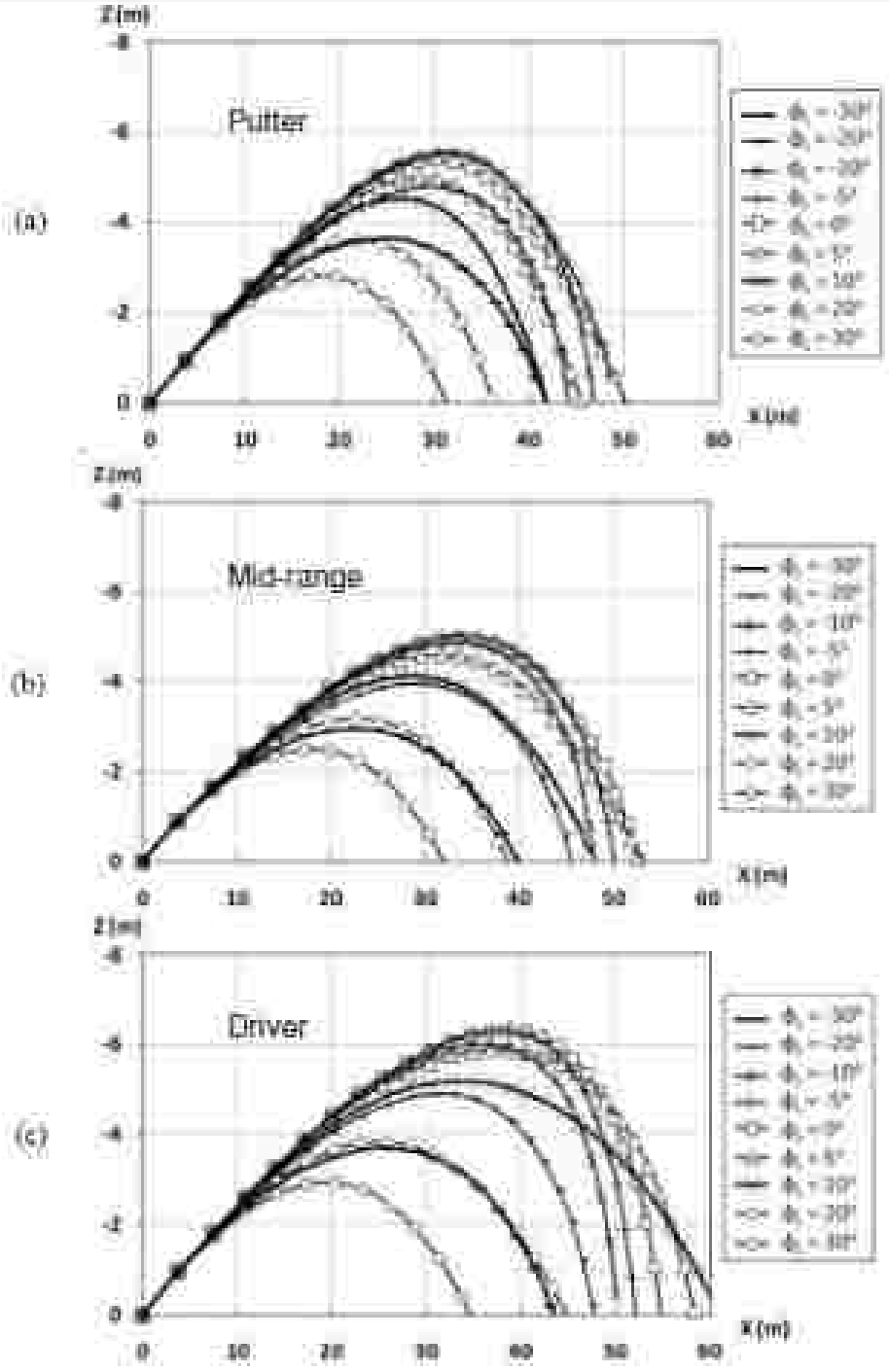

Figure 6.7: Comparison of the (a) putter, (b) mid-range and (c) driver disc in side view as the launch roll angles vary from -30° to 30°. The initial conditions are: $V_C = 20$ m s^{-1}, $\theta_L = 25°$, $\alpha_L = 0°$, $\psi_L = 0°$.

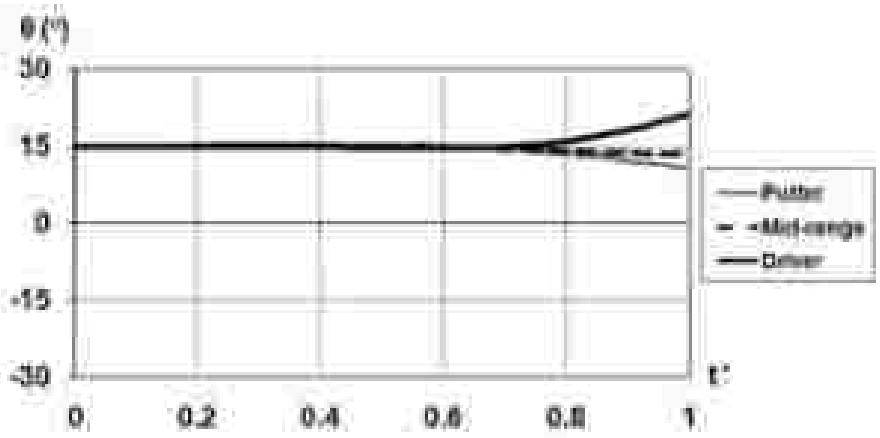

(a) Pitch angle

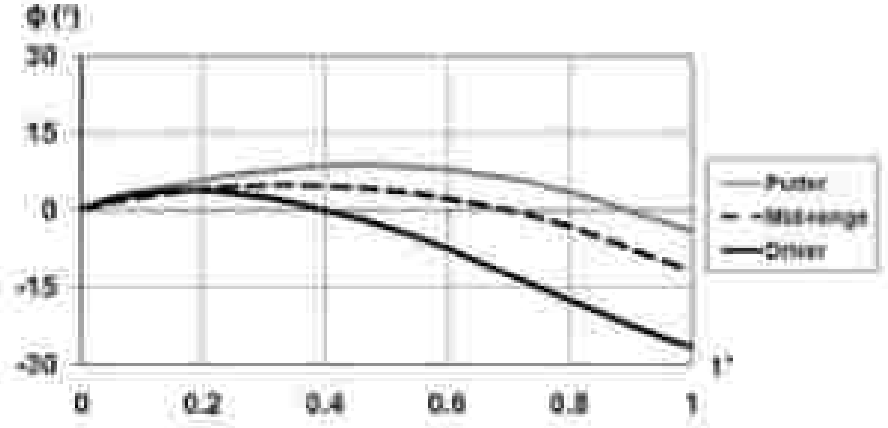

(b) Roll angle

Figure 6.8: Attitude time histories for a typical putter, mid-range and driver discs launched at $V_L = 20$ m s^{-1}, $\theta_L = 15°$, $\alpha_L = 0°$, $\psi_L = 0°$. Note that driver disc roll rate magnitude is higher than mid-range or putter disc (t* is the dimensionless time).

6.2.2 Golf disc landing locations

Figure 6.9 shows the landing locations for the putter, mid-range and driver discs at different launch speed of 15 m s^{-1}, 20 m s^{-1} and 25 m s^{-1}. In this investigation, the launch pitch angle is fixed at $\theta_L = 15°$, with the launch roll angles vary from -30° to 30°. At speed of 15 m s^{-1}, the golf discs produce a 'C' shaped locus. However, as the speed increases to 25 m s^{-1}, the 'C' shaped locus becomes less pronounced. In

sports science, the landing locus plot can be a useful tool to visualise and understand the sensitivity of landing location with respect to launch parameters. Given that a player can influence the landing location of a disc by varying the launch attitude, the landing locus plot would give some insight upon launching the disc to reach maximum distance.

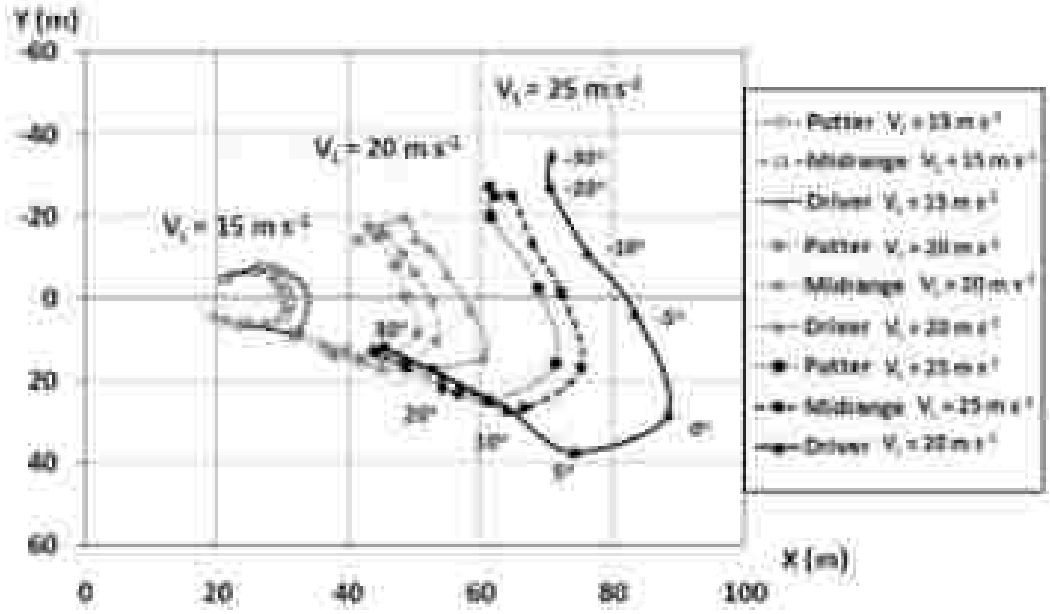

Figure 6.9: The landing locations for putter, mid-range and driver discs as a function of launch roll angles from -30° to 30° at different launch speed. The launch pitch angle is fixed at θ_t = 15° and AdvR = 0.5.

6.3 Effect of release attitude on range

6.3.1 Effect of varying launch pitch angles on range (at fixed launch roll angle)

The variation of launch pitch angles for the putter disc, mid-range disc and driver disc towards range is shown in Figure 6.10. The launch roll angle $\phi_{x,t}$ is fixed at 0° with launch pitch angles varying from 0° to 30°. As expected, the driver disc

produces the greatest range compared to the mid-range disc and the putter disc. However, the difference between the maximum range of the putter and driver discs is not so much as expected based on their difference in geometric parameters. Based on the simulation results, the local optimal launch pitch angle for the putter, mid-range and driver discs occur approximately at 13°,12° and 9°, respectively, for maximum range of 52 m, 55 m and 63 m as shown in Table 6.1. The value of local optimal launch pitch angles and the corresponding value of maximum range in this analysis is different from the value in the flight trajectories analysis (Section 6.1) due to the angle interval. In the flight trajectories analysis, the golf discs were simulated with 5° interval to capture the general trend of the golf discs flight trajectories as the launch pitch angles vary. Whereas in this analysis, the golf discs were simulated with 1° interval to determine more accurate local optimal launch pitch angle that corresponds to the maximum range.

The graph indicates that the launch pitch angle is a sensitive parameter influencing the maximum range as is expected. Note that the local optimal launch pitch angle value at which maximum distance occurs generally decreases from short-range disc to long-range disc due to the different aerodynamic characteristics of the discs.

Disc	Maximum distance (m)	Optimal launch pitch angle (θ_L)
Putter	52	13°
Mid-range	55	12°
Driver	63	9°

Table 6.1: The golf discs local optimal launch pitch angles that correspond to the disc maximum distance at $\phi_L = 0°$.

6.3.2 Effect of varying launch roll angles on range (at fixed launch pitch angle)

The effect of varying launch roll angles from -60° to 60° is shown in Figure 6.11. In this case, the launch pitch angle (θ_L) is fixed at 15°. The results in this study also found that the difference in between the maximum range of the putter and driver disc is not so large as expected. The local optimal launch roll angle for the golf disc occurs at -5°, -2° and 3° for the putter, midrange and driver, respectively, for maximum range of 51 m, 54 m, 64 m as shown in Table 6.2. The result shows that range is sensitive to launch roll angle, as well as the launch pitch angle simulated in the previous case. In contrast to the case of launch pitch angle, the local optimal launch roll angle value trend generally increases from short-range disc to long-range disc. For positive launch roll angle case, the disc distance generally reduces as the launch roll angle increases. While in the case of a negative launch roll angle, the disc distance reduces as the launch roll angles become more negative.

Disc	Maximum distance (m)	Optimal launch roll angle (ϕ_L)
Putter	51	-5°
Mid-range	54	-2°
Driver	64	3°

Table 6.2: The golf discs local optimal launch roll angles that correspond to the disc maximum distance.

Concluding remarks

It is already established in the projectile study that range is generally influenced by two parameters; the speed and the launch angle. In this thesis, the launch speed in the simulation is fixed to eliminate the influence of speed on range (as the range is proportional to the square of speed and each player has a maximum achievable launch speed). By doing this, it can focus the influence of launch angles (pitch and roll) on disc range. As a result, the thesis found that golf disc range is sensitive to

launch pitch angle and launch roll angle which modified the maximum disc distance. In addition, the optimal launch pitch angle and optimal launch roll angle are unique to the disc. This information would give a player some insight to manipulate their disc upon launching to achieve maximum distance. The roll rate also has substantial effect on the disc range as disc designed with more streamlined geometry like driver produces higher roll rate that eventually increases the range. However, the most significant results from the simulation show that the difference in between the maximum range of the putter and driver discs is not so large despite their differences in the geometry.

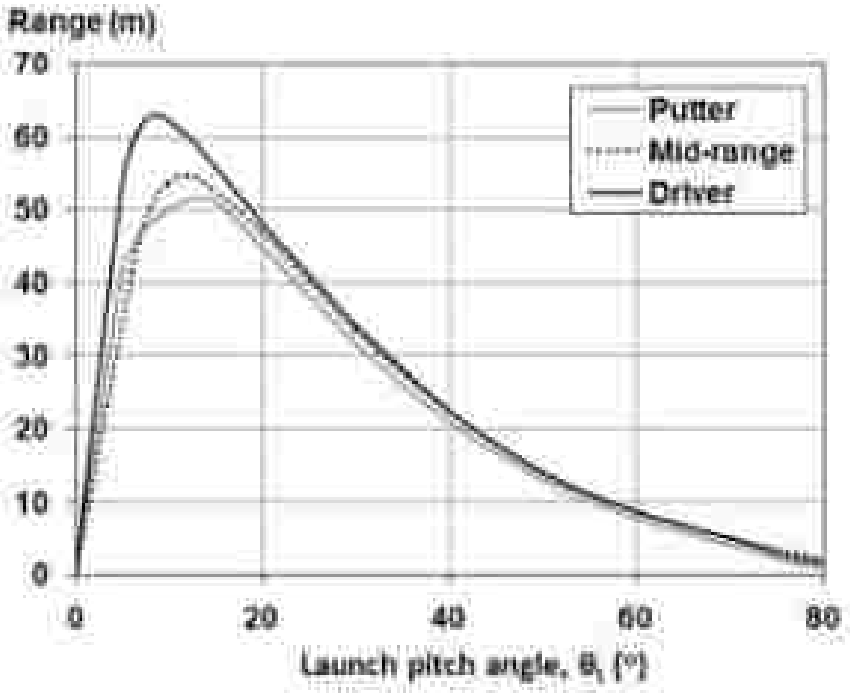

Figure 6.10: The effect of varying launch pitch angles towards range for putter, mid-range and driver discs. $V_L = 20$ m s^{-1}, $\Phi_L = 0°$, $\Phi_R = 0°$, $\Psi_L = 0°$, Adv$R = 0.5$.

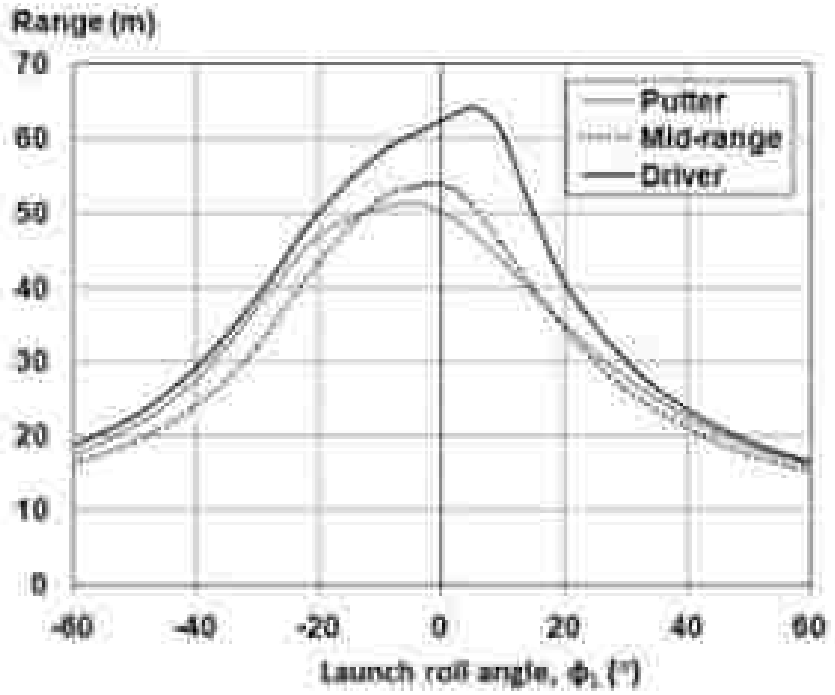

Figure 6.11: The effect of varying launch roll angles towards range for putter, mid-range and driver discs. $V_L = 20$ m s^{-1}, $\theta_L = 15°$, $\Omega_L = 0°$, $V_w = 0°$, Adv$R$ = 0.5.

6.4 Golf disc range and sensitivity

The thesis has established that the variation of disc geometry did change the disc aerodynamic characteristics as the quantitative data measured in the wind tunnel study support this. The changes eventually influence the disc performance in terms of the range as demonstrated in the comparison of short, medium and long range discs simulation. Of particular interest now is how these results can be interpreted to help the player improve their performance in the game. This section will discuss the relationship derived from the disc range with respect to changes in the launch conditions – the disc range sensitivity. A scheme to match the skill level of a player with the type of discs thrown to achieve a given target distance will be introduced. Note that the analysis only varies the launch pitch angles with respect to range. It is felt that these results are sufficient enough to demonstrate the relationship of disc

range with respect to the changes in launch conditions and how the disc range sensitivity is interpreted.

6.4.1 Disc range sensitivity as a function of launch pitch angles

First, it is important to highlight that there are two parameters that contribute to a successful flying disc game; the player accuracy combined with the disc sensitivity. It is also important to note that this thesis will only consider the disc sensitivity, as the player accuracy requires biomechanics study which is beyond the scope of this thesis. As described in Chapter 3 (Theory), the disc range can be associated with the changes of the launch conditions. This relationship will be called as disc range sensitivity from hereafter and to simplify the analysis, it can be classified as the following:

- Zero sensitivity means that any changes of the initial launch conditions would result in zero changes in the landing distance.

- As range sensitivity value increases, it means that any changes of the initial launch conditions would result in more divergence from the target distance. This suggests that the disc is more difficult to be launched and becomes less accurate at hitting the target distance.

- The level of difficulty is quantified by the width of the peak bucket, with wider width can be associated with a less sensitive disc and therefore easier to be launched. In contrast, narrower width can be associated with a more sensitive disc and therefore difficult to throw.

In Chapter 3 (Theory), an example to illustrate the basic theory of the relationship derived for the range with respect to the changes of initial conditions for a sphere has been demonstrated. As disc is more complex, the range could not be obtained

directly as in the sphere case because the disc governing equations can only be solved numerically. Therefore, the simulation is used to determine the disc range. The disc range sensitivity is then measured similar to the method demonstrated in the sphere range sensitivity.

The results in Figure 6.12 to Figure 6.15 show the plot of range with respect to launch pitch angles as a function of launch speeds for the putter and the driver discs, in dimensional and dimensionless forms. The plots shown in Figure 6.12 (a) and Figure 6.13 (a) represent the putter and driver disc dimensional range variation with respect to launch pitch angle as a function of launch speed. As expected, the disc range increases as the launch speed rises with the driver disc has a higher maximum range than the putter disc. When these results are associated with Figure 6.12 (b) and Figure 6.13 (b) that represents the data for changes of range with respect to the changes of launch pitch angle, the following information can be extracted:

- Zero sensitivity (at which changes of range with respect to the changes of launch pitch angle is zero ($dR/d\theta=0$) occurs at the maximum range.
- The shape of the peak bucket for the putter disc is generally wider than the driver disc.
- The trend of local optimal launch pitch angle that corresponds to maximum range generally decreases as the launch speed increases regardless of the golf disc categories.

In order to provide some insight to relate to the player skill level with the type of discs thrown, the extracted information can be interpreted as the following. The driver disc is generally more sensitive than the putter disc as indicated by the narrow width of the peak bucket. Although the driver disc produces a greater distance, they are highly sensitive to the changes in launch conditions which made them difficult to be thrown at launch. In contrast to driver disc, the putter disc typically covers a much shorter distance but they are less sensitive to the changes in launch conditions and therefore, easier to be controlled at launch. This suggests that disc designed for

long range requires a greater skill to throw compared to disc designed for short range.

In regards to the local optimal launch pitch angle trend that corresponds to disc maximum range, it highlights some important aspect to be considered by the player particularly the launch speed. Based from the results shown in Figure 6.14 and Figure 6.15, if the player decides to throw the disc with a low launch speed, it is advisable for the player to throw their disc at high launch pitch angle as this action is more favourable to produce a greater distance. In contrast to that, if the player decides to throw the disc with a high launch speed, it is perhaps best for the player to throw their disc at low launch pitch angle for the same reason stated previously.

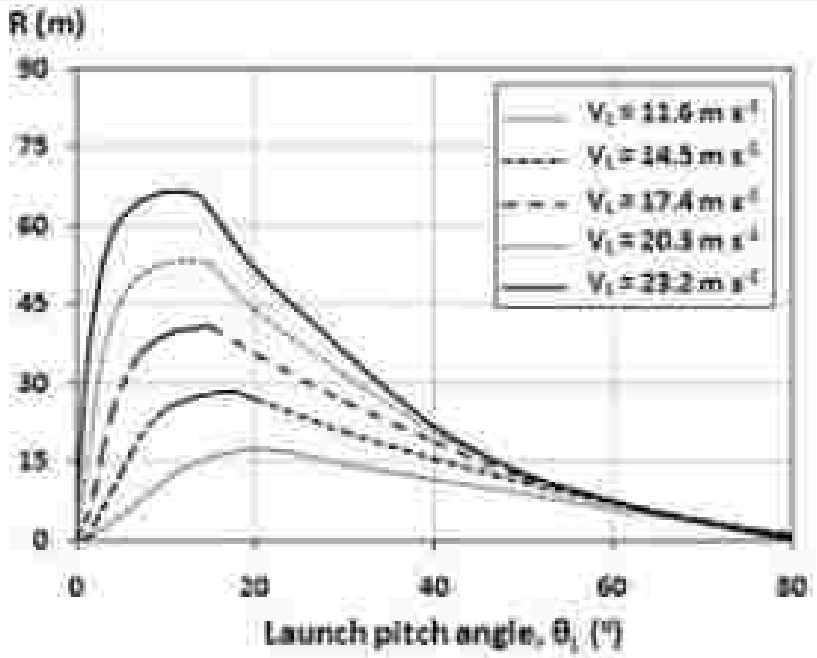

(a) Range at different launch speed for putter disc.

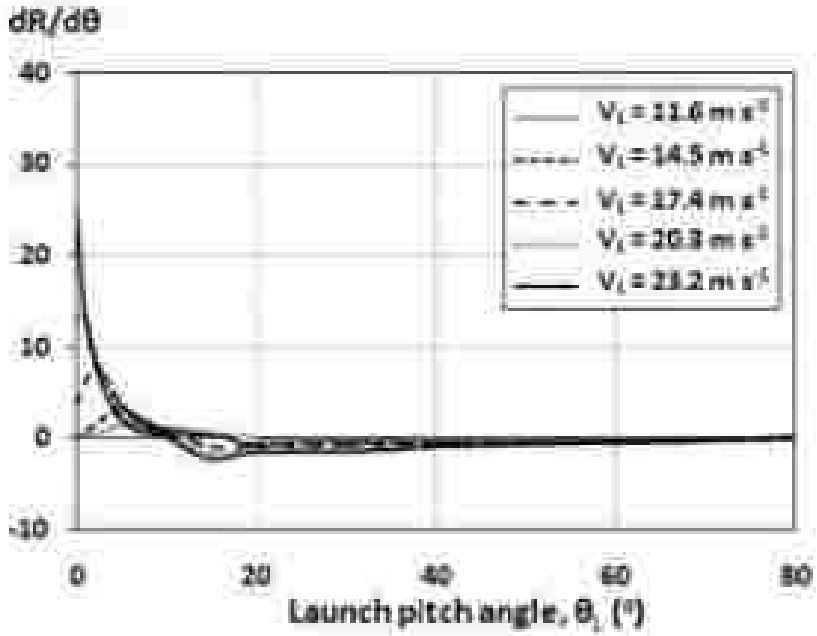

(b) The change of range with respect to launch pitch angles at varying launch speed for putter disc.

Figure 6.12: Dimensional comparison of putter disc launched at varying launch speed. The shape of the peak bucket in generally wider indicates that putter disc is less sensitive to the changes in launch conditions.

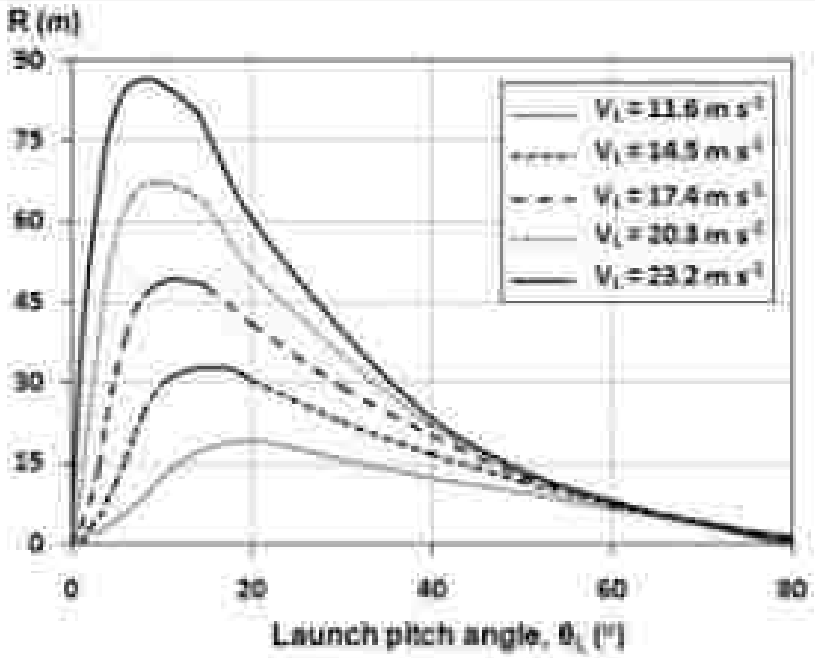

(a) Range at different launch speed for driver disc.

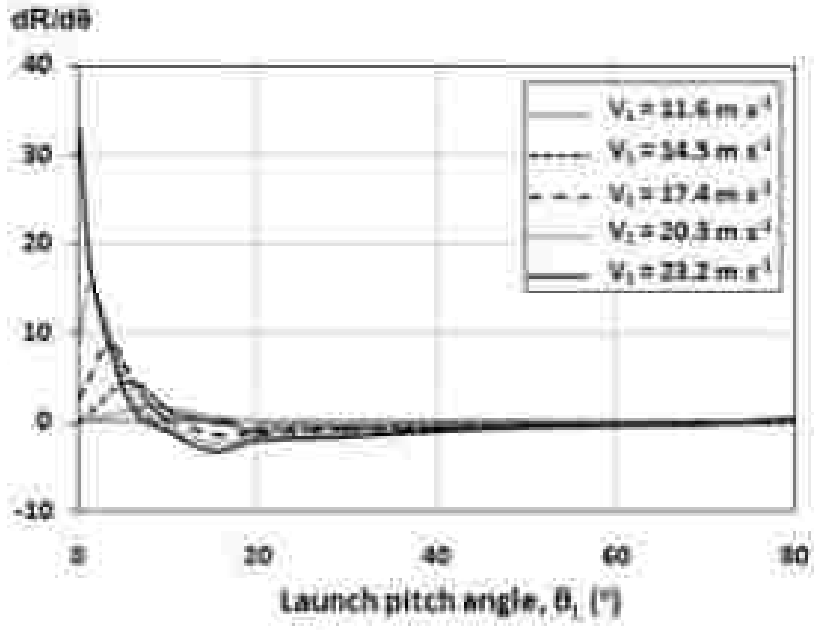

(b) The change of range with respect to launch pitch angles at varying launch speed for driver disc.

Figure 6.13: Dimensional comparison of driver disc launched at varying launch speed. The shape of the peak bucket is generally narrow indicates that driver disc is more sensitive to the changes in launch conditions.

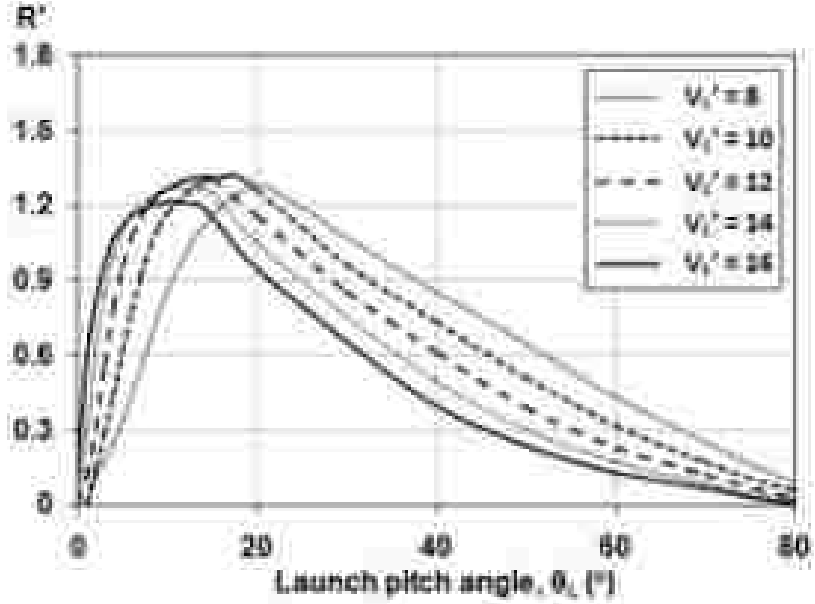

(a) Dimensionless range at different launch speed for putter disc.

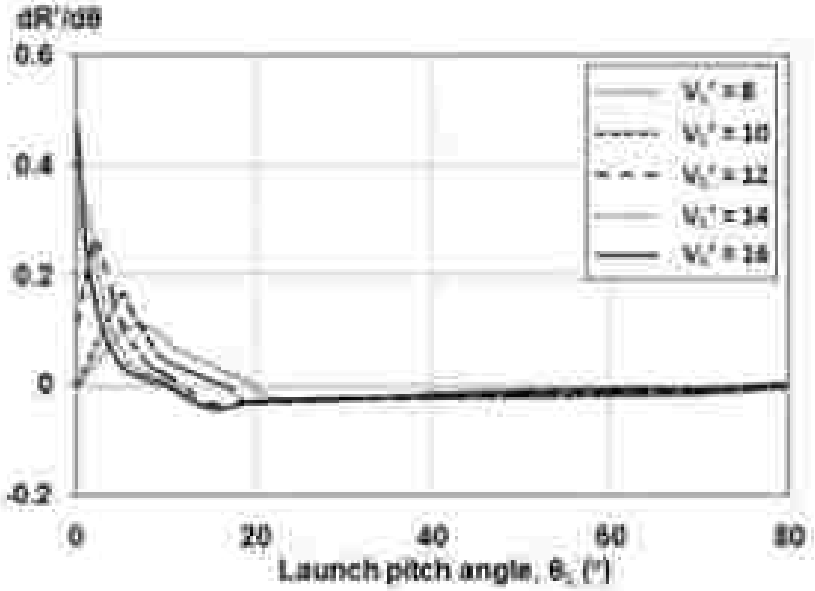

(b) The change of dimensionless range with respect to launch pitch angles at varying launch speed for putter disc.

Figure 6.14: Dimensionless comparison of putter disc launched at varying launch speed. The optimal launch pitch angle generally increases as speed reduces and the most favourable shot occurs at $dR'/d\theta = 0$ as range sensitivity is zero at this point.

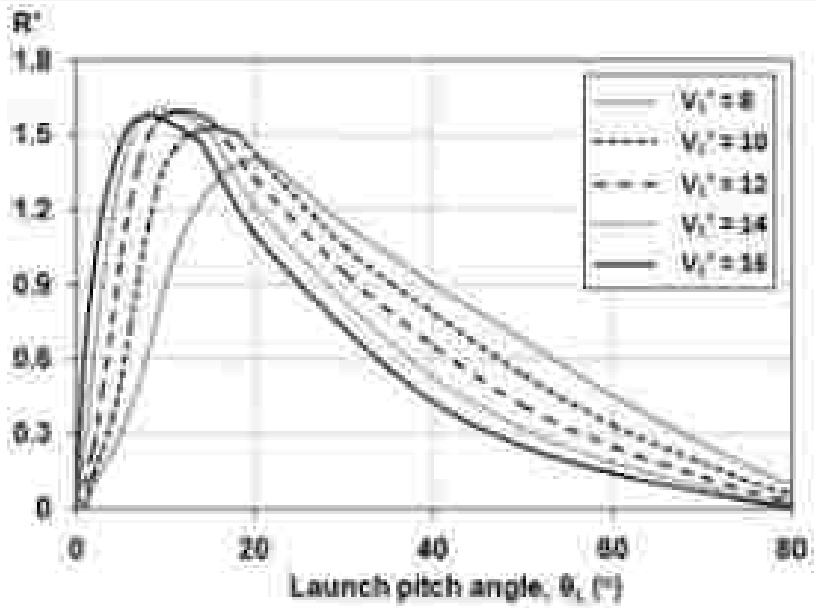

(a) Dimensionless range at different launch speed for driver disc.

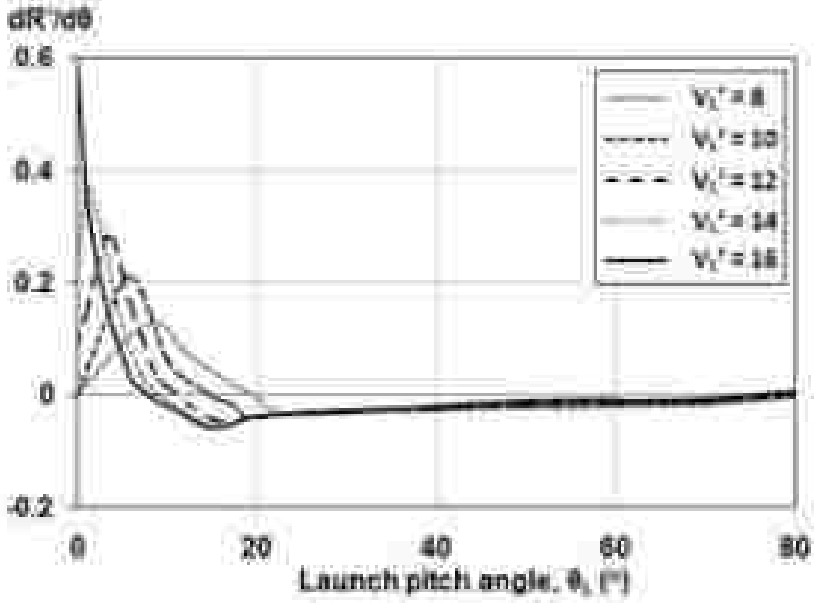

(b) The change of dimensionless range with respect to launch pitch angles at varying launch speed for driver disc.

Figure 6.15: Dimensionless comparison of driver disc launched at varying launch speed. The optimal launch pitch angle that corresponds to zero sensitivity generally increases as speed reduces.

6.4.2 Golf disc favourable shot

The previous results lead to another interesting aspect to be considered. If the player decides to throw a disc to hit a desired maximum range, the following information offers some insight. If observed carefully in Figure 6.12 (a) or Figure 6.13 (a), each maximum range has a minimum launch speed required. It is indicated by the peak of the graph and corresponds to zero value in Figure 6.12 (b) and Figure 6.13 (b). It can be considered as the most favourable shot as range sensitivity is zero at this point.

To better understand the situation, assume the player aim to throw a putter disc at about 52 m. In Figure 6.12 (a) that represents the putter disc plot, maximum range of 52 m occurs at launch speed of approximately 20.3 m s^{-1} with local optimal launch pitch angle of 13°. The player can aim to launch the disc at the stated launch conditions. However, if the player decides to throw the disc at higher launch speed, they have two available launch shot options. They can either throw it with "skimmer shot" (low) or "lob shot" (high).

A skimmer shot in this case is illustrated as positive slope of the graph and can be defined as the shot at which the launch angles are less than the local optimum launch pitch angle. Whereas a lob shot is illustrated as negative slope of the graph and can be defined as the shot where the angles are more than the local optimum launch pitch angle. Both shots would give the same maximum range value of 52 m. This is due to the fact that the maximum range does not only occur at the minimum speed required, but also occurs at a higher speed and both shots can reach the desired maximum range. However, it is important to note that if the player throws the disc less than the minimum speed required, the desired maximum range will fail to be achieved as demonstrated in the simulation result.

The next interesting aspect that is worth to be considered is the favourable shot. Based on the graph of Figure 6.14 and Figure 6.15, the most favourable shot is at the optimal launch pitch angle at which the maximum range occurred. This is due to the

fact that changes of range with respect to the changes of launch pitch angle is zero ($dR/d\theta = 0$). In practical, this shot is only possible if the player knows the specific local optimal launch pitch angle for their disc (although it would be difficult to throw the disc exactly at this angle). However, assuming that a player does not know that value and usually would opt to have either a low shot or a high shot to reach maximum distance, therefore it is important to identify which shot is more favourable. The results suggest that the high shot is more favourable than the low shot. This is due to the low range sensitivity values of high shot compared to low shot which can be seen clearly from the slope.

In summary, the golf discs sensitivity that relates the disc categories with the player skill level is illustrated in Figure 6.16.

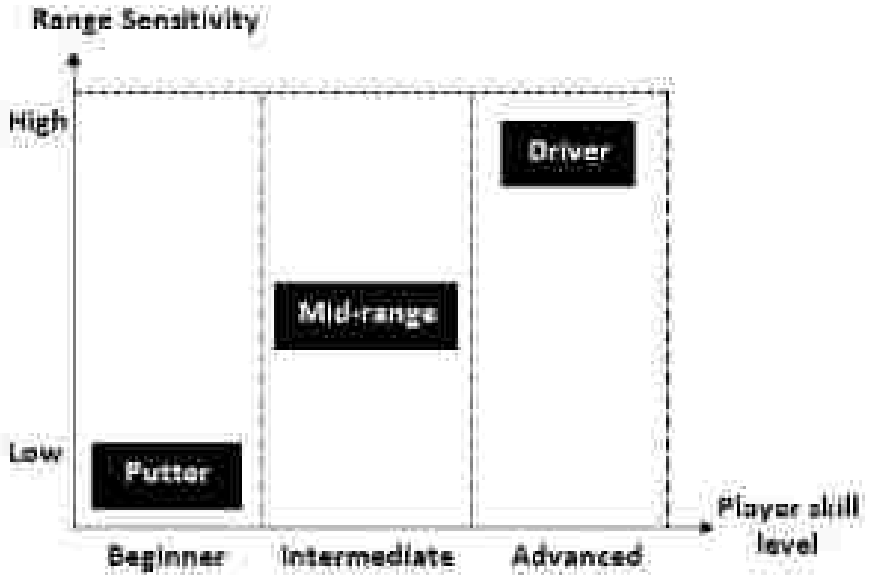

Figure 6.16: Discs designed for long range such as driver is highly sensitive to the changes in launch conditions and therefore, requires a greater skill to control. In contrast, putter disc typically covers a much shorter distance but they are less sensitive to the changes in launch conditions and therefore; easier to control at launch.

Chapter 7

Conclusions and Future Work

This thesis has studied the aerodynamics and flight dynamics of flying discs. A review of the study of flying discs, especially those used in sports, and the flight performance of other relevant sports objects were given in Chapter 2. The review highlighted the need to investigate the relationship between the designs of discs and their flight performance, particularly the range covered during flight. For this purpose, experimental and computational investigations were performed on three types of golf discs – putter, mid-range and driver discs; in addition, a number of parametric disc models were used to experimentally isolate the effect of important design features on the disc aerodynamic characteristics. Note that disc parametric study (for low aspect ratio wing less than two) has never been performed previously.

This chapter provides conclusions to the results of this work and highlights the original contributions of this work on the study of flying discs. It evaluates the achievements of the goals set forth at the beginning of the thesis and identifies some limitations of the study. Some recommendations for future work are also suggested.

7.1 Concluding remarks

1. *The experimental result shows that practical discs need to have cavities for satisfactory flying qualities.*

    - The main aerodynamic characteristic influenced by the disc cavity is the pitching moment. The experimental result demonstrates that the presence of this cavity produces a significant aft shift in the aerodynamic centre position (x_{ac}) such that the pitching moment about the centre of the disc is substantially zero for an angle of attack ranging from 0° to 7°.
    - The shift in the aerodynamic centre means that the disc will have a minimal tendency to roll about the flight axis and therefore, require less skill to throw towards a given target, and achieve a greater range

compared to a disc with the same lift-to-drag ratio (*L/D*) but with strong roll divergence.

2. *Disc thickness influences the aerodynamic characteristics of golf discs, particularly the drag.*

   - Thickness has a significant effect on drag through an increase in the profile drag. As the lift is largely unchanged by the thickness, the induced drag (lift-dependent) component is similar between discs of different thickness.
   - There is evidence from the flow visualization study that changing the thickness eventually changes the extent of the upper surface leading edge separation bubble. This behaviour as well as the profile drag has a significant contribution to the overall drag.

3. *The overall effect of fairing (i.e. rounding or tapering) the circumferential edge is to increase the lift-to-drag ratio of the disc for the range of angles of attack tested compared to the non-fairing case.*

   - The experimental result demonstrates that the effect of fairing on the disc leading or trailing edge significantly reduces the drag compared to the non-fairing case over the range of angles of attack tested. Between the faired profiles, the sharp edge disc performs better where its lift-to-drag ratio is higher than that of the rounded profile, particularly at higher angles of attack.

4. *The performance of a free flying disc does not depend on the lift-to-drag ratio (C_L/C_D) alone such as for a typical aircraft, but also the pitching moment, because the disc does not reach a steady dynamic state flight as the aerodynamic and flight dynamics are constantly changing due to its spin.*

- The experimental result shows that the driver disc is designed to have a relatively higher lift-to-drag ratio compared to the putter disc over the range of angles of attack tested. Although the putter disc has a low lift-to-drag ratio, it has the advantage of reduced nose-down pitching moment (as a result of the position of the aerodynamic centre located closer to the disc centre of gravity) which leads to a minimal tendency to roll about the flight axis.
- The range of a trimmed fixed-wing flying vehicle is directly proportional to its lift-to-drag ratio. In contrast, the range of a disc is influenced by both its lift-to-drag ratio and its pitching moment, which is coupled to the disc rolling motion via its spin. Although the driver has the highest lift-to-drag ratio, its actual range is reduced from a potentially larger range due to this rolling motion.

5. *The difference between the range of the short and long range discs is small and not as large as expected because disc dynamics and trajectories vary widely throughout the flight.*

- The putter disc has a maximum range that is 21% less than that for a driver disc, while the mid-range disc has a maximum range that is 12% less than that for a driver disc. Meanwhile, the putter disc has a maximum C_l/C_D that is 24% less than that for a driver disc, while the mid-range disc has a maximum C_l/C_D that is 20% less than that for a driver disc.
- The range computed from the disc simulation measures the ground range (between the launch to landing point) instead of the actual ground distance followed by the disc trajectory. A more curved disc trajectory reduces the maximum potential range it could achieve. The range of a driver disc is less than expected because of its more curved flight path compared to that of the putter disc.

6. *A novel method to quantify disc sensitivity with respect to changes in launch conditions has been developed.*

   - This approach of quantifying the disc sensitivity is useful because it provides a method to determine the ability to 'control' the disc when throwing it at a target: a less sensitive disc is easier to control compared to a more sensitive one. As the control of a disc can be related to the difficulty level of throwing the disc, the sensitivity analysis could be used as a metric to analyse the skill level required to throw the disc, or other objects in general (e.g., ball, discus, javelin, etc).
   - The simulation result shows that different flight characteristics exist between the long and short range disc.
   - A driver disc can fly the furthest but was highly sensitive to divergence from the optimal release conditions. A putter disc typically covers a much shorter distance but was less sensitive to throwing perturbations.
   - A correlation exists between skill level and divergence from the intended target position. Discs designed for long range require a higher skill level compared to discs designed for short range.

7.2 Future research recommendations

The thesis has established the mapping between the geometry of a disc and its aerodynamic characteristics and subsequently its flight dynamics. The findings in this study can be utilized or extended to benefit a number of related works. These potential future works are described below.

1. *The performance of an athlete based on his or her throwing accuracy could be assessed quantitatively by combining the study of disc sensitivity and the biomechanics of disc throwing.*

- The overall performance of a disc to achieve its goal (of reaching a target) in reality is a combination of the disc sensitivity and the athletic throwing accuracy. The disc sensitivity determines its chances of reaching a certain target given a tolerance in the input conditions. The throwing accuracy of a player, on the other hand, describes his or her ability to produce consistent throws. While the sensitivity of a disc has been shown in this work to be quantifiable using flight simulations, the quantification of a player's throwing accuracy (i.e. his or her ability to reproduce similar or identical repeatable throwing actions) requires knowledge on the biomechanics of throwing. By using a point-mass sphere for a demonstration, a method is proposed here to couple variables related to both aspects of disc performance (i.e. sensitivity and accuracy) based on the technique of analysing uncertainty (BSI, 2003). The overall uncertainty dR of reaching a desired target range when throwing a sphere, given that only two independent variables can be varied, is given as

$$dR = \sqrt{\left(\frac{\partial R}{\partial V} dV\right)^2 + \left(\frac{\partial R}{\partial \theta} d\theta\right)^2} \qquad (7.1)$$

where dV is the change in the launch speed and $d\theta$ is the change in the launch pitch angle. The values for $\frac{\partial R}{\partial V}$ and $\frac{\partial R}{\partial \theta}$ are the measures of the 'sphere sensitivity' to initial launch conditions, which depends on the value of the initial launch speed V_o and the initial launch angle θ_o. However, the values for dV and $d\theta$ measures a player's throwing accuracy. These accuracy measures depend on a player's unique throwing skills which differ between players; these values can only be measured through field experiments. Note that the square root summation follows the basic technique of summing uncertainties for

a number of independent variables to obtain the total uncertainty dR of a parameter R as expressed below:

$$dR = \sqrt{\sum \left(\frac{\partial R}{\partial x_i} dx_i\right)^2}. \quad (7.2)$$

In the case of throwing a disc, where R is range, then dx_i is the change in the independent launch variables and $\frac{\partial R}{\partial x_i}$ is the change of range with respect to the change of the launch variables.

2. *The experimental data can be used as a benchmark to validate computational fluid dynamics (CFD) study. The understanding of complex airflow around disc with a cavity could be enhanced using the tools of CFD. Parametric variations of various design features could be performed much faster and more efficiently with better visualization techniques.*

- The aerodynamics of golf discs have been evaluated experimentally in this study from wind tunnel experiments. These experiments, albeit valuable, were time consuming, challenging particularly when dealing with equipment malfunctions, and limited in terms of the type of information collected. These limitations could be addressed and minimized by studying the same problem using CFD tools. The data gathered herein from experiments can serve as the benchmark data to validate any CFD study.
- Following a proper validation, a CFD study could be fully utilized to expand the current study. One example would be to extend the parametric study in this work by including other design parameters not included here. In addition, the aerodynamic analysis could be detailed further by extending the regimes of angles of attack, to include more pronounced stages of flow separation, or varying the flow speeds to study the effect of Reynolds number on flow regimes

beyond those common to low-speed disc flight, i.e. for medium to large a Mach number flow. More importantly, the effect of disc geometrical properties could be studied in more details with relative ease.

- These computational analyses are useful as they provide further understanding on disc aerodynamic characteristics, as well as allow improvement on disc design at low cost.
- More uniquely, a CFD study would allow one to visualize the flow dynamics with greater details at various configurations. Based on the findings in this thesis, it would be interesting to be able to visualize the flow dynamics underneath a cavity with greater detail. It should also be possible to track how the complex flows inside the cavity evolve with varying angles of attack, for example. Studying the evolution of tip vortex around disc side edges could also prove to be important with respect to the overall disc aerodynamics and flight dynamics.

3. *The optimization of disc geometric parameters requires some compromise in design.*

- It is clear from the study that minimizing the pitching moment is necessary to improve disc stability; however, the parametric study shows that this minimization (i.e., increasing the cavity height) also increases the drag. As such, specific design requirements on a disc must be tailored to the purpose of the disc – for example, a long distance disc must be designed to have low drag characteristics while a disc designed for high accuracy must have minimal pitching moment characteristics.
- In this regard, a future work is recommended to study the detailed effect of combining different disc features for specific purposes. This detailed analysis could be used to identify dominant geometrical features associated with any required flight characteristics. Such

study could be of immediate interest to improve the efficiency of flying discs in any practical applications (e.g., sports, military projectile, etc). Another future work could focus on the fundamental aspect of a flying disc with regards to the different disc geometrical features studied in this thesis. Here, detailed experimental and/or computational studies could be conducted to understand how each disc feature influence, or govern, the flow dynamics surrounding the disc. Understanding gained from this type of fundamental study on flow dynamics could help identify better disc geometries (not studied in this thesis) that could have superior flying qualities.

References

Abbott, I. H. and Von Doenhoff, A.E., 1959. Theory of Wing Sections: including a summary of airfoil data, Dover Publications.

Achenbach, E., 1971. Influence of surface roughness on the cross-flow around a circular cylinder. Journal of Fluid Mechanics, 46 (02), p. 321.

Achenbach, E., 1972. Experiments on the flow past spheres at very high Reynolds numbers. Journal of Fluid Mechanics, 54 (03), p. 565.

Achenbach, E., 1974. The effects of surface roughness and tunnel blockage on the flow past spheres. Journal of Fluid Mechanics, 65 (01), p. 113.

Alaways, L.W. and Hubbard, M., 2001. Experimental determination of baseball spin and lift. Journal of Sports Sciences, 19 (5), pp. 349-58.

Anderson JR, J.D., 2007. Fundamentals of Aerodynamics, McGraw-Hill.

Ashley, H. and Landahl, M., 1985. Aerodynamics of Wings and Bodies, Dover Publications.

Barlow, J.B., Rae, W.H. and Pope, A., 1999. Low-speed wind tunnel testing, John Wiley & Sons.

Bartlett, R.M., 1992. The biomechanics of the discus throw: a review. Journal of Sports Sciences, 10 (5), pp. 467-510.

Bartlett, R. M., 2000. Principles of throwing. Biomechanics in Sport: Performance Enhancement and Injury Prevention (edited by Zatsiorsky, V.M.), pp. 365-380.

Bartlett, K., Best, R.J. and Borgstrom, A., 1995. The throwing events at the World Championships in Athletics 1995, Göteborg – technique of the world's best athletes, part 2: Discus and javelin.

Bartlett, K., 2000. Javelin Throwing: An Approach to Performance Development, (edited by Zatsiorsky V.M. Biomechanics in Sport: Performance Enhancement and Injury Prevention, pp. 401–434.

Bearman, P.W. and Harvey, J.K., 1976. Golf Ball Aerodynamics. Aeronautical Quarterly, 27, pp. 112-122.

Best, R.J., Bartlett, R.M. and Sawyer, R.A., 1995. Optimal javelin release. Journal of Applied Biomechanics, 11, pp. 371-394.

British Standards Institute, 2003. General metrology – Part 3: Guide to the expression of uncertainty in measurement.

British Standards Institute, 2004. General metrology – Part 4: Practical guide to measurement uncertainty.

Carre, M.J., Asai T, Akatsuka, T. and Haake, S.J., 2002. The curve kick of a football II: flight through the air. Sports Engineering, 5 (4), pp. 193-200.

Chiu, C.-hua, 2009. Estimating the Optimal Release Conditions for World Record Holders in Discus. International Journal of Sport and Exercise Science, 1 (1), pp. 9-14.

Chiu, C.-hua, 2009. Discovering Optimal Release Conditions for the Javelin World Record Holders by Using Computer Simulation. International Journal of Sport and Exercise Science, 1 (2), pp. 41-50.

Cotroneo, P. W., June 1980. Biomechanical and Aerodynamical Aspects of the Backhand and Sidearm Frisbee-Disc Throws for Distance. MS Thesis, California State University.

Crowther, W.J. and Potts, J.R., 2007. Simulation of a spin-stabilised sports disc. Sports Engineering, 10 (1), pp. 3-21.

Damowsky, B. and Columin, B., 2002. Analysis of a Flying Disc. Senior Project Report No. SP-502-000-R-BPD, Iowa State University, USA.

Davies, J.M., 1949. The Aerodynamics of Golf Balls. J. Appl. Phys., 20, pp. 821-828.

de Mestre, N.J., Hubbard, M. and Scott, J., 1998. Optimizing the shot put. In Proceedings of the Fourth Conference on Mathematics and Computers in Sport (edited by de Mestre, N. and Kumar, K.), pp. 249-257.

de Mestre, N., 1990. The Mathematics of Projectiles in Sport, Cambridge Univ Press, Cambridge.

Deutsches Bundesarchiv (German Federal Archive) [Online]. Available from: http://www.bild.bundesarchiv.de/archives/barchpic/search/_1310232113/?search[view]=detail&search[focus]=1 [Accessed: 20 May 2009]

Etkin, B. and Reid, L.D., 1996. Dynamics of Flight: Stability and Control, John Wiley & Sons.

Ferrer, R.G. and Watts, R., 1987. The Lateral Force on a Spinning Sphere: Aerodynamics of a Curveball. American Journal of Physics, 55, pp. 40-44.

Ginter, S., 1992. Chance Vought V-173 and XF5U-1 Flying Pancakes. Naval Fighters, 21.

Gordon, R. and Ram, J., 1985. Calculation of nonlinear subsonic characteristics of wings with thickness and camber at high incidence. AIAA Journal, 23 (6), pp. 817-825.

Haake, S.J., Goodwill, S.R. and Carre, M.J., 2007. A new measure of roughness for defining the aerodynamic performance of sports balls. Proceedings of the Institution of Mechanical Engineers, Part C: Journal of Mechanical Engineering Science, 221 (7), pp. 789-800.

Higuchi, H., Goto Y., Hirumoto, R. and Meisel, L. August 2000. Rotating Flying Disks and Formation of Trailing Vortices. AIAA 2000-4001, 18th AIAA Applied Aerodynamics Conference. Denver, CO, USA.

Hildebrand, F., 2001. Modelling of discus flight. In: Blackwell, J.R. (Ed.), Proceedings of Oral Sessions. XIX International Symposium on Biomechanics in Sports. International Society of Biomechanics in Sports, San Francisco, pp. 371-374.

Hoerner, S., 1993. Fluid Dynamic Drag: Practical information on aerodynamic drag and hydrodynamic resistance, Midland Park N.J.

Hubbard, M., 2000. The Flight of Sports Projectiles. Biomechanics in Sport: Performance Enhancement and Injury Prevention (edited by Zatsiorsky, V.M.), pp. 381-400.

Hubbard, M., 2002. Optimal discus release conditions including pitching moment-induced roll. In: Proceedings of World Congress of Biomechanics, University of Calgary, Calgary.

Hubbard, M., 1989. The Throwing Events in Track and Field. In Biomechanics of Sport (edited by Vaughan, C.L.) Boca Raton, Florida: CRC Press, pp. 213-38.

Hubbard, M., 1984.Optimal Javelin Trajectories. Journal of Biomechanics, 17 (10), pp. 777-783.

Hubbard, M. and Alaways, L.W., 1987. Rapid and accurate estimation of release conditions in the javelin throw. Journal of Biomechanics, 22 (6-7), pp. 583-95.

Hubbard, M. and Cheng, K.B., 2007. Optimal Discus Trajectories. Journal of Biomechanics, 40, pp. 3650-3659.

Hubbard, M., de Mestre, N.J. and Scott, J., 2001. Dependence of release variables in the shot put. Journal of Biomechanics, 34 (4), pp. 449-56.

Hubbard, M. and Hummel, S.A., 2000. Simulation of Frisbee Flight. In 5th Conference on Mathematics and Computers in Sport. Sydney, Australia, pp. 14-16.

Hubbard, M. and Rust, H.J., 1984. Simulation of javelin flight using experimental aerodynamic data. Journal of Biomechanics, 17 (10), pp. 769-76.

Hubbard, M. and Rust, H.J., 1984. Javelin dynamics with measured lift, drag, and pitching moment. Transactions of the ASME, 51, pp. 406-408.

Hummel, S.A., 2003. Frisbee Flight Simulation and Throw Biomechanics. MS Thesis, The University of California, Davis, California, USA.

Hummel, S. and Hubbard, M., July 2001. A Musculoskeletal Model for the Backhand Frisbee Throw. In 8th International Symposium on Computer Simulations in Biomechanics. Milan, Italy: Politecnico di Milano, Milan, Italy.

Hummel, S.A. and Hubbard, M., Sept. 2002. Identification of Frisbee Aerodynamic Coefficients using Flight Data. In 4th International Conference on the Engineering of Sport. Kyoto, Japan.

Hummel, S.A. and Hubbard, M., September 2004. Implications of Frisbee Dynamics and Aerodynamics on Possible Flight Patterns. In 5th International Conference on the Engineering of Sport, Davis, California, USA.

Hummel, S.A. and Hubbard, M., 2002. Identification of Frisbee Aerodynamic Coefficients using Flight Data. In 4th International Conference on the Engineering of Sport, Kyoto, Japan.

Hutchings, I., 1976. The ricochet of spheres and cylinders from the surface of water. International Journal of Mechanical Sciences, 18, pp. 243-247.

International Association of Athletics Federation (IAAF) [Online]. Available from: http://www.iaaf.org/statistics/records/inout=O/index.html [Accessed: 14 February 2010].

James, D. and Haake, S., 2008. The spin decay of sports balls in flight (P172) 2-Experimental Arrangements. The Engineering of Sport 7, 2, pp. 165-170.

Katz, P., 1968. The Free Flight of a Rotating Disc. Isreal J. Tech., 6 (1-2), pp. 150-155.

Laitone, E.V., 1997. Wind tunnel tests of wings at Reynolds numbers below 70 000. Experiments in Fluids, 23 (5), pp. 405-409.

Lanka, J., 2000. Shot Putting. Biomechanics in Sport: Performance Enhancement and Injury Prevention (edited by Zatsiorsky V.M.), pp. 435-457.

Lazzara, S., Schweitzer, C. and Toscano, J., May 1980. Design and Testing of a Frisbee Wind Tunnel Balance. Unpublished Report, Code: Engin 12, Brown University, Advisor: Prof. Karlson S.K.F.

Leigh, S., Gross, M.T., Li, L. and Yu, B., May 2008. The relationship between discus throwing performance and combinations of selected technical parameters. Sports Biomechanics, 7 (2), pp. 173-193.

Leigh, S., Liu, H. and Hubbard, M., 2010. Individualized optimal release angles in discus throwing. Journal of Biomechanics, 43 (3), pp. 540–545.

Leigh, S. and Yu, B., 2007. The associations of selected technical parameters with discus throwing performance: A cross-sectional study. Sports Biomechanics, 6 (3), pp. 269-284.

Lichtenberg, D.B. and Wills, J.G., 1978. Maximizing the range of the shot put. American Journal of Physics, 46, pp. 546–549.

Lindenbaum, B. and Blake, W., 1998. The VZ-9 "Avrocar".

Linthorne, N.P., 2001. Optimum release angle in the shot put. Journal of Sports Sciences, 19 (5), pp. 359-72.

Linthorne, N., January 2006. Throwing and jumping for maximum horizontal range. Arxiv: physics/0601148v1, pp. 1-6.

Linthorne, N.P. and Everett, D.J., 2006. Release angle for attaining maximum distance in the soccer throw-in. Sports biomechanics / International Society of Biomechanics in Sports, 5(2), pp. 243-60.

Liseaman, P.B.S., 1994. Stability and Dynamics of a Spinning Oblate Spheroid. Unpublished Document. The University of Southern California.

Liseaman, P.B.S., 1996. The Meaning of Lift. AIAA 96-0161, In 34th Aerospace Sciences Meeting & Exhibit. Reno, Nevada.

Linsaman, P.H.S., Dec. 1998. Disc Flight Dynamics. Unpublished Document. The University of Southern California.

Linsaman, P.H.S., Jan. 1999. Disc Flight Description. Unpublished Document. The University of Southern California.

Linsaman, P.H.S., Jan. 2001. Range of a Free Disc.Unpublished Document. The University of Southern California.

Linsaman, P.H.S., Dec. 2003. Physics of the Far Flung Frisbee. Unpublished Document. The University of Southern California.

Linsaman, P.H.S., Dec. 2003. Upper Bounds on Range of a Free Disc. Unpublished Document. The University of Southern California.

Lorenz, R.D., 2005. Flight and attitude dynamics measurements of an instrumented Frisbee. Measurement Science and Technology, 16 (3), pp. 738-748.

Lorenz, R., 2006. Spinning Flight: Dynamics of Frisbees, Boomerangs, Samaras, and Skipping Stones. Springer.

Maccoll, J., 1928. Aerodynamics of a spinning sphere. J. R. Aeronaut. Soc., 32, pp. 777-798.

Maheras, A.V., 1995. The relationship between the angle of release and the velocity of release in the shot-put, and the application of a theoretical model to estimate the optimum angle of release (throwing). Ph.D Thesis, University of Kansas.

McCoy, M.W., Gregor, R.J., Whiting, W.C., Rich, R.C. and Ward, P.E., 1984. Kinematic analysis of elite shot putters. Track Technique, 90, pp. 2868-2870.

Mehta, R. D. 1985. Aerodynamics of Sports Balls. Annual Review of Fluid Mechanics, 17 (1), pp. 151-189.

Mehta, R.D. and Pallis, J.M., 2001. Sports ball aerodynamics: Effects of velocity, spin and surface roughness. Materials and Science in Sports, 7514 (724), pp. 185–197.

Mero, A., Komi, P.V., Korjus, T., Navarro, E. and Gregor, R.J., 1994. Body segment contributions to javelin throwing during final thrust phases. J. Appl. Biomech., 10, pp. 166-177.

Mitchell, T.L., 1999. The Aerodynamic Response of Airborne Discs. MS Thesis, The University of Nevada, Las Vegas, NV, USA.

Morriss, C. and Bartlett, R., Biomechanical factors critical for performance in the men's javelin throw. Sports Medicine, 21 (6), pp. 438-446

Nakamura, Y. and Fukamachi, N., 1991. Visualization of the flow past a Frisbee. Fluid Dynamics Research, 7 (1), pp. 31-35.

Nathan, A.M., 2008. The effect of spin on the flight of a baseball. American Journal of Physics, 76 (2), p. 119.

Passmore, M.A., Tiplin, S. Spencer, A. and Jones, R., 2008. Experimental studies of the aerodynamics of spinning and stationary footballs. Proceedings of the Institution of Mechanical Engineers, Part C: Journal of Mechanical Engineering Science, 222 (2), pp. 195–205.

Pelletier, A. and Mueller, T.J., 2000. Low Reynolds Number Aerodynamics of Low-Aspect-Ratio, Thin/Flat/Cambered-Plate Wings. Journal of Aircraft, 37 (5), pp. 825-832.

Podesta, M.D., 2007. Bouncing steel balls on water. Physics Education, 42 (5), pp. 466-477.

Potts, J. R., 2005. Disc-wing Aerodynamics. PhD Thesis, The University of Manchester.

Potts, J.R. and Crowther, W.J., April 2000(a). The Flow Over a Rotating Disc-wing. In RAeS Aerodynamics Research Conference. London, UK.

Potts, J. R. and Crowther, W. J., August 2000(b). Visualisation of the Flow Over a Disc-wing.In Proc. of the Ninth International Symposium on Flow Visualization, Edinburgh, Scotland, UK. pp. 1-10.

Potts, J.R. and Crowther, W.J., Jan. 2001(a). Flight control of a spin stabilised axi-symmetric disc-wing. In 39th AIAA Aerospace Sciences Meeting & Exhibit, Reno, Nevada.

Potts, J.R. and Crowther, W.J., April 2001(b). Application of Flow Control to a Disc-wing UAV. In 16th UAV Systems Conference, Bristol, UK.

Potts, J.R. and Crowther, W.J., June 2002(a). A Feasibility Study in Aerodynamics & Control. In CEAS Aerospace Aerodynamics Research Conference, Cambridge, UK.

Potts, J.R. and Crowther, W.J., June 2002(b). Frisbee Aerodynamics. In 20th AIAA Applied Aerodynamics Conference & Exhibit, St. Louis, Missouri, USA.

Potts, J.R. and Crowther, W.J., Jan. 2003. Aerodynamics and Control of a Spin-stabilised Disc-wing. In CEAS Aerospace Aerodynamics Conference Highlights (Invited), 41st AIAA Aero. Sciences Meeting & Exhibit, Reno, Nevada, USA.

Pozzy, T., Winter 2002. Getting More Distance - How The Pros Do It. Disc Golf World News, No. 60.

Professional Disc Golf Association (PDGA) [Online]. Available from: http://www.pdga.com/introduction?i=f702ca43c853a4e73c76534b97cb254e> [Accessed: 6 Jun 2009].

Red, W.E. and Zogaib, A.I., 1977. Javelin dynamics including body interaction. Journal of Applied Mechanics, 44, pp. 496-498.

Rohde, A., 2000. A Computational Study of Flow around a Rotating Disc in Flight. PhD Thesis, Florida Institute of Technology.

Smits A.J., and Smith, D.R., 1994. A New Aerodynamic Model of a Golf Ball in Flight. Science and Golf II: In Proceedings of the World scientific congress of golf (edited by Cochran, A.J. and Farrally, M.R.), pp. 340-346.

Soodak, H., 2004. Geometric top theory of football, discus, javelin. In: Hubbard, M., Mehta, R.D., Pallis, J.M. (Eds.) Engineering of Sport 5: Proceedings of the 5th International Conference on the Engineering of Sport, Davis, CA, vol. 1. September. ISEA, Sheffield, UK., pp. 365-371.

Soong, T.C., 1970. The Dynamics of the Discus Throw, J. Appl. Mech. 98, pp. 531-536.

Stilley, G.D. and Carstens, D.L., 1972. Adaptation of Frisbee Flight Principle to Delivery of Special Ordinance. AIAA Paper No.72-982.

Watts, R. and Ferrer, R.G., 1987. The Lateral Force on a Spinning Sphere: Aerodynamics of a Curveball. American Journal of Physics, 55, pp. 40-44.

Wesson, J., 2009. The Science of Golf, Oxford University Press.

Wesson, J., 2002. The Science of Soccer, Institute of Physics Publishing.

Young, M., 2000. Preparing for the Specific Neuromuscular and Biomechanical Demands of the Javelin Throw. Human Performance Consulting.

Zatsiorsky, V.M., 1995. Science and Practice of Strength Training (1st ed.). Champaign, IL: Human Kinetics.

Zimmerman, C.H., August 1935. Aerodynamic Characteristics of Several Airfoils of Low Aspect Ratio. NACA Langley Memorial Aeronautical Laboratory. NACA-TN-539.

Appendix A

A. Golf disc flight trajectories (individual case)

The flight trajectories for putter, mid-range and driver are shown in Figure A1 to A3. The data plotted are the same as in Chapter 6: Simulation Results and Discussion. However, the data is plotted again to highlight the individual golf disc trajectories at varying launch angles.

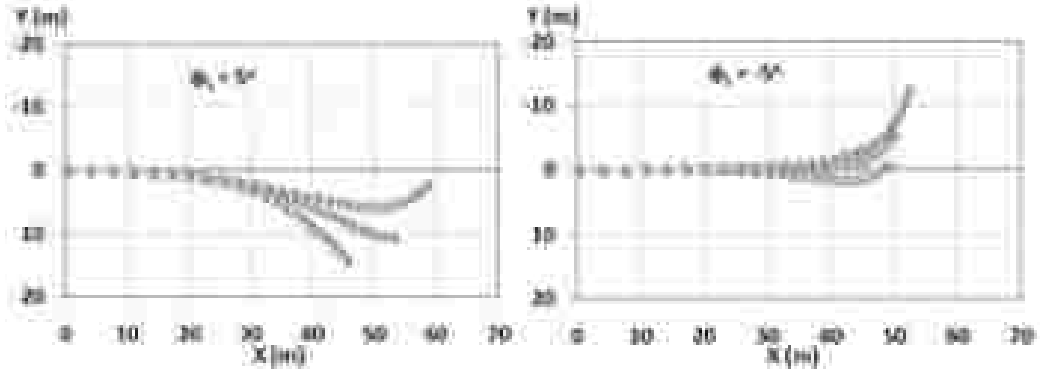

(a) Launch roll angle, $\Phi_L = 5°$.

(b) Launch roll angle, $\Phi_L = -5°$.

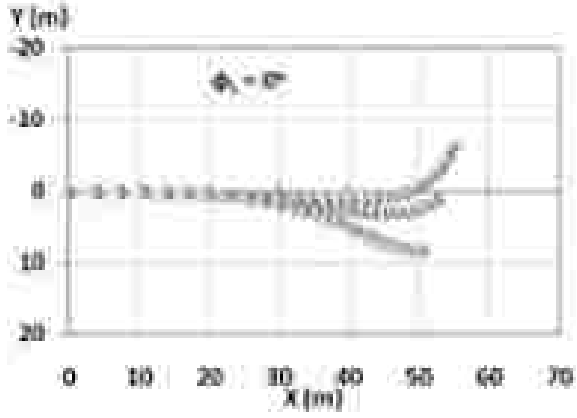

(c) Launch roll angle, $\Phi_L = 0°$.

Figure A1: Flight trajectories for typical putter, mid-range and driver discs at varying launch roll angles: 5°, -5°, 0°. The initial conditions are: $V_L = 20$ m s^{-1}, $\theta_L = 15°$, $\alpha_L = 0°$, $\Psi_L = 0°$, AdvR = 0.5, unless stated otherwise.

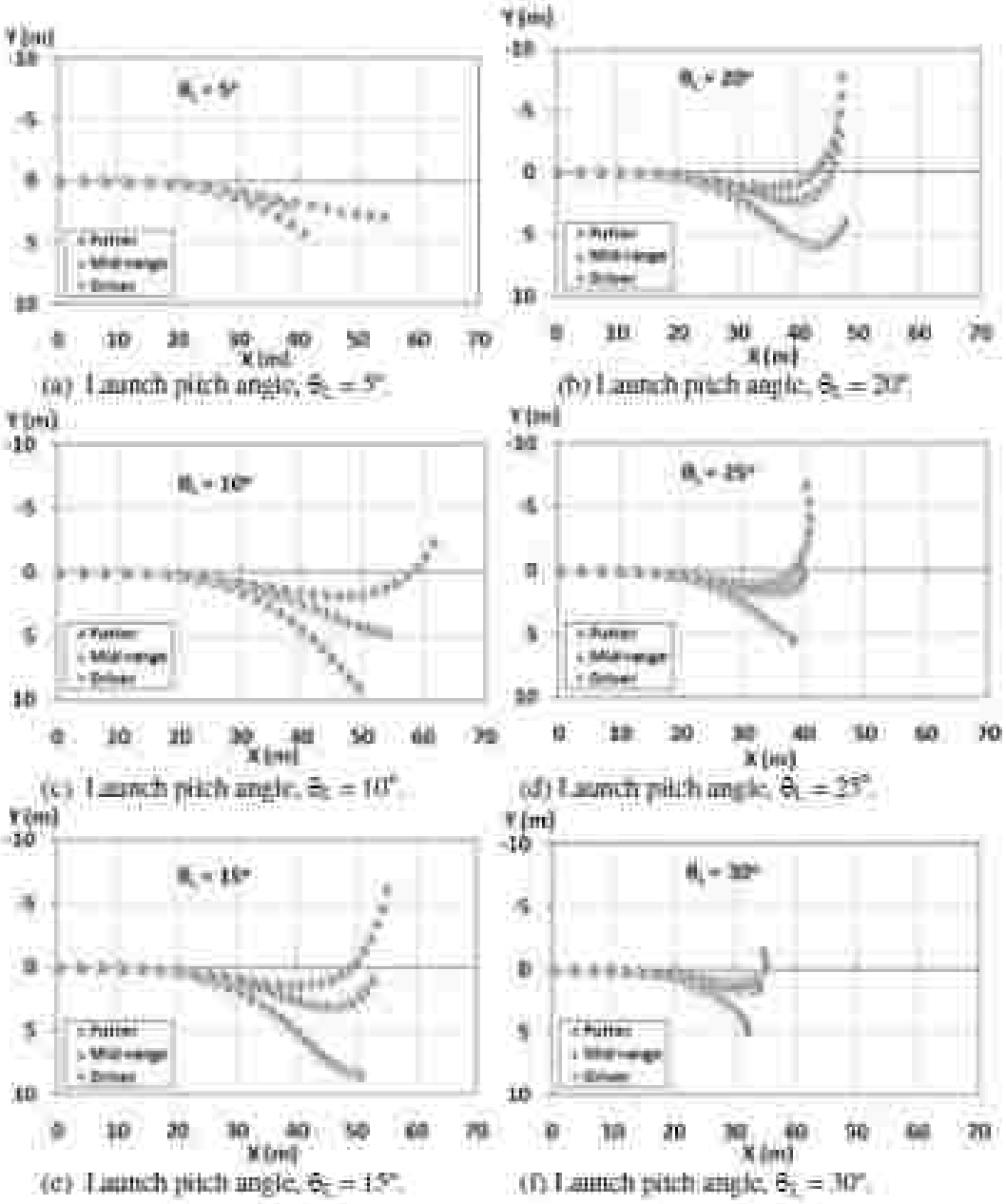

(a) Launch pitch angle, $\theta_L = 5°$.
(b) Launch pitch angle, $\theta_L = 20°$.
(c) Launch pitch angle, $\theta_L = 10°$.
(d) Launch pitch angle, $\theta_L = 25°$.
(e) Launch pitch angle, $\theta_L = 15°$.
(f) Launch pitch angle, $\theta_L = 30°$.

Figure A2: Flight trajectories for typical putter, mid-range and driver discs at varying launch pitch angles from 5° to 30°. The initial conditions are: $V_L = 20$ m s^{-1}; $\alpha_L = 0°$; $\alpha_R = 0°$; $\psi_L = 0°$; AdvR = 0.5, unless stated otherwise.

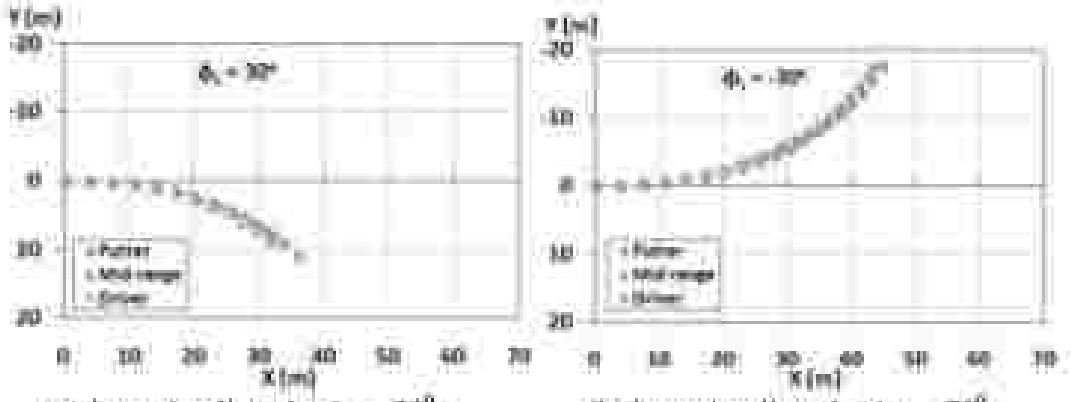

(a) Launch roll angle, $\phi_L = 30°$.

(b) Launch roll angle, $\phi_L = -30°$.

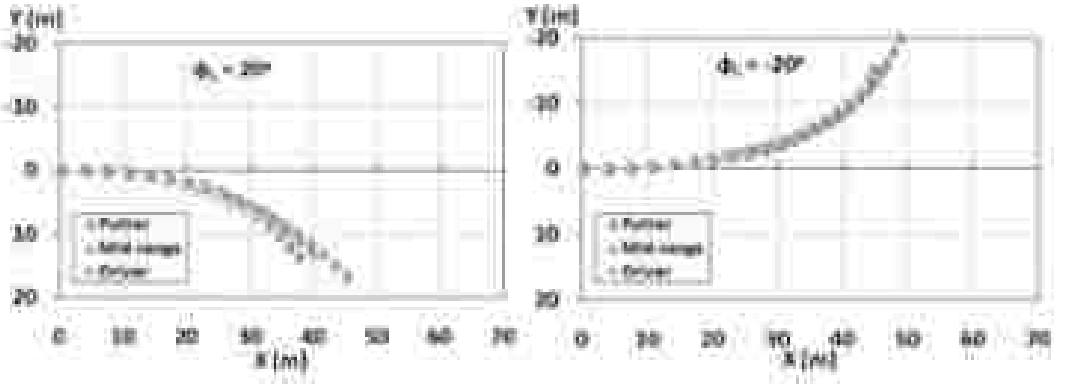

(c) Launch roll angle, $\phi_L = 20°$.

(d) Launch roll angle, $\phi_L = -20°$.

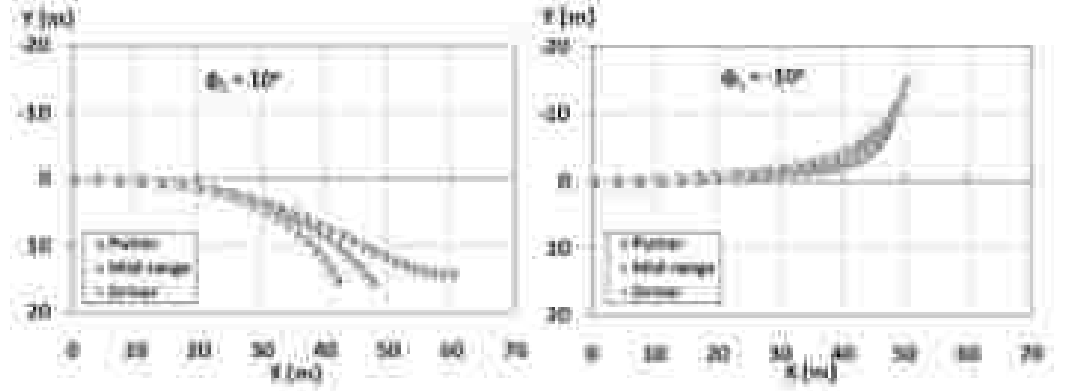

(e) Launch roll angle, $\phi_L = 10°$.

(f) Launch roll angle, $\phi_L = -10°$.

Figure A3: Flight trajectories for typical putter, mid-range and driver discs at varying launch roll angles: 30°, -30°, 20°, -20°, 10°, -10°. The initial conditions are: $V_L = 20$ m s^{-1}, $\delta_L = 15°$, $\alpha_L = 0°$, $\psi_L = 0°$, Adv-R = 0.5, unless stated otherwise.